

THESIS
2
2004
565628.21

**LIBRARY
Michigan State
University**

This is to certify that the
dissertation entitled

**POSITION-DEPENDENT REGULATION OF THE *NOR-1*
PROMOTER IN THE AFLATOXIN GENE CLUSTER AND
IMMUNO-LOCALIZATION OF PROTEINS INVOLVED IN
AFLATOXIN BIOSYNTHESIS**

presented by

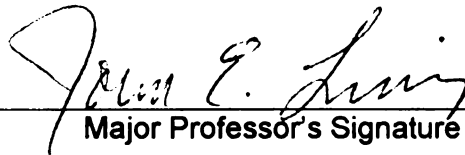
Ching-Hsun Chiou

has been accepted towards fulfillment
of the requirements for the

Doctoral

degree in

Food Science and
Environmental Toxicology


Major Professor's Signature

12-3-03

Date

PLACE IN RETURN BOX to remove this checkout from your record.
TO AVOID FINES return on or before date due.
MAY BE RECALLED with earlier due date if requested.

DATE DUE	DATE DUE	DATE DUE

**POSITION-DEPENDENT REGULATION OF THE *NOR-1* PROMOTER IN THE
AFLATOXIN GENE CLUSTER AND IMMUNO-LOCALIZATION OF PROTEINS
INVOLVED IN AFLATOXIN BIOSYNTHESIS**

By

Ching-Hsun Chiou

A DISSERTATION

**Submitted to
Michigan State University
in partial fulfillment of the requirements
for the degree of**

DOCTOR OF PHILOSOPHY

Department of Food Science and Human Nutrition

2003

ABSTRACT

POSITION-DEPENDENT REGULATION OF THE *NOR-1* PROMOTER IN THE AFLATOXIN GENE CLUSTER AND IMMUNO-LOCALIZATION OF PROTEINS INVOLVED IN AFLATOXIN BIOSYNTHESIS

By

Ching-Hsun Chiou

Aflatoxins (AF) are highly toxic and carcinogenic fungal secondary metabolites. AF contamination in crops including corn, peanuts, cottonseed, and specific tree nuts has caused significant agricultural economic and human health concerns throughout the world. My research goal was to study regulation of AF biosynthesis in *Aspergillus parasiticus*. As a long term goal, these studies should aid efforts to discover strategies to efficiently eliminate AF contamination of agricultural commodities and in turn to ensure product safety and consumer health.

Biosynthesis of AF in the filamentous fungi in the genus *Aspergillus* utilizes a complex pathway consisting of at least eighteen enzymes and at least one positive regulatory factor, AflR; these genes are clustered within a 75 kb chromosomal region. Expression of most of the AF genes in the cluster is co-regulated but the mechanisms are not clear. The localization and interaction of these enzymes to synthesize AF at the cellular level has yet to be determined. Therefore, two hypotheses are included in my study. 1) Expression of genes involved in aflatoxin biosynthesis is positively regulated within the AF gene cluster. 2) Enzymes involved in AF biosynthesis are localized within developmental structures (e.g., conidiophores) in the colony.

The objectives of my research were to: 1) study the positional-effects on AF gene (*nor-1*) expression in the gene cluster; 2) generate highly-specific antibodies against an AF protein (anti-VBS) for immuno-localization studies; 3) develop methods to localize AF proteins within a fungal colony; and 4) localize proteins involved in AF biosynthesis in a time-course dependent fractionated colony.

To study positional effects on *nor-1* promoter function, a plasmid pAPGUSNP containing the *nor-1* promoter sequence fused to a reporter gene (*uidA* encoding β -glucuronidase, GUS) plus a *pyrG* selectable marker was constructed. Transformation of pAPGUSNP into CS10 (*ver-1*, *wh-1*, *pyrG*) resulted in homologous recombination at 5' *nor-1*, 3' *nor-1*, or the *pyrG* locus. The plasmid integration site was screened by a novel rapid DNA extraction/PCR assay and confirmed by Southern hybridization analysis. The *nor-1* promoter was positively regulated in the AF gene cluster while outside the cluster (*pyrG* locus), *nor-1* promoter activity decreased dramatically. The data supported the hypothesis that expression of AF genes is cluster position-dependent.

The second hypothesis was tested by studying localization AF proteins utilizing anti-VBS antibodies raised against recombinant Maltose Binding Protein-VBS expressed in *Escherichia coli* (generated in this study), and other antibodies available in the laboratory (anti- Nor-1, Ver-1, and OmtA). A 72 h-old colony was fractionated based on 24 h intervals to correlate the time of growth with AF protein distribution. Colony fractions were fixed and embedded in paraffin to generate 4-5 μm sections for immunofluorescence labeling. Confocal Laser Scanning Microscopy (CLSM) demonstrated that Nor-1, Ver-1, OmtA, and VBS were evenly distributed among different cell types and not concentrated in conidiophores, contrary to the hypothesis. These proteins were not evenly distributed throughout a 72 h-old colony. Among three fractions, colony fraction S2 (24 to 48 h growth) exhibited the highest abundance of Nor-1, Ver-1, OmtA, and VBS (analyzed by CLSM and quantitative fluorescence intensity analysis), the highest levels of AFB₁ (determined by enzyme-linked-immunosorbent-assay), and the highest numbers of newly-developed conidiophores. These data support a spatial and temporal association between AF protein expression/AF production and sporulation at the colony level.

ACKNOWLEDGMENTS

I would first like to thank my major professor, Dr. John Linz, for his support and guidance throughout this study. He is a good mentor who teaches me science and many other precious things beyond the science. I admire Dr. Linz as a good scientist and a knowledgeable person.

Appreciation is also expressed to Dr. Karen Klomparens, Dr. James Pestka, Dr. Gale Strasburg, and Dr. Jay Schroeder for serving on my guidance committee.

I am also especially grateful to Dr. Shirley Owens and others who assisted me in the Center for Advanced Microscopy at Michigan State University.

Thanks to Li-Wei Lee, Mike Miller, Matt Rarick, and other members in the Linz laboratory for all the help they have provided.

I also appreciate my parents, family, and friends, who always stand by me and show me their support and encouragement.

TABLE OF CONTENTS

LIST OF TABLES	ix
LIST OF FIGURES	x
CHAPTER 1	
Literature review	1
DELETERIOUS EFFECTS OF AFLATOXINS	1
Background and history	1
Economic impact and regulation of AF in foods	3
Environmental factors and controlling AF contamination	4
Toxicological effects of AF	5
Aflatoxin and liver cancer	6
Bioactivation of AFB ₁	6
Detoxification of AF	6
AFB ₁ -DNA adducts and AFB ₁ induced <i>p53</i> gene mutations	6
A synergistic effect between AFB ₁ and hepatitis B virus (HBV)	8
AFLATOXIN BIOSYNTHESIS	9
Aflatoxin gene cluster	9
Regulation of AF biosynthesis	9
Partially-duplicated AF gene cluster	13
Sugar utilization gene cluster	14
SECONDARY METABOLISM AND FUNGAL DEVELOPMENT	14
Association between secondary metabolism and fungal development	14
G-Protein signaling pathway	14
FluG	15
AF biosynthesis and conidiation	15
LOCALIZATION OF AF ASSOCIATED PROTEINS	17
Penicillin biosynthesis as an example	17
Organelles possibly involved in AF biosynthesis	18
Microbodies	18
Woronin bodies	18
Vesicles	19
Vacuoles	19
Endoplasmic reticulum (ER)	21
CONFOCAL LASER SCANNING MICROSCOPY (CLSM) IN THE STUDY OF FUNGAL BIOLOGY	22
Introduction to CLSM	22
Image quality enhancement by CLSM	23
CLSM Imaging	25
Optical sections	25

Z-series	25
<i>Phi-z</i> sectioning	26
Time-lapse and live imaging	26
Fluorescence imaging	26

CHAPTER 2

A rapid DNA extraction method for screening large numbers of <i>Aspergillus</i> transformants via polymerase chain reaction	31
ABSTRACT	31
INTRODUCTION	31
MATERIAL AND METHODS	32
RESULTS AND DISCUSSION	33
ACKNOWLEDGEMENTS	41

CHAPTER 3

Position-dependent regulation of the <i>nor-1</i> promoter in the aflatoxin gene cluster	42
ABSTRACT	42
INTRODUCTION	43
MATERIALS AND METHODS	45
Strains and growth conditions	45
Construction of pAPGUSNP	45
Fungal transformation	48
Identification of the site of plasmid integration	48
Rapid DNA extraction procedure for PCR analysis	48
PCR analysis	48
Solid-culture GUS activity assay	49
Southern hybridization analysis	49
5' <i>nor-1</i> integration	51
3' <i>nor-1</i> integration	51
Integration at <i>pyrG</i>	51
RESULTS	51
Generation of pAPGUSNP	51
Transformation of <i>A. parasiticus</i> CS10 with pAPGUSNP	56
Solid-culture GUS assay	56
Determination of pAPGUSNP integration site within the chromosome	56
Confirmation of <i>pyrG</i> expression in <i>pyrG</i> ⁺ transformants	59
DISCUSSION	59
ACKNOWLEDGEMENTS	63

CHAPTER 4

Immuno-localization of Nor-1, Ver-1, and OmtA proteins involved in aflatoxin biosynthesis in <i>Aspergillus parasiticus</i>	64
INTRODUCTION	64
MATERIALS AND METHODS	67

Fungal strains	67
Time-dependent fractionation of colonies grown on solid medium	67
Preparation of paraffin-embedded fungal sections	67
Immuno-fluorescence labeling of fungal cells	69
Confocal Laser Scanning Microscopy (CLSM)	70
Quantitative fluorescence intensity analysis	70
RESULTS	71
Immuno-localization of Nor-1 and Ver-1	71
Immuno-localization of OmtA	71
Quantitative fluorescence intensity analysis	79
DISCUSSION	85
ACKNOWLEDGEMENTS	89

CHAPTER 5

Distribution and sub-cellular localization of the aflatoxin enzyme versicolorin B synthase (VBS) in time-fractionated colonies of <i>Aspergillus parasiticus</i>	90
ABSTRACT	90
INTRODUCTION	91
MATERIALS AND METHODS	94
Fungal strains and growth conditions	94
Production of antibodies against native VBS	94
Generation of MBP (Maltose Binding Protein)-VBS fusion protein	95
Production and purification of PAb against MBP-VBS	95
Time-dependent fractionation of fungal colonies	96
Fungal protein extraction	96
SDS-Polyacrylamide Gel Electrophoresis (SDS-PAGE) and Western blot analysis	97
Detection of AFB ₁ in colony fractions	97
Thin Layer Chromatography (TLC)	97
Enzyme-Linked-Immunosorbent-Assay (ELISA)	97
Preparation of paraffin-embedded fungal sections and immuno-fluorescence labeling	98
Confocal Laser Scanning Microscopy (CLSM)	99
Quantitative fluorescence intensity analysis	99
Statistical analysis	100
Preparation of ultra-thin fungal sections, immuno-gold labeling, and TEM analysis	100
RESULTS	100
Generation of PAb against native fungal VBS	100
Expression of MBP-VBS fusion protein and production of PAb against VBS	101
Expression of VBS in <i>A. parasiticus</i> grown on solid medium	106
Confocal Laser Scanning Microscopy (CLSM) of time-dependent expression of VBS in a 72 h-old fungal colony	109
Fluorescence intensity quantification and statistical analysis	109
Production of AFB ₁ in colony fractions	109

Sub-cellular localization of VBS	109
DISCUSSION	116
ACKNOWLEDGEMENTS	124
BIBLIOGRAPHY	125

LIST OF TABLES

Table 2.1. Primer sequences and PCR cycling parameters used for analysis of fungal genomic DNA templates.....	34
Table 3.1. Primer sequences and PCR cycling parameters used for analysis of site of integration using DNA templates prepared by the rapid method.....	50
Table 3.2. Summary of GUS activities and plasmid integration sites in <i>A. parasiticus</i> CS10 transformants carrying the <i>nor::GUS</i> fusion plasmid pAPGUSNP (Chiou), and NR-1 harboring pAPGUSNNB (Wilson, 1998) and pNG3.0 (Miller, 2003).....	61
Table 4.1. Quantative fluorescence intensity analysis of <i>A. parasiticus</i> SU-1 and AFS10 immuno-fluorescence labeled with Nor-1, Ver-1 and OmtA antibodies.....	86
Table 5.1. Quantitative fluorescence intensity analysis of <i>A. parasiticus</i> SU-1 and AFS10 labeled with polyclonal antibodies to VBS and OmtA.....	113
Table 5.2. Quantitative detection (ELISA) of AFB ₁ in colony fractions of SU-1 cultured on YES solid media for 72 h.....	114

LIST OF FIGURES

Figure 1.1. Chemical structures of AFB ₁ , AFB ₂ , AFG ₁ , AFG ₂ , AFM ₁ , AFM ₂ , and AFB ₁ -8, 9-epoxide.....	2
Figure 1.2. Generally accepted pathway for sterigmatocystin and aflatoxin biosynthesis.....	10
Figure 1.3. The G-protein signaling pathway involved in ST biosynthesis in <i>A. nidulans</i>	16
Figure 1.4. Diagram of the light path in a confocal instrument.....	24
Figure 1.5. CLSM Z-series of <i>A. parasiticus</i> SU-1 conidiophores stained with SYTOX green fluorescence dye.....	26
Figure 1.6. CLSM single optical section and <i>phi-z</i> scan of <i>A. parasiticus</i> SU-1 microbodies.....	28
Figure 2.1. Homologous recombination of pAPGUSNP into the <i>A. parasiticus</i> chromosome and primers used in integration analysis.....	35
Figure 2.2. Amplification of PCR targets using the rapid DNA extraction technique...	37
Figure 3.1. Restriction endonuclease maps of plasmids containing the <i>nor-1::GUS</i> construct related to this study.....	46
Figure 3.2. Southern hybridization analysis of site of integration in pAPGUSNP transformants.....	52
Figure 3.3. Southern hybridization analysis of pAPGUSNP integrated at <i>pyrG</i>	54
Figure 3.4. PCR analysis to detect site of integration in pAPGUSNP transformants...	57
Figure 3.5. Solid-culture GUS activity assay on CS10 transformants harboring pAPGUSNP.....	58
Figure 4.1. Time-dependent fractionation of fungal colonies.....	68
Figure 4.2. Immuno-fluorescence confocal microscopy of Nor-1 and Ver-1 in <i>A. parasiticus</i> SU-1 and AFS10 (<i>aflR</i> knockout mutant) grown on YES agar for 72 h.....	72
Figure 4.3. CLSM immuno-fluorescence detection of Nor-1 in <i>A. parasiticus</i> SU-1.....	74

Figure 4.4. CLSM immuno-fluorescence detection of Ver-1 in <i>A. parasiticus</i> SU-1.....	76
Figure 4.5. Immuno-fluorescence labeling of Ver-1 antibodies in the control strain <i>A. parasiticus</i> AFS10 and the wild-type strain SU-1.....	78
Figure 4.6. OmtA protein localization in time-fractionated colonies of <i>A. parasiticus</i> SU-1, AFS10 (<i>afR</i> knockout), CS10 and LW1432 (<i>omtA</i> knockout) grown on YES agar for 72 h.....	80
Figure 4.7. Protein localization using OmtA PAb and anti-SKL, and detection of nuclei using SYTOX Green.....	82
Figure 4.8. CLSM immuno-fluorescence detection of OmtA in <i>A. parasiticus</i> SU-1....	84
Figure 5.1. Western blot analysis of VBS detected by PAb raised against native fungal VBS.....	102
Figure 5.2. SDS-PAGE of recombinant MBP-VBS fusion protein.....	103
Figure 5.3. MBP-VBS treated with Factor Xa to generate MBP (42 kDa) and VBS (52 kDa).....	104
Figure 5.4. Western blot analysis of VBS produced in liquid culture using highly specific PAb raised against MBP-VBS.....	107
Figure 5.5. Western blot analysis of VBS expressed in <i>A. parasiticus</i> SU-1 colonies (solid culture) and colony fractions.....	108
Figure 5.6. CLSM of VBS protein distribution in time-fractionated colonies of <i>A. parasiticus</i> SU-1 (S1, S2, S3) and AFS10 (R1, R2, and R3) grown on YES agar for 72h.....	110
Figure 5.7. Thin Layer Chromatography analysis of AFB ₁ production in colony fractions.....	111
Figure 5.8. CLSM immuno-fluorescence of VBS <i>A. parasiticus</i> SU-1 grown in solid culture	112
Figure 5.9. CLSM dual detection for localization of VBS and nuclei in <i>A. parasiticus</i> SU-1.....	115
Figure 5.10. Immuno-gold labeling of VBS in <i>A. parasiticus</i> AFS10 and SU-1 analyzed by TEM.....	117

CHAPTER 1

Literature review

DELETERIOUS EFFECTS OF AFLATOXINS

Background and history. Aflatoxins (AF) are secondary metabolites mainly produced by the filamentous fungi *Aspergillus flavus* and *A. parasiticus* (Wilson and Payne, 1994; CAST, 2003). They are less frequently produced by *A. nomius*, *A. pseudotamari*, *A. bombycis*, and one isolate of *A. ochraceoroseus* (Klich et al., 2000; Ito et al., 2001; Bhatnagar et al., 2003). *A. parasiticus* synthesizes four major aflatoxins including aflatoxin B₁(AFB₁), AFB₂, AFG₁, and AFG₂ (Asao et al., 1963). Animals ingest AF and produce metabolites AFM₁ and AFM₂ in milk (Fig. 1.1). Among these AF molecules, AFB₁ is the most toxic and carcinogenic (Eaton and Groopman, 1994; Mclean and Dutton, 1995).

AF contamination of corn, peanuts, cotton seed, and certain tree nuts has caused significant agricultural economic and human health problems throughout the world (CAST, 2003). This mycotoxin first aroused public attention in the early 1960s with the incidence of "Turkey X" disease (Blount, 1961). Large quantities (approximately 10, 000) of turkeys died from acute hepatotoxicity caused by contamination of AF in their peanut feed (Siller and Ostler, 1961). Rainbow trout that received AF contaminated diets were discovered to develop liver cancer in the United States (Sinnhuber et al., 1977). In the 1970s, severe pre-harvest AF contamination was reported in the Southern and midwestern United States (Anderson, 1975). *A. flavus* and AF contamination are frequently seen in the Southern US., consistent with the observation that serious outbreaks are related to below-average rainfall and above-average temperature (Payne, 1998). Dietary exposure to AF has been associated with a significant incidence of human liver cancer. Studies on experimental animals indicated that AFB₁ is a potent mutagen

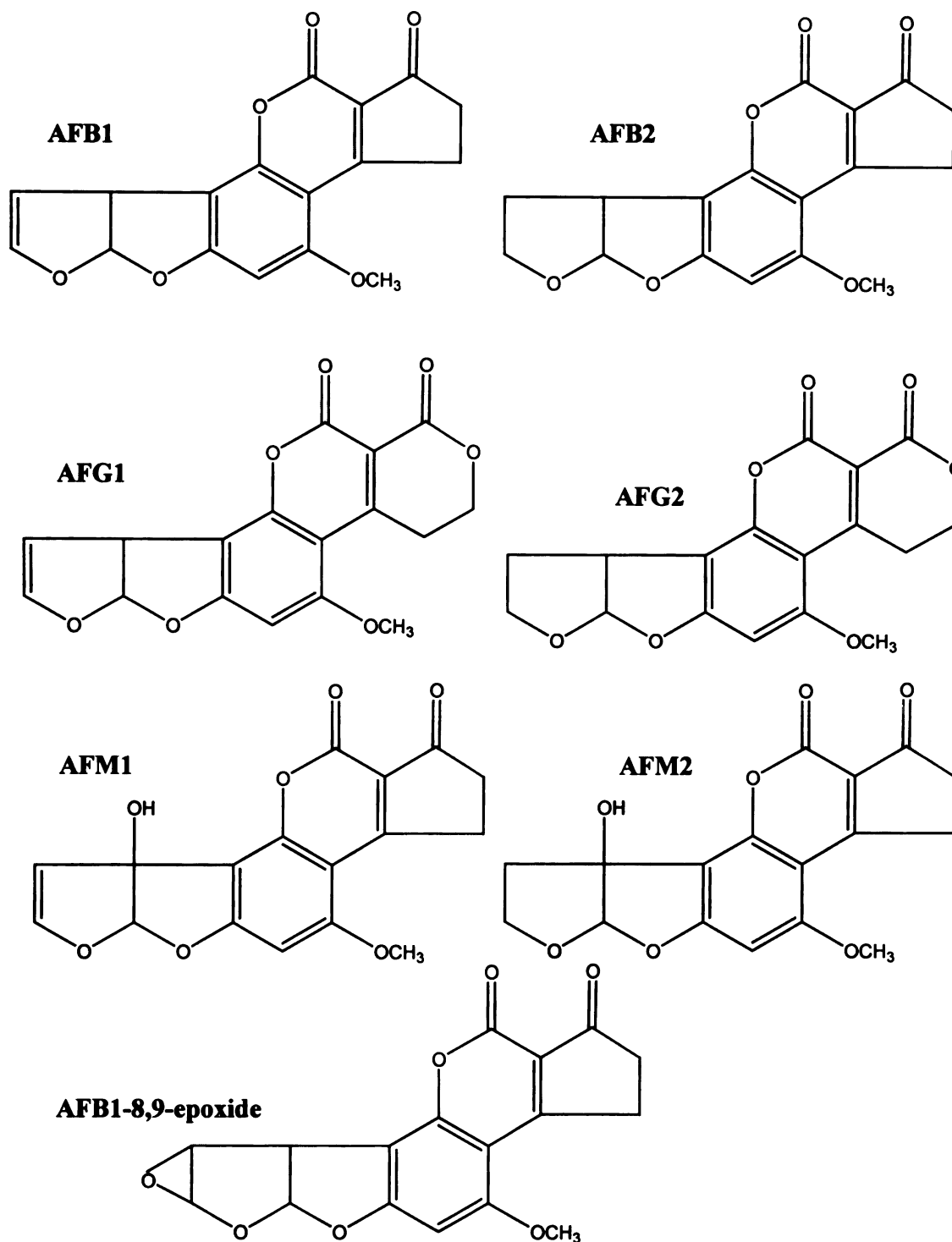


Figure 1.1. Chemical structures of AFB₁, AFB₂, AFG₁, AFG₂, AFM₁, AFM₂, and AFB₁-8, 9-epoxide.

and hepato-carcinogen (reviewed in Eaton and Groopman, 1994). Based on this information, the International Agency for Research on Cancer (IARC) identified AFB₁ as a group I carcinogen in humans (IARC, 1993). Several studies also indicated that infection of hepatitis B virus (HBV) causes a synergistic effect with AFB₁ induced *p53* mutation related to hepatocarcinogenesis (HCC) (Hsia et al, 1992; Harris and Hollstein, 1993; Jackson and Groopman, 1999, CAST, 2003). Hepatitis C viral (HCV) infection is the most important risk factor for HCC in western countries; however, no adequate epidemiological data on the relative roles of HCC and AF were available (Henry et al., 1999; Montalto et al., 2002).

Economic impact and regulation of AF in foods. Approximately 25% of food crops are affected by mycotoxin contamination (including AF) every year throughout the world and this results in serious health and economic concerns (Mannon and Johnson, 1985). Since 1977, documents regarding mycotoxin regulation and control have been published by the Food and Agricultural Organization (FAO) (Boutrif, 1995). Over 50 countries developed guidelines to regulate mycotoxins. The United States set action levels for aflatoxin under the Food, Drug and Cosmetic Act (Sec. 402) (Sharma and Salunkhe, 1991; Bhatanagar et al., 2002; CAST, 2003). The US. Food and Drug Administration (FDA) prohibits interstate commerce of feed grain containing more than 20 parts per billion (ppb, or µg/kg) AFB₁ and prohibits the sale of milk and eggs containing more than 0.5 ppb AFM₁. The action level for a feed crop varies for different animals depending on their sensitivity to AF. Over the world, the maximum allowed levels for aflatoxins in foodstuff range from zero tolerance to 50 ppb (Van Egmond, 1993; Bhatanagar et al., 2002).

Contamination of agricultural commodities with AF poses a significant threat to the food supply world-wide. In the United States, the mean economic losses of crops due to mycotoxin contamination (including AF, fumonisins, and deoxynivalenol) are estimated to be \$932 million. The loss attributed to AF contamination on food crops

(corn and peanuts) was approximately \$47 million per year and approximately \$225 million per year in feed corn (CAST, 2003). Thus, prevention and control of mycotoxin contamination is an important issue.

Environmental factors and control of AF contamination. In the field, *A. flavus* and *A. parasiticus* are able to grow over the temperature range from 12 to 48 °C (optimum 35 to 37 °C) and with a water activity as low as 0.80 (optimum 0.95). However, AF production in these fungi requires a smaller range of temperature (28 to 33 °C, optimum 31°C) and water activity (0.85 to 0.97, optimum 0.90) (Hussein and Brasel, 2001; Bhatnagar et al., 2002).

Pre-harvest contamination of AF on agriculture commodities is usually related to the environmental conditions that generate fungal growth and toxin synthesis. Several methods have been applied to control AF at this stage, including use of fungicides and insecticides (insects facilitate *Aspergillus* infection of plants), modified irrigation practice, and the use of atoxigenic biocompetitive strains (Cotty and Bhatnagar, 1994; Cary et al., 2000; Bhatnagar et al., 2002). However, these procedures have limited effects, particularly in years of drought when fungal growth and toxin synthesis are elevated. Ongoing research is focused on alternative strategies to control AF contamination in the field.

Time of harvest is also critical to restrain the levels of AF contamination. For example, contaminated corn should be harvested early and a subsequent drying procedure may help to prevent an increase in AF contamination that occurs post-harvest. Post-harvest contamination can also be controlled by maintaining proper storage conditions (CAST, 2003). For example, limiting the water activity of the harvest grains below 0.85 and maintaining the storage temperature below 10°C may prevent *A. flavus* spore germination (Marin et al., 1998; CAST, 2003).

Toxins on contaminated products can be removed or detoxified by various physical, chemical and biological methods (Bhatnagar et al., 2002; CAST, 2003). For

example, toxins can be removed by filtration or adsorption onto clays or activated charcoal. Oil roasting or dry roasting peanuts (Marth and Doyle, 1979) and microwave treatment (Farag et al., 1996) may partially destroy AF although they are heat stable. AF in contaminated grains may be extracted by a selected solvent mixture (e.g., 95% ethanol, 90% aqueous acetone, and 80% isopropanol), yet this procedure is costly and product safety remains a concern (CAST, 2003).

Toxicological effects of AF. The degree of AF-induced toxic effects in animals varies, depending on species, dose, exposure duration, and nutritional status of the host (CAST, 2003). The major organ targeted by AF is the liver. Acute aflatoxicosis often produces hepatitis in animals and humans, and ingestion of a high dose may be lethal. Acute hepatitis has been related to consumption of foodstuff contaminated with high doses of AF, especially corn (Ngindu et al., 1982). Under severe conditions, 25% mortality has been reported in outbreaks in India (Krishnamachari et al., 1975).

Sublethal doses generate chronic toxicity and low levels of chronic exposure can result in cancer. A sensitive model to study AF toxicity is trout, and the LD₅₀ was estimated to be 0.5 to 1.0 mg/kg (CAST, 2003). A high incidence of hepatoma was seen in trout fed with 80 ppb AF contaminated diet. Studies in cattle showed chronic clinical signs including reduced weight gain, immuno-suppression, lower milk production, liver damage, and lower reproduction (Bodine and Mertens, 1983). In humans, chronic dietary exposure to AF has a high risk of generating hepatocellular carcinoma (HCC). A high level of AF daily intake (1.4 µg)(Wild et al., 1992) and a high incidence of hepatitis B infection were associated with HCC (Jackson and Groopman, 1999). Epidemiological studies indicated that an increase in AF ingestion from 3 to 222 ng/kg body weight per day corresponded to elevated liver cancer incidence (from 2 to 35 cases per 100,000 population per year) (Jackson and Groopman, 1999).

Aflatoxin and liver cancer.

Bioactivation of AFB₁. AFB₁ naturally produced in the fungus is not a potent mutagen and carcinogen to humans (and other animals); however, the liver cytochrome P450 enzymes generate highly reactive molecules during the oxidative metabolic processes (Eaton and Groopman, 1994). Hence, the major targets for AFB₁ toxicity are hepatocytes. *In vitro* studies have shown that biotransformation of AFB₁ requires molecular oxygen and NADPH. The biotransformed AFB₁, the AFB₁-8,9-epoxides (Fig. 1.1), are potent bioreactive compounds causing mutation and carcinogenesis. The epoxide molecules covalently bind to proteins, DNA and RNA molecules to generate adducts. Adduct formation in turn impairs the normal molecular and cellular functions for the targets (McLean and Dutton, 1995).

Detoxification of AF. Detoxification of AFB₁-8,9-epoxides mainly depends on conjugation with glutathione (GSH). Glutathione S transferase (GST) activity is therefore an important determinant for the susceptibility of different species to the toxic effects of AFB₁ (Eaton and Gallagher, 1994). Different animal species also showed different responses to AFB₁ toxicity due to variability in bioactivation and detoxification processes. In addition to humans, rat, rainbow trout and turkey are susceptible to AFB₁ induced toxicity, whereas mice, ducks and chickens showed lower toxic response (Mclean and Dutton, 1995). It is likely that genetic variability in the expression of cytochrome P450 enzymes may result in substantial differences between individuals in susceptibility to the carcinogenic effects of aflatoxins. For example, glutathione S transferase is the predominant detoxifying activity of AFB₁-8,9-epoxides in mice. However, in humans, GST has very little activity toward AFB₁-8,9-epoxides, suggesting higher human sensitivity to the genotoxic effect of AFB₁ (Hussein and Brasel, 2001).

AFB₁-DNA adducts and AFB₁ induced p53 gene mutations. The N7-guanine residue of DNA is a potential target for AFB₁-8,9-epoxides, forming a AFB₁-N7-guanine adduct. Adduct formation or depurination can lead to mutations in DNA during DNA

replication, mainly resulting in GC→TA transversions (Eaton and Groopman, 1994). Mutation in the *p53* tumor suppressor gene by AFB₁ epoxide has also proposed to be involved in hepatocarcinogenesis (Massey et al., 1995; Mclean and Dutton, 1995; Jackson and Groopman, 1999).

The *p53* gene is a tumor suppressor gene that regulates cell growth. The biological functions of P53 are involved in control of cell cycle, DNA replication and repair, cell differentiation and apoptosis (Harris and Hollstein, 1993; Shen et al., 1996). Mutations in the *p53* tumor suppressor gene were frequently detected in HCC patients (Greenblatt et al., 1994). For example, codon 249 in exon VII of *p53* has been identified as a mutational hot-spot in HCC but not in other tumor types (Yang, et al., 1997; Jackson and Groopman, 1999). A point mutation in the third base of codon 249 of *p53* results in a G→T transversion (AGG→AGT) and a change in amino acid sequence from Arg to Ser. This mutation has been frequently associated with high levels of AFB₁ exposure in HCC patients.

The mutation of the *p53* tumor suppressor gene at codon 247-250 (nucleotide 14067-14075) induced by AFB₁ has been studied (Aguilar et al., 1993). AFB₁ was activated by rat liver microsomes and mutagenesis at codons 247-250 of *p53* gene was analyzed in human hepatocarcinoma cells, HepG2, by restriction fragment length polymorphism/polymerase chain reaction (RFLP/PCR). The results indicated that AFB₁ induces the G→T transversion at the third position of codon 249 with relatively high frequency. However, cells exhibiting different bioactivation and detoxifying systems may influence the results. Mace et al. (1997) investigated AFB₁-induced DNA adduct formation and *p53* mutations in human liver cells expressing various cytochrome p450 isozymes. The results suggested that CYP1A2 is the most effective isoform in the activation of AFB₁ to cytotoxic products and CYP3A4 for genotoxic metabolite formation. Cells containing CYP1A2 and CYP3A4 also showed a higher level of AFB₁-DNA adduct formation and increased levels of *p53* mutations (Mace, et al., 1997).

A synergistic effect between AFB₁ and hepatitis B virus (HBV). Exposure to AFB₁ alone has been verified as an important risk factor for development of human HCC. A high prevalence of hepatitis B virus (HBV) infection frequently occurred along with a high level of aflatoxin contamination in many regions of the world. HBV infection and AFB₁ exposure have been suggested to have synergistic effects on tumor formation as well as *p53* gene mutation, (Lunn et al., 1997; Yang, et al., 1997). This was supported by a study using a transgenic mouse model that expresses hepatitis B surface Ag (HBsAg) and genetic inbred *p53* null mice to determine the association of AFB₁, HBV and *p53* expression on liver tumor formation (Ghebranious and Sell, 1998). The results showed that AFB₁ induced a higher level of tumor formation than HBV infection alone. A synergistic effect between AFB₁ and HBV infection increased HCC. The highest risk group for liver cancer formation was generated with combinations of AFB₁ ingestion, HBV expression and *p53* mutation.

Epidemiological studies also suggest that high levels of AFB₁ exposure and HBV infection may have synergistic effects on HCC induction. Shen and Ong (1996) summarized the results from more than thirty reports from 1991 to 1995 with more than 1500 human HCC samples that were examined for *p53* mutation with respect to different AFB₁ exposure levels. It was found that the frequency of codon 249 mutations in the *p53* tumor suppressor gene directly parallels the environmental AFB₁ exposure level. Lasky and Mahden (1997) performed similar research by retrieving twenty studies that provided analytical data in *p53* mutations in HCC patients. The analysis suggested that high levels of AF exposure (such as Southern Africa and China) were associated with the hot-spot mutation (codon 249) in *p53* in a high proportion (approximately 50%) of HCC patients. On the contrary, codon 249 mutations were not detected in areas with low AF exposure such as Japan, Europe and the USA (Jackson and Groopman, 1999).

AFLATOXIN BIOSYNTHESIS

Aflatoxin gene cluster. Biosynthesis of AF in *A. flavus* and *A. parasiticus* from the starter unit, acetate, requires at least eighteen enzymatic activities (Woloshuck and Prieto, 1998; Payne and Brown, 1998; Minto and Townsend, 1998; Motomura et al., 1999; Cary et al., 2000; Bhatnagar et al., 2003). *A. nidulans* possesses a similar biosynthetic pathway to synthesize the secondary metabolite Sterigmatocystin (ST), a precursor of AF, but this species lacks the final enzymatic activities (OmtA and OrdA) to convert ST to AF (Brown, et al., 1996). Many of the ST/AF genes have been identified and they were found clustered within a 75 kb chromosomal DNA region (Trail et al, 1995a; Woloshuck & Prieto, 1998; Payne & Brown, 1998; Bhatnagar et al., 2003)(Figure 1.2). These genes include *aflR*, a pathway specific regulatory factor of this gene cluster (Chang et al., 1993; Woloshuck et al, 1994), and many structural genes including *pksA* (Chang et al., 1995; Feng and Leonard, 1995), *fas1*, *fas2* (Mahanti et al., 1996; Trail et al., 1995), *nor-1* (Chang et al, 1992), *avnA* (Yu et al., 1997), *avf-1* (Prieto et al., 1996), *estA* (Yu et al., 2002), *vbs* (Silva et al., 1996), *ver-1* (Skory et al., 1992), *omtA* (Yu et al., 1993) and *orda* (Yu et al., 1998).

Expression of the AF genes appears to be co-regulated within the gene cluster. Most of the structural genes are activated under AF producing conditions and the timing of their expression is similar (Skory et al., 1993; Trail et al., 1995b; Brown et al., 1996). However at least one AF gene, *estA* (encodes an esterase activity that converts versiconal hemiacetal [VHA] to versiconal [VAL]), was recently reported to have a different expression pattern compared to other AF genes (Yu et al., 2002).

Regulation of AF biosynthesis. An important positive regulator of the AF biosynthetic pathway is AflR. This GAL4-type transcription factor contains a Cys₆Zn₂-type DNA binding domain and is required for biosynthesis of AF (Chang et al., 1995b; Ehrlich et al., 1999a; Ehrlich, et al., 2003). Many of the structural genes involved in AF biosynthesis such as *nor-1*, *ver-1*, and *omtA*, as well as *aflR* itself, contain the

Figure 1.2. Generally accepted pathway for sterigmatocystin and aflatoxin biosynthesis.
(Adapted from Bhatnagar et al., 2003)

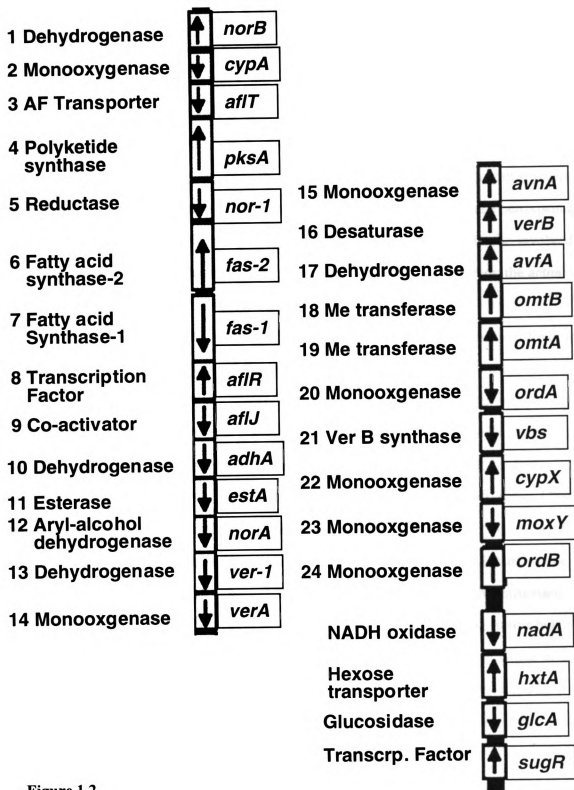


Figure 1.2

palindromic consensus AflR binding site (5'-TCGN₅CGR-3') in their promoter region and require AflR for expression (Ehrlich et al., 1999b). In addition to *aflR*, an adjacent gene *aflJ* possibly plays a role in regulation of AF biosynthesis. *aflR* and *aflJ* are divergently transcribed; both genes share part of the promoter regions (Meyer et al., 1998). Disruption of *aflJ* down-regulated AF production but the transcripts of other structural genes including *pksA*, *nor-1*, *ver-1*, and *omtA* were still present (Meyer et al., 1998). AflJ protein did not show any known sequence identity to other enzymes, yet its peptide sequence contains three putative membrane spanning domains and a peroxisomal targeting sequence, PTS1 (Meyer et al., 1998). Thus, AflJ was suggested to be involved in transport of AF proteins to specific targets (Meyer et al., 1998). However, the actual function of AflJ has not been identified.

It is not known why AF genes are clustered but the organization and coordination of expression of AF genes appears to be important (Trail et al., 1995b; Brown et al., 1996). In AF producing *Aspergillus* spp., the transcription factor AflR is an important positive regulator but AflR alone is not sufficient to regulate AF biosynthesis. Some *Aspergillus* spp., e.g. *A. sojae* and *A. oryzae* used in fermentation of foods, contain homologues of AF biosynthesis genes including *aflR* but they are not aflatoxigenic (Trail, 1995a). A 28-amino acid zinc finger binding domain located at the C-terminus of AflR (CTSCASSK-VRCTKEKPACARCIERGLAC) was present in *A. flavus*, *A. parasiticus*, *A. sojae*, and some strains of *A. oryzae* (Chang et al., 1995b). *aflR* and other structural genes such as *nor-1* and *ver-1* were present in some *A. sojae* and *A. oryzae* strains but they do not produce AF (Watson et al., 1999). Transcripts of the *aflR* homologue in the non-AF producing *A. oryzae* were also not detected under AF inducing conditions by reverse-transcription polymerase chain reaction (RT-PCR) (Kusumoto et al., 1998). Absence of AF biosynthesis in koji mold (*A. sojae*) was later confirmed to be caused by defects in *aflR* expression, resulting in lack of expression of AF related genes (Matsushima et al., 2001). In addition, some mutant strains contain an incomplete gene

cluster affecting gene expression and ST/AF production, and implicating a loss of functional regulation in these species (Cary, et al., 1999; Butchko, et al., 1999). These data also suggested that in addition to AFLR, other mechanisms appear to regulate biosynthesis of AF.

The cluster effects for expression of AF genes play an important role in AF biosynthesis. Significance of AF genes organized in a cluster was investigated as one major objective in my study (using *nor-1* gene as an example, Chapter 3). The results confirmed that the AF gene cluster exerts a positive position-dependent regulatory influence on the *nor-1* promoter (Chiou et al., 2002).

Partially-duplicated AF gene cluster. A second, partially-duplicated AF cluster was discovered in some strains of *A. parasiticus* (Liang et al., 1996; Chang and Yu, 2002). This partial AF gene cluster contains homologs of *aflR-aflJ-adhA-estA-norA-ver1* plus *omtB*, yet is missing *verA-avnA-verB-avfA*, *omtA*, *ordA*, and *vbs* present in the complete AF cluster in *A. parasiticus* strain 56775 (Fig. 1.2) (Chang and Yu, 2002). The truncated AF gene cluster contained several mutations and did not seem to be functional. Several structural genes were found to be defective, including pre-termination of *ver1B* (Liang et al., 1996) and *norA2*, point mutations in *adhA2*, and a large deletion in *omtB* (Chang and Yu, 2002).

Mutations were also found in the second copy *aflR* (*aflR2*), and a specific point mutation in nucleotide residue 896 (with a T to A substitution) can be used to discriminate between *aflR1* and *aflR2* (Cary et al., 2002). However, this mutation did not result in a pre-terminated gene product. *AflR2* was not able to activate transcription in a yeast two hybrid system (Cary et al., 2002), and it could not complement the loss of functional activity of the primary *AflR1* (Chang and Yu, 2002). An *A. parasiticus* *aflR* knockout mutant AFS10, was disrupted in *aflR1* but not *aflR2*. This strain did not produce AF, any precursors in the pathway, or transcripts of *aflR2* and other AF genes such as *nor-1*, *ver-1*, and *omtA* analyzed by Northern hybridization analysis. However,

using RT-PCR, the transcripts of *aflR2* and these AF genes were detected at low levels (Cary et al., 2002). The *aflR1* knockout strain AFS10 was used as a negative control in my AF protein localization studies (Chapter 4 and 5).

Sugar-utilization gene cluster. Downstream of the AF gene cluster following a 5 kb spacer region, a sugar utilization gene cluster consisting of 4 genes (*sugR*, *hxtA*, *glcA*, and *nadA*) was identified (Yu et al., 2000). Expression of *hxtA*, which encodes a hexose-transport protein, followed the same timing of expression under AF inducing conditions (glucose minimum salt medium) as AF genes such as *omtA* (Yu et al., 2002). This sugar utilization cluster, or the hexose-transporter HxtA specifically, may play a role in regulation of AF biosynthesis, since simple sugars, e.g. glucose, were found to induce AF biosynthesis (Buchanan and Lewis, 1984; Skory et al. 1993; Miller, 2003).

SECONDARY METABOLISM AND FUNGAL DEVELOPMENT

Association between secondary metabolism and fungal development. In *Aspergillus* as well as many other microorganisms, the production of secondary metabolites is frequently associated with developmental processes, e.g., sporulation (Bennett, 1983; Horinouchi et al., 1994, Guzman-De-Pena and Ruiz-Herrera, 1997; Adam and Yu, 1998; Adams et al., 1998; Calvo et al., 2002). The hypothesis is best supported by the gram-positive bacterial genus *Streptomyces* in which morphological differentiation resembles development of filamentous fungi. In *Streptomyces griseus*, secondary metabolism and formation of aerial mycelium, a structure required for subsequent generation of spores, are both triggered by a γ -butyrolactone containing molecule, A-factor (Horinouchi and Beppu, 1994; Kato et al., 2002).

G-Protein signaling pathway. In *A. nidulans*, coordinated regulation of asexual sporulation and biosynthesis of the mycotoxin sterigmatocystin (ST) has been demonstrated (Adams and Yu, 1998; Adams et al., 1998). The balance between vegetative growth, sporulation, and ST production is regulated by two antagonistic

factors, FadA (Fluffy Autolytic Dominant), and FlbA (Fluffy, Low brlA; *brlA* is a conidial vesicle specific gene) involved in a G-protein signaling pathway (Yu et al., 1996; Hicks et al, 1997)(Figure 1.3). The *fadA* gene encodes the G α subunit of a heterotrimeric G protein and activation of this gene facilitates cell proliferation and vegetative growth, while *flbA* encodes a RGS (Regulator of G protein signaling) domain that antagonizes the function of FadA. Inactivation of the FadA G protein signaling pathway is required for both ST biosynthesis and asexual sporulation (Hicks et al, 1997). Conversely, developmental activation requires at least partial inactivation of *fadA*. Dominant activating mutations of *fadA* as well as loss of function mutations of *flbA* resulted in inhibition of both conidiation and ST production. Conversely, overexpression of *flbA* or a dominant interfering mutation of *fadA* leads to precocious ST gene expression and ST accumulation, as well as unscheduled conidiation (Hicks et al, 1997).

FluG. Another factor FluG, acting up-stream of this G-protein linked pathway, is associated with synthesis of an extracellular, low molecular weight diffusible factor leading to asexual conidiation and ST production (Lee and Adams., 1994). Loss of function mutations in *fluG* resulted in a complete block in ST production and sporulation, similar phenotypes to loss of function mutations in *brlA* and dominant activation mutation in *fadA* (Hicks, et al., 1997). The FluG-dependent asexual sporulation pathway seems to be in competition with the vegetative growth pathway promoted by FadA. Whereas FadA negatively regulates ST biosynthesis, FluG is believed to promote ST production via inactivation of FadA signaling (D'Souza et al., 2001). The detailed mechanisms of this G-protein signaling pathway observed in *Aspergillus* are under investigation.

AF biosynthesis and conidiation. Secondary metabolites and conidiation are usually observed when cells enter the stationary phase of growth (Betina, 1995). In *A. flavus* and *A. parasiticus*, AF was detected in developmental structures including conidia

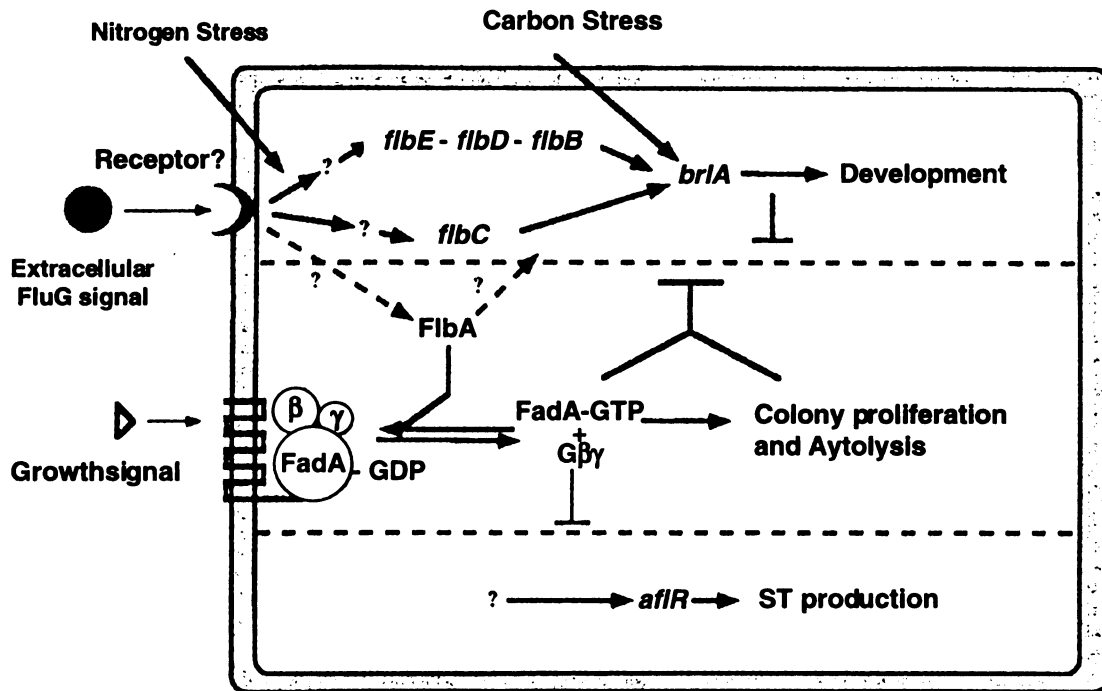


Figure 1.3. The G-protein signaling pathway involved in ST biosynthesis in *A. nidulans*.
(Adapted from Adams et al., 1998)

and sclerotia (Wicklow and Schotwell, 1983). *A. parasiticus* with a defect in *fluP*, a gene that encodes a large polyfunctional enzyme with sequence similarity to polyketide synthetases, did not develop conidiospores and AF production was reduced 3 to 5 fold compared to the wild type (Zhou et al., 1999). Production of ST/AF in *Aspergillus* spp. typically accompanies conidiation but the converse is not always true because ST/AF can be synthesized in liquid and submerged shake culture where conidiation does not usually occur (Kale et al. 1994). However, Guzman-de-Pena et al. (1998) indicated a lower level production of AF in liquid culture compared to AF production from the same mass of *A. parasiticus* grown on solid media with conidiation. Also, chemicals that suppress conidiation such as fluoroacetic acid (Reiß, 1982) and diaminbutanone, an ornithine decarboxylase inhibitor (Guzman-de-Pena et al., 1998) reduced production of AF in *A. parasiticus*.

LOCALIZATION OF PROTEINS INVOLVED IN AF BIOSYNTHESIS

One of the goals of my study was to determine where AF proteins are synthesized within a cell and to understand how these enzymatic activities associate with each other in order to make the final AF molecules.

Penicillin biosynthesis as an example. In *Penicillium chrysogenum*, biosynthesis of the secondary metabolite penicillin is similar to ST/AF biosynthesis in *Aspergillus* because penicillin biosynthetic genes are also organized in a cluster. Three gene products, ACVS (aminoadipyl-cysteinyl-valine tripeptide synthetase), IPNS (isopenicillin N-synthetase), and AT (acyl CoA: 6-iso-penicillin-N-acyltransferase) involved in penicillin biosynthesis have been isolated and localized (Muller et al., 1991). ACVS was thought to be associated with a Golgi-like organelle (Kuryłowicz et al., 1987) and vacuoles (Lenderfeld et al., 1993), but later was confirmed to be localized in the cytoplasm (Van der Lende et al., 2002). The second enzyme IPNS was also found to be a cytosolic protein (Van der Kamp et al., 1999; Van der Lende et al., 2002). By immuno-

transmission electron microscopy, only the final enzyme activity, AT, was found associated with microbodies (*aka.* peroxisomes) (Muller et al., 1995).

Organelles possibly involved in AF biosynthesis. This section reviews several organelles that may be associated with AF biosynthesis in *A. parasiticus*.

1) Microbodies. Microbodies (*aka.* peroxisomes) are found universally in fungi, but the number, shape and function are highly variable (Markham, 1995). Even within a species, generation of microbodies may be affected by various factors including age, developmental stage, and nutrient source. Microbodies contain a variety of enzyme activities and are potentially involved in a wide range of degradative and biosynthetic activities (Carson and Cooney, 1990). There are two types of microbodies with different enzyme activities. The peroxisome contains catalases and enzymes involved in fatty acid β -oxidation, while the glyoxysome houses the glyoxylate cycle and also enzymes involved in fatty acid β -oxidation (Keller et al., 1991). Microbodies are common in fungal spores, where they are associated with lipid inclusions (Maxewell et al., 1977).

Two types of Peroxisomal Targeting Sequence (PTS) have been identified. PTS1 is a carboxyl-terminal tri-peptide sequence Ser-Lys-Leu (SKL) and conserved variants (S/A/(C)(K/R/H)(L/M)(Gould et al., 1987). The second matrix protein targeting signal, PTS2, is an N-terminal nonapeptide motif with the consensus sequence (R/K)(L/V/I)X5-(H/Q)(L/A)(Subramani, 1996). However, many peroxisomal enzymes have neither a PTS1 nor a PTS2 motif (Waterham and Cregg, 1999). None of the AF proteins contains the conserved PTS1 or PTS2 located at the C-terminus or N-terminus, respectively. However, the PTS1 sequence was detected in AflJ, OmtA and OrdA, but not at the C-terminus (predicted by PSORT version 6.4).

2) Woronin bodies. Woronin bodies are highly refractile particles seen in over 50 species of filamentous fungi (Markam and Collinge, 1987; Jedd and Chua, 2000). This organelle is bounded by a single bilayer membrane and the major component is protein (Head, 1989). The Woronin body has a spherical to oval shape and the size is

approximately 0.1-0.75 μm , slightly larger than the septal pore (Markham, 1995; Markham and Collinge, 1987; Jedd and Chua, 2000).

Woronin bodies are usually located in the septa and have been suggested to function by plugging the damage within the septal pore in response to hyphal injury (Colling and Markham, 1985; Tenney et al., 2000). This function indicates that the Woronin body is capable of moving within hyphal cells, implying a possible role in transport of AF. The phytotoxin prehelminthosporol has been found localized in Woronin bodies in *Bioplaris sorokiniana* (Akesson, et al., 1996).

The Woronin body was suggested to be derived from peroxisomes in *A. nidulans* (Valenciano et al., 1998). A gene encoding a major Woronin body protein, *hex1*, was recently identified in *Neurospora crassa* (Tenney et al., 2000; Jedd and Chua, 2000). The Hex1 protein contains the C-terminal PTS1 sequence, suggesting a relationship between the woronin body and the peroxisome. In *Neurospora crassa*, Woronin bodies are associated with catalase-negative peroxisomes (Jedd and Chua, 2000).

3) Vesicles. Vesicles are small but they are important and very abundant in filamentous fungi (Markam, 1995). Vesicle sizes vary with diameters ranging from approximately 30 nm to 400 nm (Markam, 1995). A high density of vesicles is usually clustered in the hyphal apex; they are involved in transport of various structural proteins, enzymes, and other cellular components including lipids and polysaccharides (Markam, 1995). The vesicles are able to migrate through the septal pore and the movement is associated with microtubule components (Hoch et al, 1987). There are many types of vesicles such as wall vesicles, microvesicles, and chitosomes, with respect to their particular functions.

4) Vacuoles. Vacuoles are the largest organelles in eukaryotic microorganisms. The large vacuoles of fungi have many features similar to animal lysosomes. Fungal vacuoles, similar to higher plant vacuoles, are acidic compartments containing hydrolases and lysosomal activities (Klinlosky, 1997; Ashford, 1998); the acidic environment is

regulated by a vacuolar ATPase (Wada and Anraku, 1994). The functions of vacuoles are associated with intracellular homeostasis, storage of metabolites, and degradation of proteins (Thrumm, 2000). This organelle is also involved in intracellular protein transport such as endocytosis, protein secretion, and intracellular protein localization (Wendland et al., 1998). The structure and dynamic activities of fungal vacuoles indicate that this organelle has the capacity to interact and transport material over long hyphal distances (Ashfor, 1998).

Under the microscope, the vacuole appears as a large, hemi-spherical hollow-like, fluid-filled organelle surrounded by a single membrane (Markham, 1995; Ohsumi et al., 2001; Ohneda et al., 2002). Vacuoles are often observed in aged cells and they are not usually present in the active apical tip regions (Markham, 1995). Some large fungal vacuoles may contain small membrane-bound vesicles, which are derived from fusion of multivesicular bodies with large vacuoles (Hoch and Staples, 1983).

Over 40 vacuolar protein-sorting (*vps*) and vacuolar-morphology (*vam*) associated genes have been identified in *Saccharomyces cerevisiae* (Raymond et al., 1992). One vacuole resident protein, carboxypeptidase Y (CPY), has been used as a vacuole marker protein (Johnson et al., 1987). In *A. nidulans*, *cypA* that encodes CPY (Ohsumi et al., 2001), and *vpsA* involved in vacuolar biogenesis (Tarutani et al., 2001) have been cloned and characterized.

Klinonsky (1998) reviewed vacuole-related functions and suggested that of all the organelles, the vacuole may be the most adaptive compartment as a delivery mechanism. In fed-batch fermentation of *P. chrysogenum*, during the switch from the rapid growth to the production phase as nutrients became limited, a high degree of mycelial fragmentation was seen along with heavy vacuolation (Paul et al., 1994), implicating an association of vacuole biogenesis and secondary metabolism. In addition, immunogold-transmission electron microscopy localized OmtA, an enzyme involved in a late stage AF biosynthesis, in the cytoplasm as well as in the vacuole in cells located near the substrate surface of the

colony (Lee et al., manuscript submitted). In this regard, the vacuole is hypothesized to play a role in AF biosynthesis.

5) Endoplasmic reticulum (ER). The ER is a continuous membrane system, yet various domains are present in this single organelle that perform different functions (Markhem, 1995; Voeltz et al., 2003). The ER appears to make physical contact with the membranes of many organelles such as nuclei (nuclear envelopes) and vacuoles, and dynamic contact with cytoplasmic vesicles *via* the continuous traffic system (Beckette et al., 1974; Wedlich-Sölender et al., 2002). This organelle is involved in protein folding and several post-translational modifications in the ER lumen, and translocation of proteins (e.g. secretory proteins) across the ER membrane (Voeltz et al., 2003; Ellgaard and Helenius, 2003).

N-glycosylation of proteins along the secretory pathway is an important protein quality control mechanism. This proof reading system serves beyond the levels of transcription and translation to ensure native conformation of newly synthesized proteins and the fidelity of cellular functions (Ellgaard and Helenius, 2003; Roth, 2002; Helenius and Aebi, 2001; Parodi, 2000). After proteins reach their native tertiary and quaternary structure, they subsequently translocate to their final cellular destination. In general, the proteins involved in the secretory pathway are targeted to the plasma membrane, vesicles, or extracellular space for secretion (Roth, 2002; Ellgaard and Helenius, 2003). As part of the ER quality control, misfolded proteins are translocated from the ER to the cytoplasm and subjected to an ER-associated degradation (ERAD) process and subsequently destroyed by the 26S proteasome (Kostova and Wolf, 2003).

According to protein sub-cellular localization prediction programs listed in the ExPasy molecular server (<http://us.expasy.org>), proteins targeted to the ER usually require an N-terminal hydrophobic signal peptide and *N*-glycosylation site(s) (Asn-X-Ser/Thr) (Signal IP; Target P; NetGlyc 1.0; Ausubel et al., 2003). ER resident proteins further require an ER-retention signal, KDEL, within the C-terminal peptide sequence (Teasdale

and Jackson, 1996; Harter and Wieland, 1996). Among AF proteins, only VBS was confirmed to be *N*-glycosylated (Silva et al., 1996) and appeared to be modified in the ER (see Chapter 5). Based on protein sequence prediction, only one other protein, OrdA involved in the final step of AF biosynthesis, contains a putative N-terminal signal peptide and one *N*-glycosylation site, suggesting OrdA may be associated with the ER secretory pathway like VBS (ExPasy molecular server). Both proteins were not predicted to be ER resident proteins. Association of AF proteins along the ER secretory pathway may be significant to their protein functions, and possibly play a role in regulation of AF biosynthesis.

CONFOCAL LASER SCANNING MICROSCOPY (CLSM) IN THE STUDY OF FUNGAL BIOLOGY

Introduction to CLSM. Microscopy serves as an useful tool to conduct studies in cell biology including analyses of cell dynamics, morphogenesis, cytochemistry, fungal spore structure and development (Spear et al., 1999). Fungal cellular organelles can also be visualized; however, the resolution of light microscopy has limitations (theoretical maximum resolution is 0.2 μm) in traditional light microscopes (Paddock, 2000). In conjunction with fluorescence-based techniques such as immuno-fluorescence labeling as well as the recent application of the green fluorescent protein (GFP), fluorescence tagged cellular targets can be tracked by fluorescence microscopy. In the past, conventional epifluorescence microscopy has been widely used. Confocal laser scanning microscopy (CLSM) provides a wide range of advantages over traditional light microscopy (and epifluorescence microscopy) although CLSM is based on the fundamental principles used to light microscopes.

The first stage-scanning confocal microscope was invented in mid-1957 by Minsky for imaging of neural networks in unstained brain cells (Minsky, 1961; 1988). Modern confocal microscopes are based on the configuration of this prototype (with the

use of a pinhole) and an enhanced model became commercially available in 1987 after air-cooled lasers and PC computers and software became prevalent (Amos et al., 1987).

The characteristic feature of CLSM is the ability to generate "confocal images" that eliminate the interference of out-of-focus light captured by the detector. This confocal effect is achieved by use of a confocal pinhole positioned between the specimen and the detector in the light path (Figure 1.4). CLSM utilizes one or more focused beams of light illuminated by the laser (light amplification by stimulated emission of radiation) which scans across the sample generating "optical sections" at various focal planes. Thus, contrast and resolution are enhanced on each single optical section. This feature is particularly beneficial for viewing thick samples since CSLM is capable of scanning through specimens (up to hundreds of microns in thickness) instead of mechanical sectioning of samples and acquiring serial optical sections (Z-sections) (Whallon, 1998).

Image quality enhancement by CLSM. Since CLSM utilizes the basic configuration of the light microscope, the instrument resolution *per se*, that is influenced by the wavelength of light, the objective lens, and properties of the specimen itself, is not improved drastically (Paddock, 2001). However, the final image resolution of modern CLSM is improved by the following factors. First, stable multiple wavelength lasers instead of conventional tungsten-halogen and/or mercury lamps are used to generate bright point sources of light to scan the samples. Typically air-cooled lasers are used including the helium-neon laser emitting at 543 nm and 633 nm and the argon-ion laser emitting at 488 nm and 514 nm. The laser spot size affects instrument resolution; similar to scanning electron microscopy, the smaller the beam spot, the greater the resolution (Czymmeck et al., 1994). The spot size is also affected by the wavelength of light and numeric aperture (NA) of the objective lens ($D_{\text{resolution}} = 0.61 \times [\text{Wavelength}] / \text{NA}_{\text{objective}}$). For example, the spot size for the 488 nm laser with a high NA (1.4) lens is approximately 250 nm (Czymmeck et al., 1994). In addition, a laser focused to a small

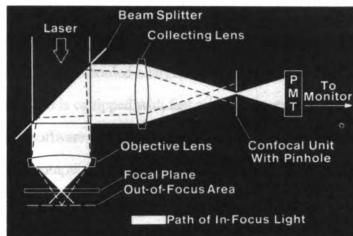


Figure 1.4. Diagram of the light path in a confocal instrument. (Adapted from Czymmek et al., 1994)

point (as equipped in the CLSM models; Zeiss 210 and Zeiss LSM5 PASCAL, Carl-Zeiss Inc., Germany) generates better resolution than a laser focused through a slit (as equipped in Meridian Insight[®], Meridian Instrument, Inc., Okemos, Mich.). Theoretical resolution of CLSM under 488 nm excitation with a 1.4 NA oil objective was estimated to be 160 nm (Brelje et al., 1993) and approximately 130 nm under ideal conditions (Carlsson and Aslund, 1987).

Second, image detection in modern confocal microscopes utilizes sensitive and low noise detectors (e.g., photomultiplier tube (PMT) or a digitized charge-coupled device (CCD) camera, particularly the cooled-charged CCD with reduced noise read out. In addition, advanced CLSM is equipped with fast microcomputers with image processing capability and elegant software to analyze images. High quality output images can be processed directly in a computer imaging system or recorded on hard copy devices (Poddock, 2001). Advanced image analysis programs also allow CLSM digitized images to be processed further, for example, reconstruction of three-dimensional (3-D) images from Z-stacks (Czymmek et al., 1994), or pixel analysis to quantify fluorescence intensity (Spear et al., 1999; Chapter 5 in this dissertation).

CLSM imaging. CLSM is capable of generating many types of microscopic images. General light microscopy applications, such as phase contrast, polarization, and differential interference contrast (DIC), can be conducted via CLSM with enhanced image qualities. However, an important feature of CLSM is detection of fluorescence. The characteristic functions are described as follows.

1) Optical sections. The basic unit of confocal microscopy is the single optical section (confocal image). The contrast of an optical section is enhanced more intensely than non-confocal images generated by epi-fluorescence microscopy.

2) Z-series. For one specific field of interest, several optical sections can be collected as a series to generate a-Z-stack. The CLSM is commonly equipped with a stepping motor to control the movement of the stage with a pre-determined distance (step

size). Using a macro program, CLSM can acquire images from the top (or from the bottom) of a specimen, scan through the sample with a pre-set step size, and acquire as well as store the whole series of optical sections on the hard drive to generate a Z-series (Z-stack). The Z-series can be further processed into a 3-D presentation, stereo images, or viewed as a movie depending on the program capabilities. A representative Z-series of *A. parasiticus* SU-1 conidiophores stained with SYTOX green nuclear staining dye (Molecular Probes, Eugene, OR) is shown in Fig. 1.5.

3) *Phi-z* sectioning. Optical sectioning is not limited to the horizontal focal plane but also can be collected in the vertical plane to generate a *phi-z* or *x-z* section. *Phi-z* sectioning is accomplished by scanning the laser across a defined single line. It allows signals to be detected from another angle of view. For example, the microbodies of *A. parasiticus* SU-1 immuno-labeled with anti-SKL antibodies followed by secondary antibodies conjugated with Alexa 488 probe are displayed in a single optical section (Fig. 1.6, A). Analysis by *phi-z* scanning indicated that several microbodies are located inside the hyphae (Fig. 1.6, B).

4) Time-lapse and live imaging. Since CLSM is capable of scanning through the sample without mechanical sectioning, live cells may be studied. This application may be somewhat difficult to accomplish, for example, if the experiment requires fixation of the cell, or if the target signals are not stable under illumination by the laser. In addition, the position of the specimen has to be maintained under the microscope. Nevertheless, time-lapse imaging allows visualization of dynamic events at a rate close to realtime or video-rate imaging (Whallon, 1998).

5) Fluorescence imaging. CLSM is a powerful tool for fluorescence imaging. The argon-ion laser emits at 488 nm and generates optimum excitation spectra for many commonly used fluorescence probes, including FITC (fluorescein isothiocyanate (*Abs/Em* 490/523 nm), Alexa 488 (*Abs/Em* 495/519 nm), the red-shift green fluorescent protein

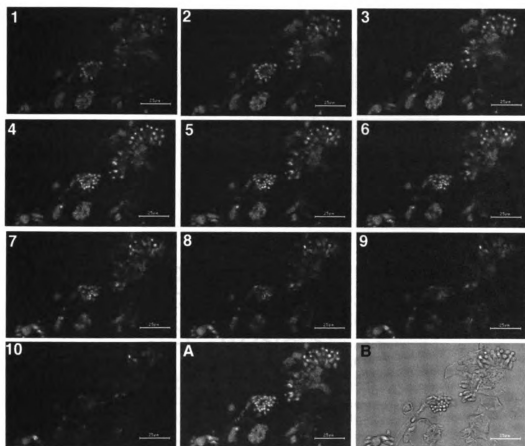


Figure 1.5. CLSM Z-series of *A. parasiticus* SU-1 conidiophores stained with SYTOX green fluorescence dye. Fungal thin sections (4 µm) derived from colony fraction S2 (24-48 h growth) of a 72 h-old SU-1 colony grown on YES agar were stained with SYTOX green dye (Molecular Probes). (1) - (10): Ten optical sections with step size (z section interval) 750 nm. (A) An extended focus image of this CLSM Z-stack. (B) A bright field image in the middle of the Z-stack. Bars, 25 µm.

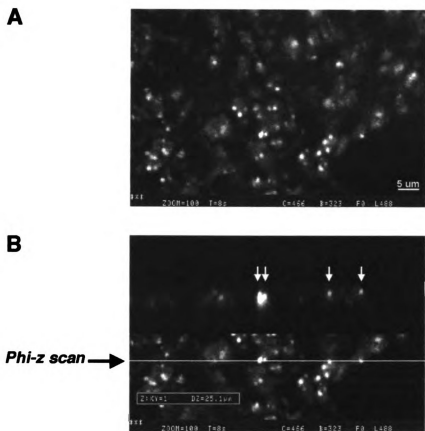


Figure 1.6. CLSM single optical section and *phi-z* scan of *A. parasiticus* SU-1 microbodies. Fungal thin sections (4 μm) derived from colony fraction S2 (24–48 h growth) of a 72 h-old SU-1 colony grown on YES agar were immuno-labeled with anti-SKL antibodies (Zymed) followed by secondary antibody conjugated with Alexa 488 probe (Molecular Probes). CLSM was performed using a Zeiss 210 confocal scanning microscope (Carl Zeiss Inc.). (A) Single optical section. (B) *Phi-z* scan. The arrows indicate the location of microbodies inside the cell. Bar, 5 μm .

variant, EGFP (*Abs/Em* 488/507 nm), and a nuclear staining dye, SYTOX green (*Abs/Em* 504/523 nm). CLSM can also perform multiple fluorescence detection, for example, dual channel detection of green and red fluorescence on the same image (Chapter 5, Fig. 5.9). This is particularly useful if these fluorophores have minimum overlapping emission spectra to avoid cross-talking signals. Mixed krypton-argon gas lasers are popular for multiple-wavelength confocal microscopy because they emit at three well-separated wavelengths (488 and 568 and 647 nm) allowing detection of green to far-red fluorophores (e.g. FITC; Lissamine rhodamine B, *Abs/Em* 570/590 nm; Cy5, *Abs/Em* 649/666 nm)(Ausubel et al., 2003). However, some fluorophores excite at shorter waves (e.g., DAPI [4,'6-diamidino-2-phenylindole, *Abs/Em* 458/461 nm] nuclear stain, and CMAC [7-amino-4-chloromethylcoumarin, *Abs/Em* 353/466 nm] vacuolar stain); detection of these probes requires CLSM equipped with expensive UV lasers.

Photobleaching may cause significant problems for fluorescence detection, particularly when samples are illuminated with high intensity lasers. It is a quenching phenomenon that causes fading of fluorescence signals, yet the mechanism is not fully understood. One important class of bleaching is photodynamics and this involves interaction of fluorophores with light and oxygen. The amount of photodamage depends on the concentration of molecular oxygen and the distance between the fluorophore, molecular oxygen and other cellular constituents (Herman, 1998). Protection against photobleaching can be achieved by reducing excitation energy or exposure time; however, this will also reduce the yield of the signal. Other methods to prevent photobleaching include deoxygenation of solutions; use of singlet oxygen quenchers such as histidine, diphenylisobenzofuran, or crocetin (a water soluble acratenoid); or antifade reagents such as *n*-propyl-gallate. Several antifade mounting media are also commercially available (e.g. Vectashield [Vector] and Prolong antifade mounting media [Molecular Probes]).

In summary, CLSM is capable of generating higher contrast and resolution images compared to traditional light microscopy by reducing background interference significantly. Advanced image detection systems and analysis programs render this instrument more capable of analyzing cellular structures or other aspects in detail. In this dissertation, CLSM is an important tool to study localization of proteins involved in AF biosynthesis in the filamentous fungus *A. parasiticus* (Chapter 4 and 5).

CHAPTER 2

A rapid DNA extraction method for screening large numbers of *Aspergillus* transformants via polymerase chain reaction

ABSTRACT

The efficiency of screening fungal transformants using available methods, particularly in large quantity, has been a problem in fungal molecular biology. A rapid DNA extraction method was developed for screening *Aspergillus* transformants via polymerase chain reaction (PCR). Fungal cells were collected directly from colonies on a culture plate into microcentrifuge tubes containing TE buffer (10 mM Tris-HCl, 1.0 mM EDTA, pH 8.0). The cell suspension was boiled for five minutes to release nucleic acids. After a brief centrifugation step (12,000 g for 5 min), fungal cell extracts (supernatant) were obtained. PCR of diluted fungal extracts with appropriate primers resulted in amplicons up to 2.5 kb with *Taq* DNA polymerase and up to 3.5 kb with *PfuTurbo* DNA polymerase. The procedure was successfully utilized for amplification of native fungal genes as well as identification of the integration site of plasmid sequences after homologous recombination.

INTRODUCTION

Fungal transformation provides an important tool for the study of fungal biology. However, limited numbers of transformants can be screened conveniently due to labor-intensive assay procedures. The presence of the fungal cell wall limits the efficiency of genomic DNA isolation. Disruption of the fungal cell wall to release nucleic acids is usually accomplished by the laborious procedure of grinding under liquid nitrogen. DNA purification also commonly includes proteolytic enzyme digestion, phenol/chloroform extraction, and precipitation of DNA (Ausubel et al., 2003; Borgia et al., 1994). The quantity and quality of the genomic DNA isolated by these procedures tends to vary

significantly. A high content of polysaccharides and nucleases represent significant obstacles for obtaining high quality fungal genomic DNA. Hence, my goal was to develop a rapid, inexpensive, and efficient DNA extraction method for screening large numbers of fungal transformants.

I present a simple procedure to obtain crude DNA templates directly from fungal colonies that was successfully used to amplify endogenous fungal genes as well as to detect the integration site of plasmid sequences after homologous recombination. Twenty-four fungal colonies can be easily assayed in a three to four hour period including time for PCR and electrophoretic analysis.

MATERIAL AND METHODS

Aspergillus parasiticus CS10 (*wh-1, ver-1 pyrG*) (Skory et al., 1990) was transformed with plasmid pAPGUSNP (Fig. 2.1, A) and the transformants were selected on Czapek-Dox medium (CZ medium, Difco) for ability to synthesize uridine monophosphate. As soon as the prototrophic transformants sporulated (approximately 2 days), spores were transferred onto duplicate CZ plates with a toothpick. After three days (or as soon as colonies could be observed), colonies were analyzed. A sterile 200 μ l plastic pipette tip (Lee and Cooper, 1995) was used to transfer a portion of the fungal colony (including conidiospores and mycelia) into a microcentrifuge tube containing 100 μ l TE buffer (10 mM Tris-HCl, 1.0 mM EDTA, pH 8.0). This process was repeated up to three times to ensure that sufficient fungal cells were transferred. Tubes were heated in a boiling water bath for 5 min and placed on ice. The samples were centrifuged at 12,000 g for 5 min at 4°C. The supernatant (fungal extract) containing crude DNA templates was transferred into a new microcentrifuge tube. The extract was further diluted with TE buffer (undiluted, 1/5, 1/20, 1/100). In most assays, 2.5 μ l of the 1:5 dilution resulted in good amplification in a 50 μ l PCR reaction. The remainder of the fungal extract was

stored at -80°C and could be successfully analyzed by PCR for at least three months.

Diluted samples stored at 4°C could be analyzed by PCR for at least one week.

PCR analysis was conducted on DNA extracted from *A. parasiticus* transformants and the recipient strain, CS10. Four primer pairs were used in the assay (Table 2.1). Primer pair JL136 and JL137 produced a 1.4 kb exon II fragment from the fungal gene encoding versicolorin B synthase (*vbs*) (Silva et al., 1996). Three primer pairs, JL99 and JL100, JL102 and JL103, JL221 and JL222 were designed to determine the integration site of pAPGUSNPyrG in the 5' region of *nor-1*, in the 3' region of *nor-1* or at the *pyrG* locus respectively. One primer from each pair targeted a sequence located within the fungal genome. The other primer targeted one site within the plasmid sequence (Figure 2.1).

A 50 µl PCR reaction mixture consisted of 2.5 µl of the diluted fungal extract, 20 mM Tris-HCl pH 8.8, 10 mM KCl, 10 mM (NH₄)₂SO₄, 0.1% Triton X-100, 0.1 mg/ml BSA, 0.5 - 1.0 µM of each primer, 200 µM each dNTP, 2.0 - 3.0 mM MgCl₂ and either 2.5 units of *Taq* thermal stable DNA polymerase (5 U/µl, Gibco BRL) or 2.5 units of *PfuTurbo* DNA polymerase (2.5 U/µl, Stratagene). PCR cycling parameters were adjusted depending on primer design and the target size (Table 2.1). PCR was performed in a Perkin-Elmer GeneAmp System 9600 thermal cycler. All PCR reactions were initialized by a denaturation step at 95°C for 3 min followed by 35 cycles of denaturation, annealing and extension. Reactions were terminated with an extension reaction at 72°C for 10 min. PCR products (10 µl of reaction) were observed by electrophoresis on a 1% agarose gel using standard procedures (Ausubel et al., 2003).

RESULTS AND DISCUSSION

DNA was extracted by the boiling procedure from seven representative transformants and the recipient strain, CS10 (Figure 2.2). The DNA was analyzed by PCR with appropriate primer pairs. A 1.4 kb fragment was generated from all eight

Table 2.1. Primer sequences and PCR cycling parameters used for analysis of fungal genomic DNA templates.

Primer	Target	Primer Sequence	PCR cycling parameters
Endogenous vbs ExonII			
JL136	1.4 kb	5' AGG CTC GAA AGG CGC ATA CGA 3'	95°C 1', 66°C 1', 72°C 2'
JL137		5' GTG GTC TAC TGC CCA GCC ATC 3'	
Integration of pAPGUSNP, 3' region of <i>nor-1</i> gene			
JL102	2.1 kb	5' CGC AAG GTG AGG GTT CGA ACC GAG G 3'	95°C 1', 65°C 1', 72°C 3'
JL103		5' CCG CAG CAG GGA GGC AAA CAA TGA A 3'	
Integration of pAPGUSNP, 5' region of <i>nor-1</i> gene			
JL 99	3.2 kb	5' TTT CAC GGG TTG GGG TTT CTA CAG G 3'	95°C 1', 62°C 1', 72°C 5'
JL100		5' GAC GGG GAA CCT CTT TAC AAA CAT C 3'	
Integration of pAPGUSNP at <i>pyrG</i>			
JL221	3.5 kb	5' CCA GAA AAT GCG AAG GTA AGT GCT TC3'	95°C 1', 55°C 1', 72°C 5'
JL222		5' GCG ACA CGG AAA TGT TGA ATA CTC AT3'	

Figure 2.1. Homologous recombination of pAPGUSNP into the *A. parasiticus* chromosome and primers used in integration analysis. (A) Plasmid map of pAPGUSNP. (B) pAPGUSNP integrated within the 5' region of the *nor-1* gene generates a 3.2 kb PCR fragment using primers JL99 and JL100. (C) pAPGUSNP integrated within the 3' region of the *nor-1* gene generates a 2.1 kb PCR fragment using primers JL102 and JL103. (D) pAPGUSNP integrated at the *pyrG* locus generates a 3.5 kb PCR fragment using primers JL221 and JL222. (E) Amplification of endogenous *vbs* gene fragment in *A. parasiticus* using primers JL136 and JL137.

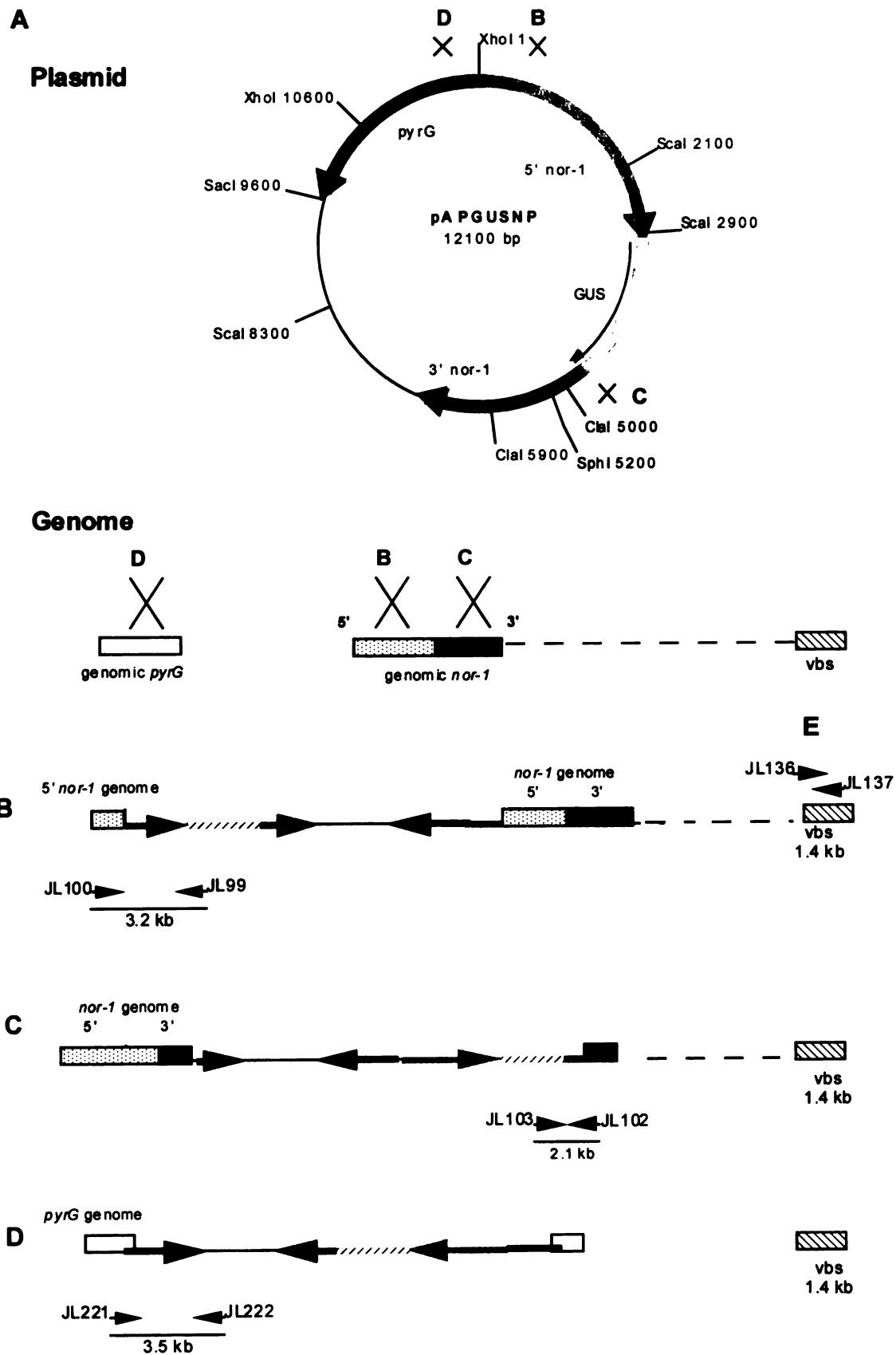


Figure 2.1

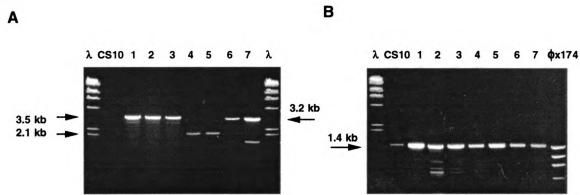


Figure 2.2. Amplification of PCR targets using the rapid DNA extraction technique.

The assay was performed on eight *A. parasiticus* colonies, including the host strain, CS10, and seven representative transformants. (A) Integration analysis using various primer sets. Cell extracts of CS10, and transformants 100, 149, 164 were PCR amplified with primers JL221 and JL222. A 3.5 kb target fragment was produced in transformants 100, 149, 164 (Lanes 1-3) but not the host strain CS10. PCR of cell extracts from 57 and 104 (Lanes 4-5) with primers JL102 and JL103 produced a 2.1 kb fragment. PCR of cell extracts from transformants 17 and 24 with primers JL99 and JL100 generated a 3.2 kb fragment (Lanes 6-7). All DNA extracts produced the endogenous 1.4 kb *vbs* fragment with primers JL136 and JL137 (shown in B).

strains from the endogenous *vbs* gene (Figure 2.2, B). Using the same fungal extracts, the three sets of primer pairs for integration analysis successfully determined the integration sites of pAPGUSNP within the genome in the transformants (Figure 2.2, A). With primer pair JL221 and JL222, PCR amplification of cell extracts from transformants 100, 149 and 164 (Lanes 1-3) produced a 3.5 kb PCR product, indicating that the plasmid integrated at the chromosomal *pyrG* locus while PCR amplification of cell extracts from the host strain CS10 did not generate this fragment. PCR amplification of cell extracts from transformants 57 and 104 (Lanes 4 and 5) produced a 2.1 kb fragment with primer pair JL102 and JL103, indicating integration of pAPGUSNP within the 3' region of the *nor-1* gene while cell extracts of transformants 17 and 24 (Lanes 6 and 7) produced a 3.2 kb fragment indicating integration within the 5' region of the *nor-1* gene. The integration location of pAPGUSNP in each strain was confirmed by Southern hybridization analysis (data shown in Chapter 3). After demonstrating the utility of this DNA extraction procedure, over 500 transformants were screened. The assay correctly identified the site of integration in over 80% of the transformants.

Several genomic DNA extraction methods for plant tissues and fungi were developed to simplify the extraction procedure and to allow large numbers of samples to be analyzed. However, these methods still have some drawbacks. For example, some procedures applied to fungi (Cenis et al. 1992) and plant tissues (Steiner et al. 1995) required mechanical grinding of tissues for isolation of DNAs. Alternatively, cell disruption was achieved by temperature extremes in *Podospora anserina* (Lecellier and Gael 1994) or by alkaline lysis in *Neurospora* and *Aspergillus* to prepare DNA for dot blot analysis (Min et al. 1995). DNA extracted from whole colonies of yeast cells treated with NaOH was used directly in PCR (Wang et al. 1996), but the method could not reliably amplify targets greater than 600 bp (Steiner et al. 1995).

The fungal cell wall can also be digested by specific enzymes to facilitate release of nucleic acids. For example, yeast cells were treated with zymolase (Ling et al. 1995)

and the filamentous fungus *Aspergillus niger* was treated with Novozyme 234 (Zeijl et al. 1998). Both assays could amplify targets up to 3 kb. However, these methods utilized costly enzymes, which require additional time for preparation and cell wall digestion.

A rapid spore PCR assay that used conidiospores of *Aspergillus fumigatus* directly from culture plates for screening gene disruption events has been reported (Aufauvre-Brown et al. 1993). Low numbers of *Magnaporthe. grisea* spores (10^4 - 10^6) were also used directly in PCR without extraction of DNA (Xu and Hamer 1995). Spores from five strains of filamentous fungi were treated with microwave irradiation to facilitate release of DNA into the supernatants (Ferreira and Glass 1996). However, it is important to note that these direct spore PCR methods could only amplify PCR targets smaller than 1 kb. Attempts to produce a 1.4 kb PCR fragment using the direct PCR methods described above were not successful.

The fungal DNA extraction procedure presented here is simple and effective. Only a small quantity of the fungal cells must be acquired directly from the culture plates eliminating the need for extended culture. Fungal colonies grown for 48 h to 72 h were easily analyzed. Alternatively, colonies could be replicated onto several assay plates reducing the growth time to less than 36 hours. I observed that too much material could introduce a high level of contaminants for PCR, reducing effectiveness. This problem was overcome in most cases by increasing the dilution of the sample prior to PCR analysis.

The initial version of our rapid DNA extraction utilized sonication to release DNA. Sonication has been used successfully with other cell types, e.g. bacterial cells (Ausubel et al. 2003). In our laboratory, conidiospores of *Aspergillus parasiticus* SU-1 (2×10^7 spores/ml) were disrupted by sonication (output control level 4, 10 pulse x 4 cycles, SONIFIER[®] cell disruptor W-350, Branson Sonic Power Co.). An increase in optical density at 260 nm ($A_{260} = 0.34$) suggested the release of nucleic acids into the lysates. High temperature treatment of cell lysates was attempted to inactivate cellular

nucleases and other PCR inhibitory factors. However, when the efficiency of sonication, boiling, and a combination of the two to release DNA was tested (A_{260} = 0.701, 0.962, 0.989 respectively), the boiling process by itself resulted in the effective release of nucleic acids. Both procedures provided DNA templates for PCR amplification (data not shown). However, the boiling method was nearly as effective and did not require expensive equipment.

Boiled fungal lysates may still contain PCR inhibitory factors which cannot be heat inactivated. This problem can be minimized by diluting the extracts with TE buffer to the point where sufficient DNA templates remain while minimizing the level of inhibitors. In our hands, a 2.5 μ l aliquot from the 1:5 dilution of the fungal extract worked well in the 50 μ l PCR reaction. Dilution of the original cell extract of transformants generated from other fungal species may have to be adjusted appropriately.

Success of PCR amplification also depended on the reaction conditions (e.g., optimum $MgCl_2$ concentration, proper annealing temperature and extension time). I observed that the activities of specific thermal stable DNA polymerases played an important role in determining success of amplifying long target fragments. *Taq* polymerase (Gibco BRL) inconsistently amplified targets up to 2.5 kb using this DNA extraction procedure. Addition of PCR adjuncts and stabilizers such as BSA (10-100 μ l/ml) and DMSO (1-10%) (Stratagene manual) had limited effects on enhancement of product yield. However, *PfuTurbo* polymerase (Stratagene) efficiently amplified target fragments up to 3.5 kb. Longer targets were not tested in this assay.

Conditions for sample storage also play a role in determining success of the analysis. In our hands, fungal colonies on plates could be stored at 4°C for at least a week before analysis. Once samples were collected into TE buffer, fungal extracts (supernatants) could be used for up to one week of storage at 4°C and up to three months of storage at -80°C. However, the sooner the extracts were used, the better the results. Preparation of fungal extracts for only 10 to 12 samples at one time is recommended.

This appears to reduce degradation of nucleic acids which occurs during sample preparation.

This rapid DNA extraction method for PCR analysis provides an easy, inexpensive, convenient and efficient assay procedure for screening a large number of *Aspergillus* transformants and may be applicable to a wide variety of other fungal genera. This rapid procedure to prepare DNA templates from fungal colonies provides sufficient purity for PCR analysis of the site of plasmid integration into the *A. parasiticus* genome (Chiou et al., 2002). This development was critical for current and future studies on the regulation of the AF promoters (such as *nor-1* and *ver-1*) because detection of the correct site of integration in the genome is essential to accurately measure environmental influences on the aflatoxin gene promoters. In this regard, the speed and effectiveness of the rapid assay makes screening of large numbers of fungal transformants practical.

ACKNOWLEDGEMENTS

Special thanks to David Wilson, a former student working in the laboratory, for providing the primers to analyze the plasmid integration sites at *nor-1* by PCR.

This rapid DNA isolation/PCR method is published as part of the data in a manuscript "Chiou, C. H., M. M. Miller, D. L. Wilson, F. Trail and J. E. Linz. 2002. Chromosomal location plays a role in regulation of aflatoxin gene expression in *Aspergillus parasiticus*. Appl. Environ. Microbiol. 68:306-315".

CHAPTER 3

Position-dependent regulation of the *nor-1* promoter in the aflatoxin gene cluster

ABSTRACT

Expression of most of the AF genes within the 75 kb gene cluster in *Aspergillus spp.* appears to be co-regulated but the mechanism is not yet clear. I hypothesized that regulation of AF genes is cluster position-dependent; i.e., AF genes are positively regulated within the AF gene cluster. In this study, the *nor-1* gene that encodes norsolorinic acid reductase, an early AF pathway enzymatic activity, was used as a study model. Promoter activity of *nor-1* was compared within the AF gene cluster (*nor-1* locus) and outside the cluster (*pyrG* locus). A plasmid pAPGUSNP containing the *nor-1* promoter sequence fused to a reporter gene (*uidA*, β -glucuronidase, GUS) plus a selectable marker (*pyrG*) was constructed to study positional effects on *nor-1* promoter function. Transformation of pAPGUSNP into CS10 (*ver-1*, *wh-1*, *pyrG*) resulted in homologous recombination at 5' *nor-1*, 3' *nor-1*, or the *pyrG* locus. The plasmid integration site was screened by a rapid DNA extraction/PCR assay and confirmed by Southern hybridization analysis. GUS reporter activity was analyzed by a solid-culture GUS assay. Among 178 transformants analyzed, 42 transformants showed positive GUS activity (24.0%). Based on a rapid PCR assay, random selection of 14 GUS⁺ transformants indicated that plasmid integration occurred within the *nor-1* gene (11 within 5' *nor-1* and 3 within 3' *nor-1*). Southern hybridization analysis confirmed that of 10 GUS⁺ isolates analyzed, they all harbored pAPGUSNP within the *nor-1* locus (7 at 5' *nor-1*; 2 at 3' *nor-1*; 1 showed multiple integration at both sites). None of the 11 transformants that harbored the *nor::GUS* fusion at the *pyrG* locus expressed detectable GUS activity. The results agree with previous observations that reduced *ver-1* and *nor-1*

promoter activity is expressed at *niaD* (encodes nitrate reductase). These data support our hypothesis that expression of AF genes is cluster position-dependent.

INTRODUCTION

Many of the genes involved in aflatoxin (AF) biosynthesis in *Aspergillus spp.* have been identified and they were found clustered within a 75 kb chromosomal DNA region (Trail et al., 1995; Payne and Brown. 1998; Woloshuck and Prieto, 1998.). Expression of these genes appeared to be coordinately regulated although details of the regulatory mechanism are not yet clear.

The *nor-1* gene in the filamentous fungus *Aspergillus parasiticus* encodes a ketoreductase activity that converts norsolorinic acid (NOR), the first stable intermediate in the AF biosynthetic pathway, to averantin (AVN) (Trail et al., 1994; Zhou and Linz, 1999). The *nor-1* gene is expressed under AF inducing conditions, concurrent with many other AF genes (Skory et al., 1993; Zhou and Linz, 1999). The timing of *nor-1* expression and protein accumulation was consistent with the accumulation of AF (Skory et al., 1993).

Previously, Liang et al. (1997) reported preliminary evidence that the organization of AF genes in a cluster may play a role in regulation of AF biosynthesis. The *ver-1* promoter, which drives expression of a gene encoding a ketoreductase activity involved in a middle step of AF biosynthesis, was fused to *uidA* (encodes β -glucuronidase; GUS) to generate a reporter plasmid, pHD 6.6, containing *niaD* (encodes nitrate reductase) as a selectable marker. pHD6.6 was transformed into *A. parasiticus* NR-1 (*niaD*) resulting in integration predominantly at the *ver-1* or *niaD* locus via homologous recombination. Single copy integration of pHD6.6 at *niaD* resulted in a 500-fold reduction in *ver-1* promoter activity when compared with single copy integration at the *ver-1* locus. Similar results have been shown for two *nor::GUS* constructs located at *niaD* and the *nor-1* locus (Wilson, 1998; Chiou et al., 2002; Miller, 2003). GUS reporter activity was detected at

high levels when the *nor-1* promoter was positioned at the *nor-1* region within the AF gene cluster but was not detected at *niaD*. However, in *A. parasiticus*, *niaD* expression is under the control of nitrogen catabolite repression mediated by *areA* and the pathway specific induction of *nirA*. In the presence of nitrate, *niaD* is positively regulated. On the other hand, nitrate has been shown to down regulate AF biosynthesis (Payne and Brown, 1998). Lack of *ver-1* and *nor-1* expression at *niaD* could have resulted from *niaD*-dependent regulation.

In this study, *nor-1* promoter activity expressed at another chromosomal locus, *pyrG*, was investigated. The *pyrG* gene encodes orotidine monophosphate (OMP) decarboxylase that converts OMP to uridine monophosphate (UMP), a compound essential for cell growth (Skory et al., 1993). Unlike *niaD*, expression of *pyrG* has not been reported to be associated with regulation of AF biosynthesis. In this study, a plasmid (pAPGUSNP) containing four major DNA fragments was constructed. This plasmid includes the 5' *nor-1* fragment (upstream promoter sequences of the *nor-1* gene), a GUS reporter (obtained from the *Escherichia coli uidA* gene which encodes β -glucuronidase), the 3' *nor-1* fragment (the *nor-1* terminator and down stream sequences), and a selectable marker *pyrG*. Transformation of pAPGUSNP into *A. parasiticus* CS10 (*ver-1*, *wh-1*, *pyrG*), an uridine auxotroph, resulted in homologous recombination of pAPGUSNP into 5' *nor-1*, 3' *nor-1* or *pyrG* locus. The plasmid integration site was screened by a rapid DNA extraction/PCR assay and confirmed by Southern hybridization analysis. GUS activity was analyzed by a solid culture GUS assay. The results showed that the *nor-1* gene was positively regulated only when the promoter was positioned at its native localization (*nor-1*). When the *nor-1* promoter was placed outside the cluster (at *pyrG*), expression of *nor-1* was reduced dramatically. This result was in agreement with our previous studies on positional effects at *nor-1* and *niaD* (Wilson, 1998; Miller, 2003). These data provide strong support for the hypothesis that the AF gene cluster exerts a positive position-dependent regulatory influence on the *nor-1* promoter.

MATERIALS AND METHODS

Strains and growth conditions. *Escherichia coli* DH5 α F^c [F'/*endA1 hsdR17* (r_k⁻ m_k⁻) *supE44 thi-1 recA1 gyrA* (Nal^r) Δ *relA1* (*lacZYA argF*)_{u169}: (m80 Δ *lacZ M15*) (Gibco BRL, Life Technologies Inc., Rockville, MD) was used to amplify plasmid DNA using standard procedures (Ausubel et al., 2003). *A. parasiticus* CS10 (*wh-1, ver-1, pyrG*) (Skory et al., 1990) was derived from *A. parasiticus* ATCC 36537 (*wh-1, ver-1*) by nitrosoguanidine mutagenesis and was used as a recipient for the reporter construct carrying the *pyrG* selectable marker (pAPGUSNP). To grow the recipient strain CS10, YES medium or Czapek Dox medium (CZ, Difco, Detroit, MI) was supplemented with uridine (100 μ g/ml).

Construction of pAPGUSNP. Plasmid pAPGUSN (Fig. 3.1, A) contains the *nor-1::GUS* backbone and was generated by Dr. Frances Trail, Department of Botany and Plant Pathology, Michigan State University. The 5' *nor-1* fragment (3.0 kb) contains flanking sequences, promoter, and nucleotides encoding the first 21 amino acid residues of Nor-1. This fragment was fused in frame to a 1.8 kb GUS reporter (β -glucuronidase) derived from *E. coli uidA*. The 3' *nor-1* fragment (2.0 kb) contains nucleotide sequences encoding the last 6 amino acids of Nor-1, the transcription terminator, and flanking sequences. To generate pAPGUSNNP, pAPGUSN was digested with *NheI* and the ends filled-in with Klenow fragment of DNA PolI (Roche Molecular Biochemicals, Indianapolis, Ind.). The 2.5 kb *pyrG* gene was amplified by PCR with *Taq* DNA Polymerase (Gibco BRL, Rockville, MD), pPG3J (Skory et al., 1990) as template, and appropriate primers (5'-GTAGAAGTTGTTTCAGTAGCTGATGG-3' and 5'-CGAGTATCACAGTCAGGACTCCACG-3'). The resulting PCR fragment was end-

Figure 3.1. Restriction endonuclease maps of plasmids containing the *nor-1::GUS* construct related to this study. Only restriction endonuclease sites relevant to this study are shown. (A) pAPGUSN contains the *nor-1::GUS* backbone (generated by Dr. Trail, Department of Botany and Plant Pathology, Michigan State University). (B) pAPGUSNP contains the *nor-1::GUS* fusion plus the *pyrG* selectable marker (Chiou, this study). (C) pAPGUSNNB contains the *nor-1::GUS* fusion plus the *niaD* selectable marker (generated by Wilson, 1998). (D) pBGN3.0 contains the *nor-1::GUS* fusion plus the *niaD* selectable marker (generated by Miller, 2003).

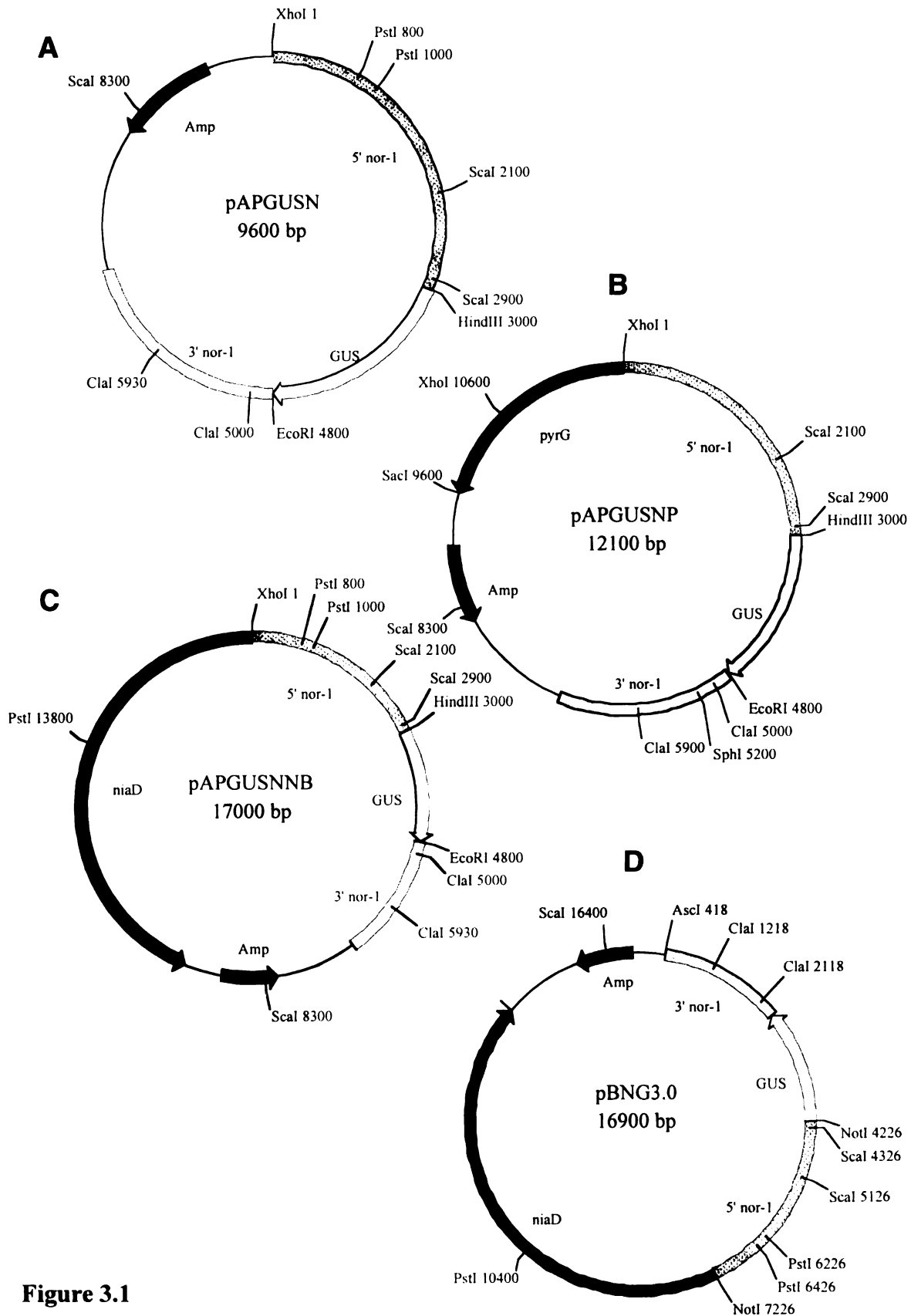


Figure 3.1

polished by *Pfu* polymerase (Stratagene, LaJolla, CA) and blunt-end ligated into pAPGUSN to generate pAPGUSNP (Fig. 3.1, B).

Fungal transformation. Plasmid pAPGUSNP (5 -10 µg) was transformed into protoplasts of CS10 (an uridine auxotroph) according to a method described previously (Horng et al., 1990; Skory, et al., 1993). Uridine prototrophic transformants were selected on CZ agar medium with 20% sucrose as osmotic stabilizer. Agar plates were incubated in the dark at 29⁰C for 3 to 5 days.

Identification of the site of plasmid integration. (i) Rapid DNA extraction procedure for PCR analysis. Plasmid site of integration was screened by a rapid DNA extraction and PCR method discussed in Chapter 2 (Chiou et al., 2002). Transformants were grown until sporulation (usually 3 to 5 days) and conidiospores were transferred to duplicate Czapek Dox agar plates using a sterile toothpick or sterile pipette tip. After 3 to 4 days (or as soon as colonies could be observed), colonies were analyzed. A sterile 200 µl plastic pipette tip was used to transfer a portion of the fungal colony (including conidiospores and mycelia) into a microcentrifuge tube containing 100 µl TE buffer (10 mM Tris-HCl, pH 8.0, 1 mM EDTA). The process was repeated up to 3 times to ensure that sufficient fungal cells were transferred. Tubes were heated in a boiling water bath for 5 min and placed on ice. The samples were centrifuged at 12,000 x g for 5 min at 4⁰C. The supernatant (fungal extract), containing DNA, was transferred to a new microcentrifuge tube. The extract was diluted with TE buffer (undiluted, 1:5, 1:20, and 1:100). In most assays, 2.5 µl of the 1:5 dilution resulted in good amplification in a 50 µl PCR reaction. The remainder of the fungal extract was stored at -80⁰C and could be analyzed by PCR for at least 3 months. Diluted samples stored at 4⁰C could be analyzed for at least 1 week.

(ii) PCR analysis. PCR analysis was conducted on DNA extracted from *A. parasiticus* transformants and the recipient strain *A. parasiticus* CS10. The primer pairs utilized depended upon the plasmid vector used and the site of integration analyzed

(Table 3.1). A 50 μ l reaction consisted of 2.5 μ l of the diluted fungal extract, 20 mM Tris-HCl (pH 8.8), 10 mM KCl, 10 mM $(\text{NH}_4)_2\text{SO}_4$, 0.15% Triton X-100, 0.1 mg/ml BSA, 0.5 to 1.0 μ M of each primer, 200 μ M of each dNTP, 2.0 to 3.0 mM MgCl_2 , and either 2.5 units of *Pfu* Turbo polymerase (2.5 U/ μ l, Stratagene, LaJolla, CA) or 2.5 units of *Taq* polymerase (5 U/ μ l) (Gibco BRL). PCR cycling depended on primer design and the target size (Table 3.1). PCR was performed in a Gene Ampli System 9600 (Perkin-Elmer) thermal cycler. All PCR reactions were initiated by a denaturation step at 95⁰C for 3 min followed by 35 cycles of denaturation, annealing, and extension. Reactions were terminated with an extension reaction at 72⁰C for 10 min. PCR products were observed by electrophoresis on a 1% agarose gel using standard procedures (Ausubel et al., 2003).

Solid-culture GUS activity assay. A solid-culture assay to analyze GUS activity was developed based on published procedures (Kolar et al., 1991; Verdoes et al., 1994). Transformants were transferred from selective medium to agar plates containing an aflatoxin-inducing solid growth medium (YES) overlaid with sterilized circular 82 mm Nytran Plus membranes (Schleicher and Schuell Inc., Keene, NH). Plates were incubated in the dark at 29⁰C for 36 to 55 h. Membranes with attached fungal colonies were removed from the surface of the agar plates and immersed in liquid nitrogen for 30 s. Membranes were allowed to thaw and immersed again in liquid nitrogen for 30 s. After thawing, membranes were incubated in GUS substrate solution (60 mM Na_2HPO_4 , 40 mM NaH_2PO_4 , 10 mM KCl, 1 mM MgSO_4 , 0.27% β -mercaptoethanol, 0.04% X GLU [Gold Biotechnology, St. Louis, MO]) for up to 24 h. Positive GUS activity resulted in a blue color in the colony

Southern hybridization analysis. The plasmid integration site was confirmed by Southern hybridization analysis. Fungal genomic DNA was purified from *A. parasiticus* transformants grown in YES liquid shake culture (the recipient strain CS10 required

Table 3.1. Primer sequences and PCR cycling parameters used for analysis of site of integration using DNA templates prepared by the rapid method.

Primer	Target size (kb)	Primer Sequence	PCR cycling parameters
Integration in 5' region of <i>nor-1</i> gene			
<u>PCR 1</u>			
JL 99	3.1 kb	5'TTT CAC GGG TTG GGG TTT CTA CAG G 3'	95°C 1', 62°C 1', 72°C 5'
JL100		5'GAC GGG GAA CCT CTT TAC AAA CAT C3'	
Integration in 3' region of <i>nor-1</i> gene			
<u>PCR 2</u>			
JL102	2.1 kb	5'CGC AAG GTG AGG GTT CGA ACC GAG G3'	95°C 1', 68°C 1', 72°C 3'
JL103		5'CCG CAG CAG GGA GGC AAA CAA TGA A3'	
Integration in <i>pyrG</i>			
<u>PCR 3</u>			
JL221	3.5 kb	5'CCA GAA AAT GCG AAG GTA AGT GCT TC3'	95°C 1', 55°C 1', 72°C 5'
JL222		5'GCG ACA CGG AAA TGT TGA ATA CTC AT3'	
Endogenous vbs ExonII			
(Control)			
JL136	1.4 kb	5'AGG CTC GAA AGG CGC ATA CGA3'	95°C 1', 68°C 1', 72°C 2'
JL137		5'GTG GTC TAC TGC CCA GCC ATC3'	

supplementation with 100 µg/ ml Uridine) for 48 h at 29°C with five, 6 mm glass beads (Skory et al., 1993). Southern hybridization analysis was performed using digoxigenin labeled probes and a non-radioactive hybridization detection procedure provided by the manufacturer (Roche Molecular Biochemicals, Indianapolis, Ind). The restriction enzymes and probes used to analyze the integration site are summarized in Table 3.1. The integration scheme and resulting blots are shown in Figures 3.2 and 3.3.

(i) 5' *nor-1* integration. Genomic DNA of transformants was digested with *XhoI* and probed with Probe 1. DNA from *A. parasiticus* CS10 generates a 5.8-kb band while DNA from a 5' integrant of pAPGUSNP generates 13.0 and 3.4-kb bands (Fig. 3.2).

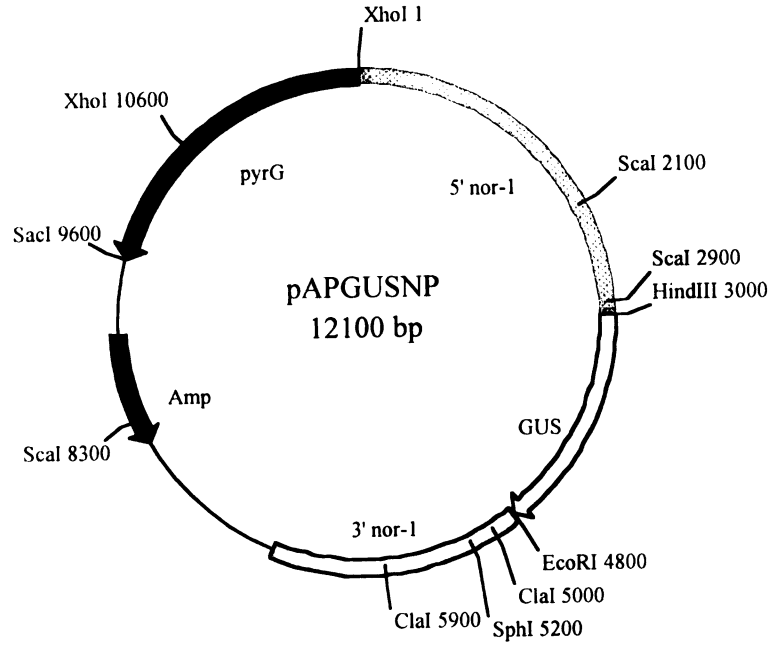
(ii) 3' *nor-1* integration. Genomic DNA of transformants was digested with *ScaI* and probed with Probe 2. DNA from *A. parasiticus* CS10 generates a 3.0-kb band while DNA from a 3' integrant of pAPGUSNP generates 4.0 and 4.4-kb bands (Fig. 3.2).

(iii) Integration at *pyrG*. Genomic DNA of transformants was digested with *SphI* and *SacI*, respectively, and probed with a 2.5-kb *pyrG* fragment generated by PCR (Probe 3). DNA from *A. parasiticus* CS10 digested with *SphI* generates a 12.6-kb band while DNA from a *pyrG* integrant generates 16.0 and 8.8-kb bands. CS10 genomic DNA digested with *SacI* generates a 8.1-kb band while DNA from a *pyrG* integrant generates 5.9 and 14.3-kb bands. (Fig. 3.3).

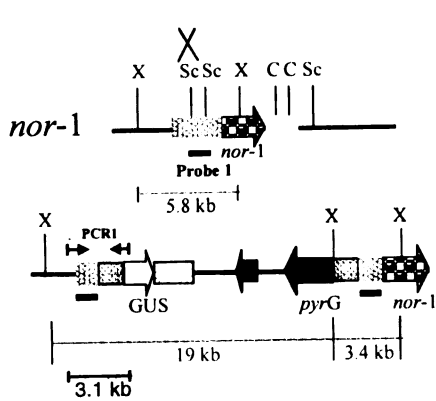
RESULTS

Generation of pAPGUSNP. Plasmid pAPGUSNP was constructed by blunt-end ligation of a 2.5 kb *pyrG* fragment into a 9.6 kb *nor-1::GUS* backbone derived from pPAPGUSN (Fig. 3.1, A). The rate of successful blunt-end ligation was low. The ligated plasmids were transformed into *E. coli* DH5α. Among 1200 transformants generated, only three transformants contained the 2.5 kb *pyrG* gene; these were identified by DNA dot blot analysis using digoxigenin-labeled *pyrG* fragment (2.5 kb) as a probe. Restriction digestion analysis indicated only one transformant harbored the correct

Figure 3.2. Southern hybridization analysis of site of integration in pAPGUSNP transformants. Restriction endonuclease map of pAPGUSNP is shown on the top. (A) Schematic for Southern hybridization and PCR analyses of pAPGUSNP integration into 5' region of *nor-1* and Southern hybridization data. *A. parasiticus* genomic DNA was digested with *XhoI* and probed with Probe 1. Single crossover integration of pAPGUSNP into the 5' region of *nor-1* results in two bands, 19 kb and 3.4 kb, and the disappearance of the 5.8-kb wild-type band. (B) Schematic for Southern hybridization and PCR analysis of pAPGUSNP integration into the 3' region of *nor-1* and Southern hybridization data. Genomic DNA was digested with *Scal* and probed with Probe 2. Single crossover integration of pAPGUSNNB into the 3' region of *nor-1* results in two bands, 4.0 kb and 4.4 kb, and the disappearance of the 3.4-kb wild-type band. Abbreviations: X = *XhoI*; Sc = *Scal*; C = *Clal*.



A 5' nor-1



B 3' nor-1

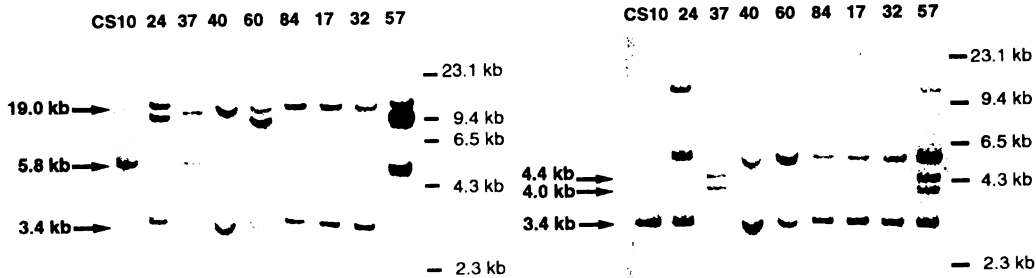
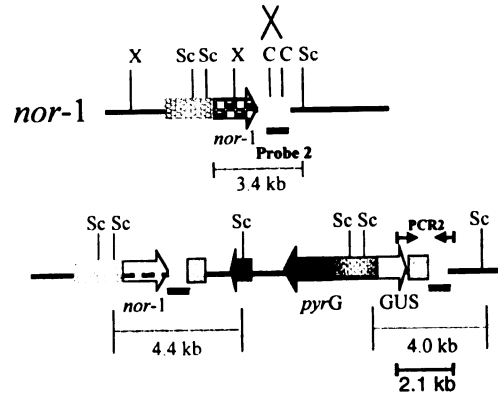


Figure 3.2

Figure 3.3. Southern hybridization analysis of pAPGUSNP integrated at *pyrG*.

Restriction endonuclease map of pAPGUSNP is shown on the top. Genomic DNA was digested with *SphI* (A) or *SacI* (B) and hybridized with the digoxigenin-labeled *pyrG* probe (2.5 kb, Probe 3). With *SphI* restriction endonuclease digestion (panel A), single crossover integration of pAPGUSNP into *pyrG* results in two bands, 16 kb and 8.8 kb, and the disappearance of the 12.6-kb wild-type band. With *SacI* restriction endonuclease digestion (panel B), single crossover integration of pAPGUSNP into *pyrG* results in two bands, 14.3 kb and 5.9 kb, and the disappearance of the 8.1-kb wild-type band.

Abbreviations: Sp = *SphI*; Sa = *SacI*.

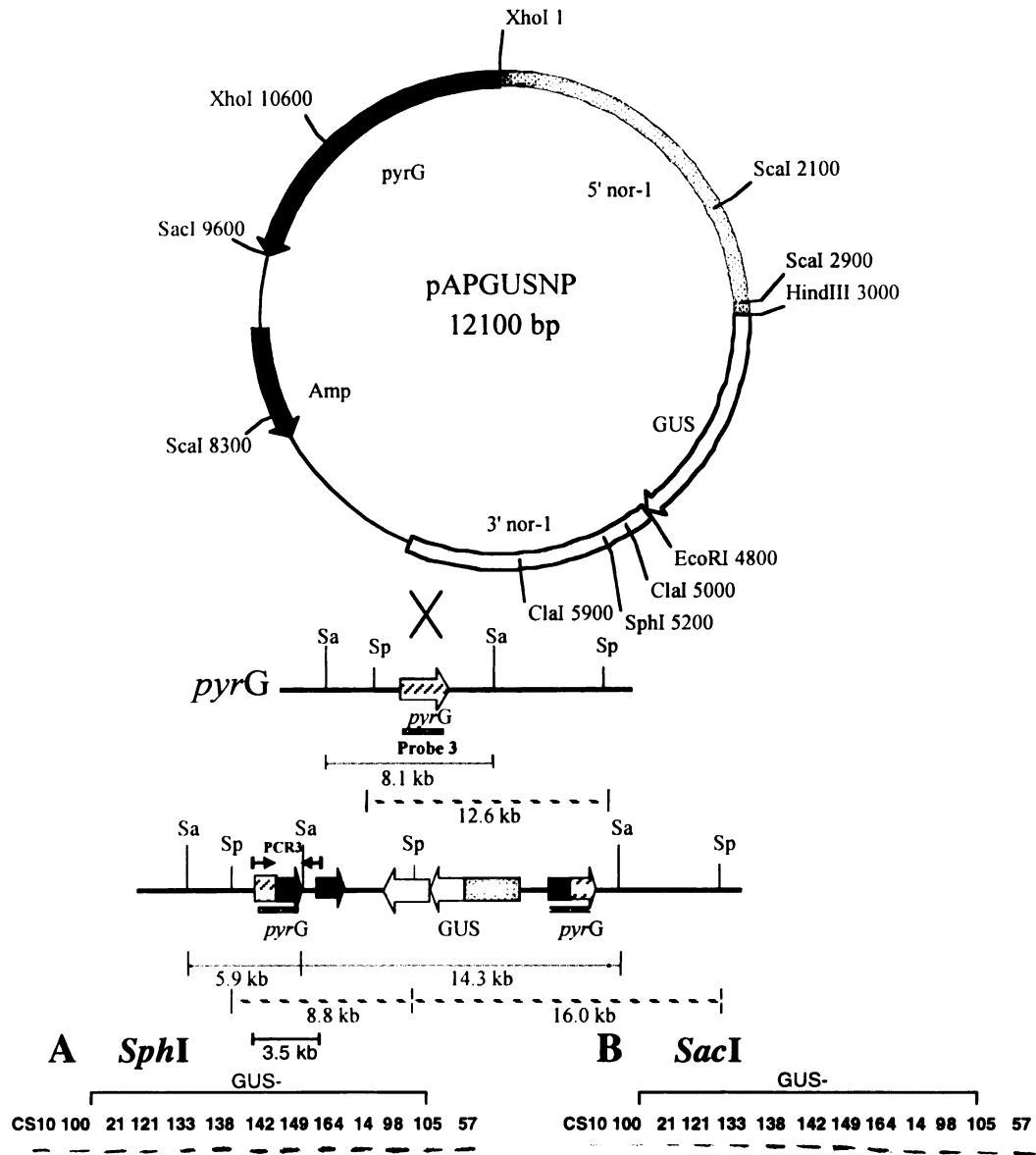


Figure 3.3

construct. This plasmid (pAPGUSNP) carries *nor-1*:: GUS and *pyrG* oriented in opposite directions, resulting in divergent transcription the two genes (Fig. 3.1, B).

Transformation of *A. parasiticus* CS10 with pAPGUSNP. Transformation of the *A. parasiticus* uridine-auxotrophic strain CS10 with plasmid pAPGUSNP was performed in three separate experiments. The *pyrG*⁺ uridine-prototrophic transformants were selected on CZ media with 20% sucrose. In total, 178 transformants were generated and subsequently analyzed using a solid-culture GUS activity assay.

Solid-culture GUS assay. All of the *pyrG*⁺ transformants selected on CZ medium were analyzed for expression of GUS on AF inducing medium (YES agar plate). Solid-culture GUS assay of these transformants (178 in total) resulted in identification of 42 GUS⁺ isolates (24%). Randomly selected GUS⁺ or GUS⁻ isolates were subsequently analyzed by PCR or Southern hybridization to determine the plasmid integration sites.

Determination of pAPGUSNP integration site within the chromosome. Fourteen GUS⁺ isolates were randomly selected and screened by a rapid PCR assay for site of integration (Fig. 3.4). The rapid PCR assay utilized a quick and easy template preparation procedure (see Materials and Methods) and the results were comparable to PCR using purified genomic DNA (Chiou et al., 2002). All 14 GUS⁺ isolates had pAPGUSNP integrated at 5' *nor-1* (11 isolates) or 3' *nor-1* (3 isolates). The site of integration of pAPGUSNP was confirmed in 4 of these isolates and 6 additional randomly selected GUS⁺ isolates by Southern hybridization analysis (Fig. 3.2). Of these 10 isolates, 7 had pAPGUSNP integrated at 5' *nor-1* and 2 carried pAPGUSNP at 3' *nor-1*. Isolate 57 was likely a multiple integrant of pAPGUSNP; these data suggested this isolate carried one copy of pAPGUSNP at both 5' and 3' *nor-1* (Fig. 3.2). In contrast, of 11 isolates with pAPGUSNP integrated at *pyrG*, none expressed GUS activity (Southern hybridization analysis shown in Fig. 3.3).

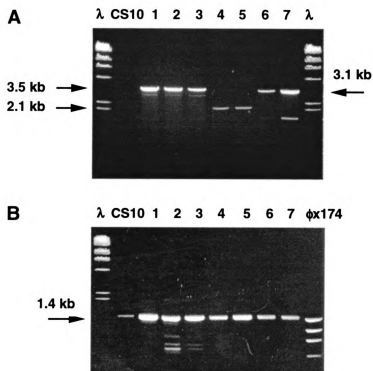


Figure 3.4. PCR analysis to detect site of integration in pAPGUSNP transformants.

Template DNA for 5' and 3' *nor-1* and *pyrG* integration assays was prepared with a rapid boiling procedure. (A) GUS^+ and GUS^- transformants (lanes 1 through 7) and CS10 (negative control) were analyzed for 5' *nor-1*, 3' *nor-1*, or *pyrG* integration. Primers PCR3 were used to detect *pyrG* integration (lanes 1, 2, and 3; GUS^- transformants) and generated a 3.5-kb PCR fragment. Primers PCR2 were used to detect 3' *nor-1* integration (lanes 4 and 5; GUS^+ transformants) and generated a 2.1-kb PCR fragment. Primers PCR1 were used to detect 5' *nor-1* integration (lanes 6 and 7; GUS^+ transformants) and generated a 3.1-kb PCR fragment. (B) DNA from all 7 transformants and the control strain CS10 was amplified with a primer pair specific for exon III of the versicolorin B synthase gene (positive control). A 1.4-kb PCR fragment was expected in all fungal isolates. Lanes containing molecular size markers in panels A and B are represented by λ HindIII digest and ϕ x174 HaeIII digest. Nucleotide sequences of all primers are found in Table 3.1.

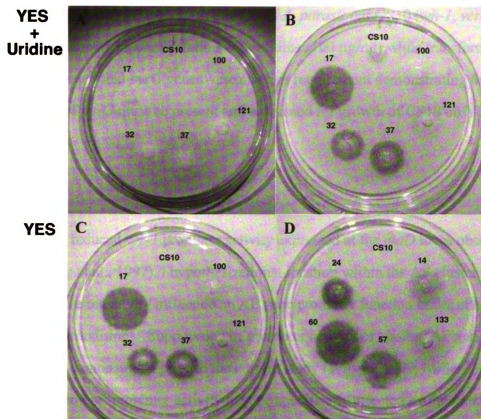


Figure 3.5. Solid-culture GUS activity assay on CS10 transformants harboring pAPGUSNP. The recipient strain CS10 (control) and representative *pyrG*⁺ transformants were inoculated onto Nytran membranes overlaid onto YES agar medium (panels C and D) or YES supplemented with 5 mg uridine per plate (panels A and B). A GUS assay was conducted on filters in panels B, C and D. Transformants carried a single copy of pAPGUSNP integrated at 5' *nor-I* (transformants 17 and 32), at 3' *nor-I* (transformant 37), or at *pyrG* (transformants 100 and 121). Transformants 24 and 60 carried multiple copies of pAPGUSNP with at least one copy integrated at 5' *nor-I*. Transformant 57 carried multiple copies of pAPGUSNP with at least one copy integrated at 3' *nor-I*. Transformants 14 and 133 carried multiple copies of pAPGUSNP with at least one copy at *pyrG* and no copies at *nor-I*.

Confirmation of *pyrG* expression in *pyrG*⁺ transformants. Expression of *pyrG* in *A. parasiticus* CS10 (used as the recipient) was analyzed under these aflatoxin-inducing growth conditions (Fig. 3.5). Growth of *A. parasiticus* CS10 (*wh-1*, *ver-1*, *pyrG*) on YES required supplementation with uridine (100 µg/ml) while transformation of CS10 with a functional *pyrG* gene overcame this requirement demonstrating that a functional copy of *pyrG* must be present and expressed for growth of CS10 on YES medium.

DISCUSSION

Based on reduced *ver-1* promoter activity expressed at the *niaD* locus observed previously (Liang et al., 1997), I hypothesized that location within the AF cluster provided a positive regulatory influence on AF gene promoter function under aflatoxin-inducing growth conditions. Suppression of promoter activity of another AF gene, *nor-1*, at *niaD* was also demonstrated prior to the current study (Wilson, 1999; Miller, 2003). However, alteration of promoter activity may be specifically affected by the *niaD* gene since *niaD* is only expressed under non-AF inducing conditions using nitrate as the sole nitrogen source; otherwise the gene is repressed. Reduction of *ver-1* and *nor-1* promoter activity at the *niaD* locus may be a consequence of regional control. Thus, investigation of positional effects of AF promoter activity at an additional locus provides supporting data for our previous observations. In this study, promoter activity of *nor-1* located in the *pyrG* locus and its native chromosomal location was investigated. The *pyrG* locus was chosen for two reasons. 1) The selectable marker (*pyrG*) that encodes uridine monophosphate decarboxylase was cloned previously (Skory et al., 1990). 2) Expression of *pyrG* is not associated with regulation of AF biosynthesis, unlike *niaD*.

The results generated in this study were consistent with results generated in analysis of *nor-1* promoter activity within the AF gene cluster and at *niaD* (Chiou et al., 2002). First, the percentage of GUS⁺ transformant is similar (approximately 24%). This

study utilized a plasmid pAPGUSNNP (Fig. 3.1, B) containing the *nor-1::GUS* fusion (derived from pAPGUSN, Fig. 3.1, A) plus *pyrG* as a selectable marker; while pAPGUSNNB (Fig. 3.1, C) and pBNG3.0 (Fig. 3.1, D) contained a similar *nor-1::GUS* construct and *niaD* as a selectable marker. Transformation of pAPGUSNNB and pBNG3.0 into *A. parasiticus* NR1 (*niaD*) resulted in 23% (25 out of 149 transformants analyzed) and 25% (29 out of 117 transformants analyzed) GUS⁺ transformants, respectively (data summarized in Table 3.2).

Second, these data confirmed the preliminary observation by Liang et al. (1997) that chromosomal location plays a role in regulation of AF gene expression. Expression of *nor-1::GUS* at the *nor-1* locus was regulated similarly to the native *nor-1* gene, while placement at two other positions (*niaD* and *pyrG*) outside of the aflatoxin gene cluster resulted in no detectable GUS activity. The targeting of reporter constructs to specific chromosomal locations for promoter analysis has been advised by other investigators studying expression of fungal genes (Hammer, and Timberlake, 1987; Timberlake and Marshall, 1989; van Gorcom et al., 1986). Although the mechanisms of position-dependent gene expression have not been fully elucidated in filamentous fungi, it has been hypothesized that enhancer elements may be responsible for the position-dependent effect (Kinsey and Rambosek, 1984). The hypothesis that positive cis-acting factors have regional control over the transcription of AF genes is reasonable, since removal of AF reporter fusions from the AF gene cluster results in reduced GUS expression.

An alternative explanation for the lack of GUS activity at the *niaD* and *pyrG* loci is that a transcriptionally inactive chromatin structure exists at these two sites. We think that such inactivation is unlikely for two reasons. First, NR-1 transformed with pGAPN2B (β -tubulin::GUS) expressed GUS activity at similar levels at 24, 48, and 72 h when integrated at the *niaD* locus, although the level of GUS activity in the pGAPN2B transformants was approximately ten-fold lower than GUS activity in D8D3

Table 3.2. Summary of GUS activities and plasmid integration sites exhibited in *A. paraciticus* transformants carrying *nor::GUS* fusion in CS10 transformants carrying pAPGUSNP (Chiou, in this study), and NR-1 harboring pAPGUSNNB (Wilson, 1998) and pBNG3.0 (Miller, 2003).

Plasmid	pAPGUSNP^a	pBNG3.0^b	pAPGUSNNB^c
Target locus	<i>pyrG</i>	<i>niaD</i>	<i>niaD</i>
Recipient strain	CS10	NR-1	NR-1
# of Total transformants	178	117	149
# of GUS+	42	29	35
% GUS +	24%	25%	23%
Integration analysis:	^aChiou (this study)	^bMiller (2003)	^cWilson (1998)
PCR on GUS+ transformants	14		
Integration at 5' <i>nor-1</i>	11		
Integration at 3' <i>nor-1</i>	3		
Southern analysis on GUS+ transformants	10	21	11
Integration at 5' <i>nor-1</i>	7	12	4
Integration at 3' <i>nor-1</i>	2	9	6
Multiple intgegration at 5' and 3' <i>nor-1</i>	1		
Unverified			1
Southern analysis for GUS- transformants	11	22	6
Integration at 5' <i>nor-1</i>	0	0	0
Integration at 3' <i>nor-1</i>	0	0	0
Integration at <i>pyrG</i>	11		
Integration at <i>niaD</i>		22	2
Single crossover at <i>niaD</i>			4

(pAPGUSNNB integrated at 3' *nor-1*; Wilson, 1998) at 48 and 72 h. In contrast, transformant D8D4 (pAPGUSNNB integrated at *niaD*; Wilson, 1998), when grown under the same conditions, produced no detectable GUS activity at any of these time points (data not shown). Second, in transformants carrying pAPGUSNP, the *nor-1* promoter carried on this plasmid was not active at the *pyrG* locus even though growth on YES medium required expression of the *pyrG* gene. In addition, several pAPGUSNP transformants had no detectable GUS activity even when they carried multiple copies of the plasmid (none integrated at *nor-1*). In contrast, other multiple integrants with at least one copy of pAPGUSNP integrated at *nor-1* were GUS⁺. Based on these data and preliminary data reported by Liang et al. (1997) I propose that aflatoxin gene expression is influenced by an enhancer element.

The clustering of genes involved in the same secondary metabolic pathway is a common theme in the filamentous fungi (Keller and Hohn, 1997). However, cis-acting elements that regulate many genes simultaneously in fungal gene clusters have not been identified. If an enhancer element does influence the regulation of *nor-1* transcription, it is located at least 3-kb upstream from the transcription initiation site in the 5' *nor-1* region, and at least 1.8-kb downstream the transcription termination site in the 3' region of *nor-1* or within the *nor-1* coding region. Because similar position-dependent expression was observed with the *ver-1*::GUS reporter construct (Liang et al., 1997), it also is possible that the same cis-acting element is influencing the regulation of both *nor-1* and *ver-1*. Studies performed on the SpoC1 gene cluster in *Aspergillus nidulans* showed that clustered genes can be coordinately expressed during development, and that placement of cluster genes at ectopic chromosomal locations results in the loss of that coordination (Miller et al., 1987; Timberlake and Barnard, 1981). The physical linkage of aflatoxin biosynthesis genes also may have a regulatory role. Studies designed to establish such a phenomenon and to determine the nature of the regulatory mechanism,

may eventually lead to a broader understanding of the expression of secondary metabolism genes and the ability to manipulate their expression in microorganisms.

ACKNOWLEDGEMENTS

We thank Dr. Frances Trail, Department of Botany and Plant Pathology at Michigan State University, for providing plasmid pAPGUSN.

Data in Chapter 3 is published in *Applied and Environmental Microbiology* in a manuscript entitled "Chromosomal location plays a role in regulation of aflatoxin gene expression in *Aspergillus parasiticus*" (Chiou et al., 2002).

CHAPTER 4

Immuno-localization of Nor-1, Ver-1, and OmtA proteins involved in aflatoxin biosynthesis in *Aspergillus parasiticus*

INTRODUCTION

The biosynthesis of aflatoxin is a complex process that involves at least 18 enzyme activities (Minto and Townsend, 1997; Payne and Brown, 1998, Cary et al., 2000). The mechanisms that coordinate these enzyme activities to synthesize AF within a cell are still not clear. In addition, the distribution of these AF enzymes in a fungal colony and their sub-cellular localization within a fungal cell have yet to be determined. The objective of this study was to investigate the distribution and sub-cellular location of representative enzymatic activities in the aflatoxin biosynthetic pathway. This study focused attention on Nor-1 (Trail et al., 1994), Ver-1 (Skory et al., 1992) and OmtA (Yu et al., 1993) that catalyze early, middle and late enzymatic steps in the aflatoxin biosynthetic pathway, respectively. Nor-1 is a NADPH-dependent keto-reductase involved in the conversion of norsolorinic acid (NA) to averantin (AVN) (Zhou and Linz, 1999). Ver-1 is another keto-reductase involved in conversion of versicolorin A (VERA) to demethyl-sterigmatocystin (DMST)(Skory et al., 1992; Liang et al., 1996). OmtA is a methyltransferase that specifically converts sterigmatocystin (ST) to O-methylsterigmatocystin (OMST) by transfer of a methyl group from S-adenosylmethionine (SAM) (Yu et al., 1993; Lee et al., 2002). Our laboratory produced polyclonal antibodies (PAb) against Nor-1 (Zhou, 1998; Lee et al., manuscript submitted), Ver-1 (Liang, et al., 1997), and OmtA (Lee et al., 2002) to localize these enzymes in *A. parasiticus* SU-1 and CS10. An *omtA* disruptant strain, LW 1432 (*wh1, ver-1, omtA*), was also generated to serve as a negative control (Lee et al., 2002).

A model for coordinate regulation of sterigmatocystin (ST) production (an AF biosynthetic pathway intermediate in *A. parasiticus*) and asexual sporulation has been

described in *A. nidulans* (Hicks, et al., 1997; Adams et al., 1998). Based on this model, I hypothesized that the enzymes involved in AF biosynthesis are localized within specific developmental structures; this study focused on an asexual spore-bearing structure, the conidiophore. At the sub-cellular level, according to the complexity of this AF biosynthetic pathway, I hypothesized that enzymes (or some of the enzymes) involved in AF biosynthesis are compartmentalized or closely associated within a cell. Physical interaction of these enzymes may facilitate efficient and accurate catalysis.

Preliminary cellular localization of Nor-1 and Ver-1 in the wild type AF producing strain *A. parasiticus* SU-1 was performed by Liang (1996) and Zhou (1998) using a slide-culture cell preparation procedure followed by indirect immunofluorescence microscopy. However, artifacts were generated by this sample preparation method for several reasons. First, growth conditions and colony morphology were different from colonies generated by center-inoculation of conidiospores on solid media. In the slide-culture method, conidiospores were inoculated on the surface of agar blocks (approximately 8 mm²) placed between 2 sterile coverslips. Mycelia as well as the conidiophores attached onto one surface of the coverslips as growth continued. Acquiring nutrients from the agar block likely became less efficient as the colony extended outwards, unlike regular fungal growth on an agar plate in which the nutrients were obtained from the agar surface directly underneath the mycelia. Slide-culture may induce stress responses and cause alteration of fungal development. Second, the fungal cell wall represents a barrier that obstructs cell permeabilization and antibody accessibility; these conditions are extremely critical to achieve success in subsequent immunolabeling. Thus, lysing the cell wall is an important step to immunolocalize proteins in the fungal cells. However, digestion of *A. parasiticus* cell wall utilizing Novozyme 234, a partially-purified cell wall lysing enzyme isolated from *Trichoderma harzianum*, did not give a constant degree of cell wall digestion, thus causing artifacts in immunolabeling. Preliminary indirect fluorescence microscopy detected Nor-1 in the

cytoplasm in the conidiophores and the substrate level mycelia (Zhou 1998). Ver-1 was detected mainly in the conidiophores and the signals were confined to particle-like structures (Liang, 1996). However, these results were not consistently reproducible, and no reliable negative control was available.

The goal of my study was to develop a growth model that would closely mimic regulation of toxin synthesis in soil and on the host plant. An improved colony fractionation scheme as well as cell preparation methods were developed. A 72 h-old colony was fractionated based on 24-h intervals to correlate the time of growth with AF protein distribution. Colony fractions were then fixed and embedded in paraffin to generate sections (4-5 μm) for immuno-labeling without the need to lyse cell walls. In addition, instead of using a conventional epi-fluorescence microscope, fluorescence microscopy was performed using a Confocal Laser Scanning Microscope (CLSM) which provides better resolution of confocal images (optical sections) and broader image analysis capabilities (described in Chapter 1).

The results of my study demonstrated that Nor-1, Ver-1 and OmtA were evenly distributed among different cell types and were not concentrated in conidiophores, contrary to the hypothesis. In a 72 h-old colony, these proteins were most abundant in colony fraction 2 where the cells had grown for 24 to 48 h. Within a cell, Nor-1 and Ver-1 were primarily localized to the cytoplasm, suggesting that they are cytosolic enzymes. OmtA was also detected in the cytoplasm and the fluorescent signal was confined to discrete areas (patches). Yet due to limitations in resolution of CLSM, it was not clear if those patches represent specific sub-cellular organelles. The pattern of labeling using anti-OmtA was not consistent with localization of OmtA only to nuclei, peroxisomes, or Woronin bodies. However, the data do not rule out the possibility that OmtA was localized to other cell locations as well as these specific organelles. Although Nor-1, Ver-1 and OmtA appeared to localize in the cytoplasm, compartmentalization of these proteins needs to be further explored.

MATERIALS AND METHODS

Fungal strains. *A. parasiticus* SU-1 (NRRL5862, ATCC 56775) is a wild-type, aflatoxin-producing strain. A non-aflatoxin producing *aflR* knockout strain, AFS10 (kindly provided by Dr. Jeff Cary, USDA, New Orleans, LA.), was used as a negative control. AFS10 was generated from *A. parasiticus* NR-1 (*niaD*) which was derived from parental strain SU-1 (Cary et al., 2002). Two additional strains, *A. parasiticus* CS10 (*ver-1 wh-1 pyrG*) (Skory et al., 1993) derived from *A. parasiticus* ATCC36537 (*ver-1 wh-1*), and an *omtA* disrupted mutant strain LW1432 (*ver-1 wh-1 omtA*) generated by disrupting the *omtA* gene in CS10 (Lee et al., 2002) were also used to study localization of OmtA.

Time-dependent fractionation of colonies grown on solid medium. To determine the accumulation and distribution of Nor-1, Ver-1, and OmtA in fungal colonies grown on solid culture media, conidiospores (2×10^5) of *A. parasiticus* SU-1 and AFS10, as well as CS10 and LW1432 (to specifically localize OmtA), were inoculated onto the center of YES (2% yeast extract, 6% sucrose, pH 5.8) agar overlaid with sterile cellophane membranes and incubated at 29° C in the dark. Three-day-old colonies of SU-1 (S) and AFS10 (R) were fractionated into three concentric rings based on area covered at 24, 48, or 72 h of growth (fraction 1, 48-72 h old; fraction 2, 24-48 h, and fraction 3, 0-24 h) to generate fractions S1, S2, S3 and R1, R2, R3 (Lee et al., 2002). *A. parasiticus* CS10, and LW1432 colonies were fractionated following the same scheme to generate analogous fractions C1, C2, C3, and L1, L2, L3, respectively (Figure 4.1).

Preparation of paraffin-embedded fungal sections. Samples from fungal colony fractions were embedded in paraplast (Sigma, St. Louis, MO) using a published procedure (Ausubel et al., 2003) with the following modifications. Fungal tissues were fixed with Streck tissue fixative (Streck Laboratory Inc., Omaha, NE) at 4° C overnight,

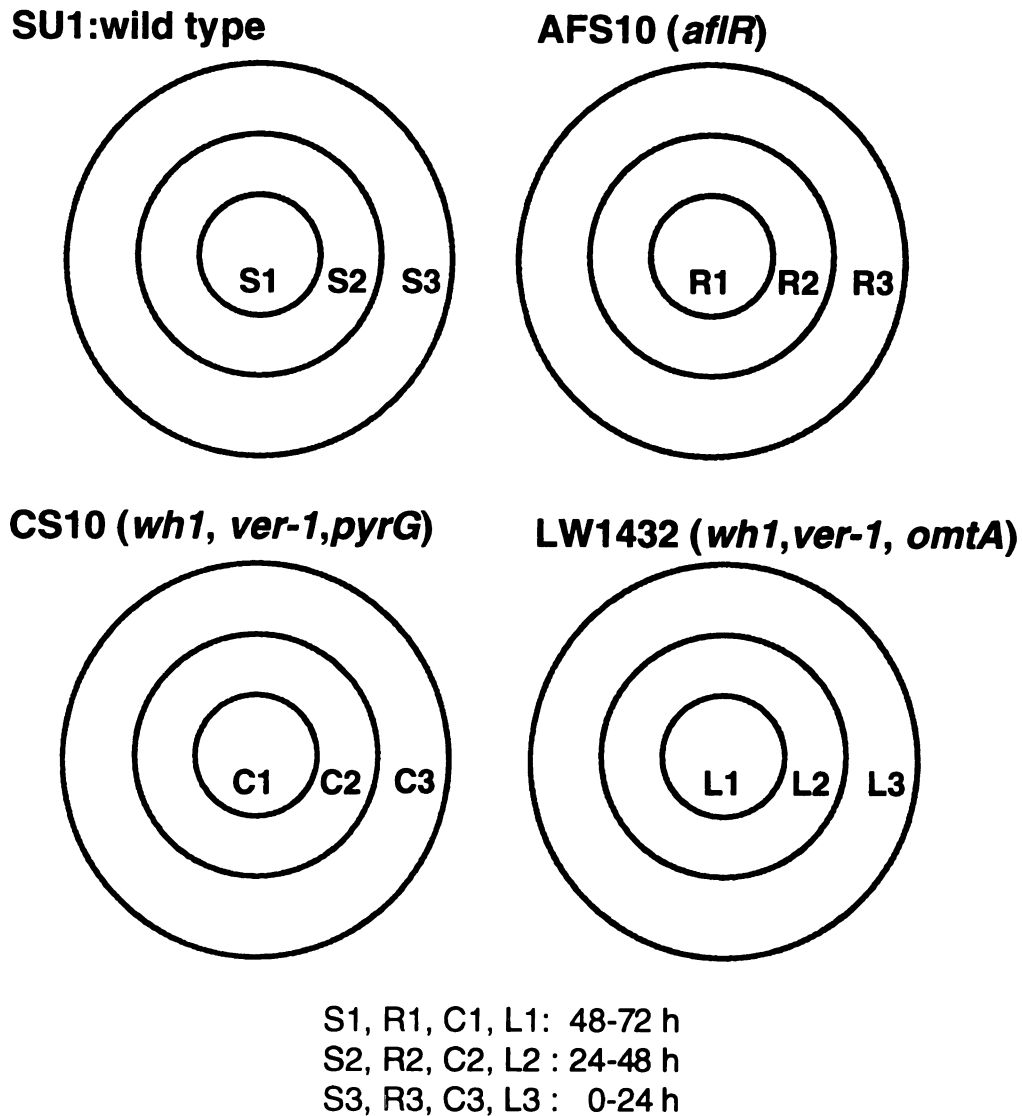


Figure 4.1. Time-dependent fractionation of fungal colonies. A 72 h culture of SU-1 (wild type AF producing) grown on YES medium (2% yeast extract, 6% sucrose) was divided into 3 fractions based on 24 h growth intervals (S1: 48- 72 h growth; S2: 24- 72 h growth; S3: 0- 24 h growth). The control strain AFS10, an *aflR* knockout mutant, was prepared similarly to generate R1, R2 and R3. For detection of OmtA, additional strains, LW1432 (*ver-1 wh-1 omtA*) and its parent strain CS10 (*ver-1 wh-1 pyrG*), were used to generate L1, L2, L3 and C1, C2, C3, respectively.

and then dehydrated in a graded series of ethanol: 30% (30 min, room temperature); 50% (30 min, room temperature); 70% (overnight, 4° C); 85% (30 min, room temperature, 2 times); 95% (30 min, room temperature, 2 times); 100% (30 min, 4° C, 2 times), followed by incubation in 100% xylene (10 min, room temperature, 3 times). Fungal tissues were then incubated in a paraffin/xylene mixture (1:1; v/v) for 15 min, 60 min and overnight at 60°C and finally for 8 h in 100% paraffin at 60° C (three changes of paraffin during incubation). The paraffin embedded sample blocks were hardened in a plastic mold (VWR Scientific, Detroit, MI) at RT. Sample blocks were cut into 4 µm thick sections using a tissue section microtome (AO Spencer 820 microtome, Fisher Scientific). The sections were attached to poly-L-Lysine (Sigma) coated coverslips (22 mm square).

Immuno-fluorescence labeling of fungal cells. Coverslips with paraffin-embedded fungal sections were placed in a coverslip holder (EMS, Fort Washington, PA) for de-paraffinization and antigen retrieval. Sections were de-paraffinized twice in 100% xylene for 10 min, then rehydrated with a decreasing concentration of ethanol: twice in 100% for 10 min, once in 95%, 70%, 50% for 5 min each, and finally in deionized distilled H₂O. Antigen retrieval was performed by heating the sections in 10 mM citrate buffer (pH 6.0) at 95° C for 5 min followed by cooling at room temperature for 20 min. Coverslips were rinsed with TBS (Tris buffer saline, pH 7.5) and incubated in blocking solution (1% BSA with 0.1% saponin in TBS) at 4°C overnight. The samples were probed with primary antibodies against Nor-1 (1 to 500 dilution)(Zhou, 1998; Lee et al., submitted), Ver-1 (20 µg/ml) (Liang et al., 1997), OmtA (20 µg/ml) (Lee et al., 2002), or anti-SKL (1:500, Zymed, So. San Francisco, CA) as a positive control, followed by secondary antibody conjugated to a fluorescent probe (goat anti-rabbit IgG- Alexa 488 conjugate [5 µg/ml]; Abs 495 nm/ Em 519 nm) at RT for 1 h. Coverslips were washed after each antibody treatment with TBS containing 1% BSA and 0.1% saponin followed by two washes with TBS for 10 min. Fungal nuclei were detected using SYTOX Green

fluorescence dye (Molecular Probes). The samples were mounted onto microscopic slides with Prolong anti-fade mounting media (Molecular Probes, Eugene, OR).

Confocal Laser Scanning Microscopy (CLSM). Fluorescence image detection was performed on a Zeiss 210 Laser scanning microscope or Zeiss LSM5 Pascal Laser Scanning Microscope with a 488 nm laser line. The 40 X oil objective lens (Zeiss Plan-NeoFlura, NA= 1.3) was used to obtain most images. The Alexa 488 fluorescence probe (Abs 495 nm/Em 519 nm) was detected using LP 520 or BP 520-560 barrier filters. Fluorescence image analysis of SU-1, AFS10, CS10 and LW1432 was conducted under the same instrument parameter settings. High resolution images were generated using a Zeiss Plan-APOCHROMAT (63 X/ 1.4 Oil Dic, N.A.=1.4) objective along with higher zoom levels in the Zeiss LSM5 Pascal CLSM specifically to demonstrate the localization of Nor-1, Ver-1, and OmtA within a SU-1 cell. Single optical sections or extended focus images from CLSM Z- stacks were obtained.

Quantitative fluorescence intensity analysis. To quantitate fluorescence intensity, a Meridian INSIGHT[®] plus laser-scanning system (Meridian Instruments, Inc., Okemos, MI) connected to a Zeiss Axioskop microscope equipped with IQ Master Program (V2.31) image analysis software was used. The Alexa 488 green fluorescence was detected using a BP 530/30 barrier filter under the 488 nm laser line. All images were captured using a 40X Zeiss Plan-NEOFLUAR oil objective lens (N.A.=1.3) (Carl Zeiss Inc., Germany) with a 1X cooled charged-couple detector (CCD) allowing analysis of a large number of cells in one 512 x 480 pixel resolution image. Fluorescence image analysis of strains SU-1 and AFS10, as well as CS10 and LW1432 was conducted using the same instrument parameter settings. For each colony fraction, twenty images were acquired for intensity analysis and the average pixel number was reported.

RESULTS

Immuno-localization of Nor-1 and Ver-1. CLSM detected Nor-1 and Ver-1 in all colony fractions of SU-1 (Fig. 4.2a for Nor-1 and Fig. 4.2d for Ver-1). Under the same instrument settings, very little signal was detected in AFS10 (Fig. 4.2b for Nor-1 and Fig. 4.2e for Ver-1). Therefore, bright field images of the AFS10 colony fractions are shown to illustrate the typical size and numbers of cells analyzed (Fig. 4.2c and 4.2f). Highest fluorescence intensity was detected in fraction S2 for both Nor-1 and Ver-1. Both proteins were equally distributed in substrate level mycelia and conidiophores (Fig 4.3 for Nor-1; Fig. 4.5, C for Ver-1).

Within a cell, high resolution optical sections taken using Zeiss LSM5 PASCAL microscope with a Zeiss Plan-APOCHROMAT (63 X Oil Dic, NA=1.4) objective showed that both Nor-1 and Ver-1 were mainly localized in the cytoplasm. Nor-1 did not associate with specific organelles in either hyphae (Fig 4.3, A to D) or conidiophores (Fig. 4.3, E). Ver-1 was mainly present in the cytoplasm (Fig. 4.4, A, and B), frequently associated with the cell wall as well as spore coat, and occasionally detected in particle-like structures (Fig. 4.4, C, and E). However, the presence of Ver-1 in locations other than cytoplasm appeared to be non-specific since these labeling patterns were also observed in the control strain AFS10 (Fig. 4.5, A). Thus, both Nor-1 and Ver-1 are concluded to be cytosolic proteins. Although the Ver-1 antibodies bound to AFS10 non-specifically, the overall fluorescence intensities detected in AFS10 were significantly lower than in SU-1 (Fig. 4.2, B and Fig. 4.5).

Immuno-localization of OmtA. To compare the fluorescence labeling intensity between SU-1 and CS10 and their non-aflatoxin producing counterparts, AFS10 and LW1432, respectively, the samples were viewed under the lowest zoom level using the Zeiss 210 CLSM (zoom = 20) in order to acquire maximum cell number within a field. Under the same contrast and brightness settings, the samples prepared from the control

Figure 4.2. Immuno-fluorescence confocal microscopy of Nor-1 and Ver-1 in *A. parasiticus* SU-1 and AFS10 (*aflR* knockout mutant) grown on YES agar for 72 h. Colonies of SU-1 and AFS10 were divided into 3 fractions (see Material and Methods). The paraffin embedded fungal sections were immuno-labeled with anti-Nor-1 antiserum (panel A) (1:500) or anti-Ver-1 IgG (panel B) (20 µg/ml) followed by Alexa 488 conjugated goat anti-rabbit IgG. Fluorescence intensities of SU-1 sections immuno-labeled with anti-Nor-1 and anti-Ver-1 are shown in Rows a and d, respectively; and of AFS10 sections in Rows b and e. The related bright field images of the AFS10 colony fractions are shown in Rows c and f (legends labeled in black). Bars, 100 µm.

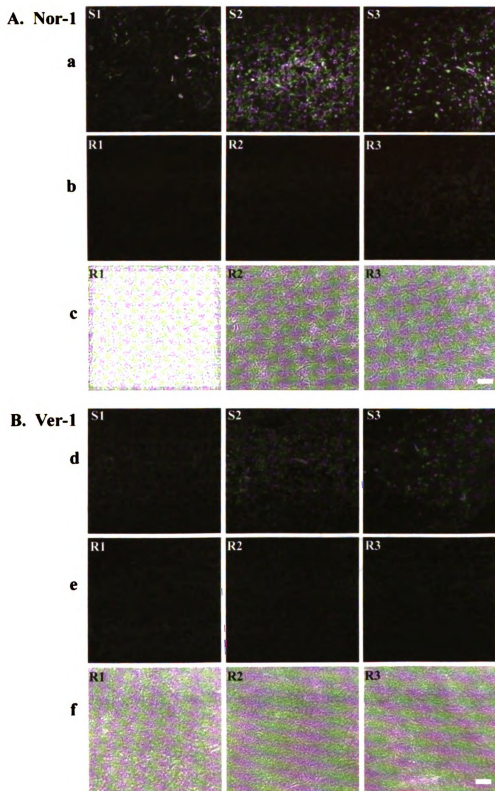


Figure 4.2

Figure 4.3. CLSM immuno-fluorescence detection of Nor-1 in *A. parasiticus* SU-1. Fungal cells derived from colony fraction S2 were immuno-labeled with the Nor-1 antibody followed by goat-anti-rabbit IgG conjugated with Alexa 488 probe. Fluorescence images were acquired in a Zeiss LSM5 Pascal CLSM using a Plan-APOCHROMAT (63 X Oil Dic, NA=1.4) objective and zoom level 3. Immuno-fluorescence of Nor-1 was detected in the cytoplasm of SU-1 hyphae shown in single optical sections (panels A, B, C, and D). Immuno-fluorescence of Nor-1 was also detected in conidiophores (panel E). The DIG image related to panel E is shown in panel F. Bars = 2 μ m.

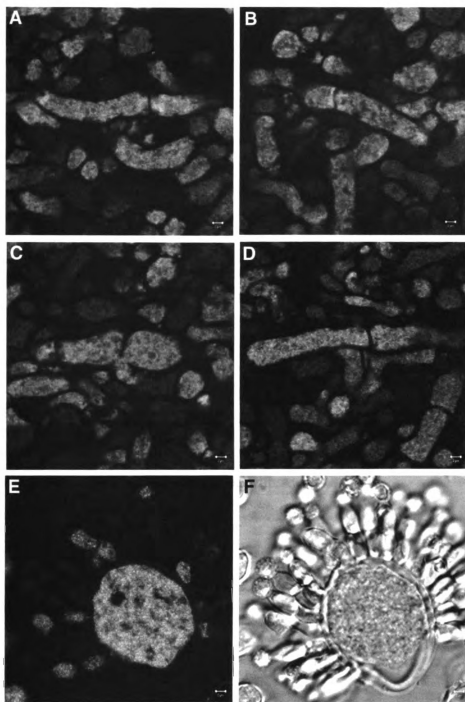


Figure 4.3

Figure 4.4. CLSM immuno-fluorescence detection of Ver-1 in *A. parasiticus* SU-1. Fungal cells derived from colony fraction S2 were immuno-labeled with the Ver-1 antibody followed by goat-anti-rabbit IgG conjugated with Alexa 488 probe. Fluorescence images were acquired in a Zeiss LSM5 Pascal CLSM using a Plan-APOCHROMAT (63 X Oil Dic, NA=1.4) objective and zoom level 3. Immuno-fluorescence of Ver-1 was detected in the cytoplasm of SU-1 hyphae shown in single optical sections (panels A and B). Immuno-fluorescence of Ver-1 was also detected in conidiophores (panels C and E). The DIG images related to C and E are shown in D and F, respectively. Bars = 2 μ m. The non-specific signals of Ver-1 associated with cell wall, spore coat, or particle structures are indicated with arrows.

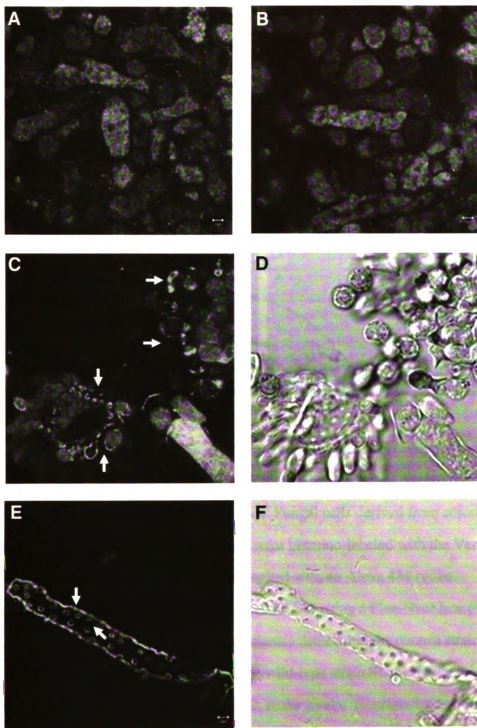


Figure 4.4

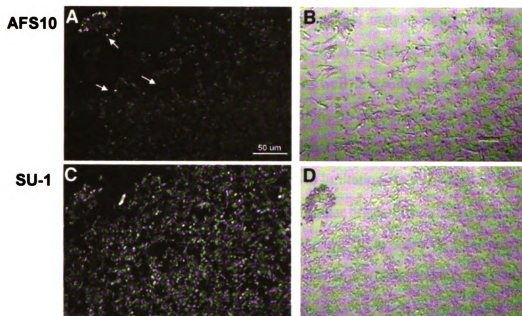


Figure 4.5. Immuno-fluorescence labeling by Ver-1 antibodies in the control strain *A. parasiticus* AFS10 and the wild-type strain SU-1. Fungal cells derived from colony fraction R2 and S2 (see Material and Methods) were immuno-labeled with the Ver-1 antibody followed by goat-anti-rabbit IgG conjugated with an Alexa 488 probe. Fluorescence images were acquired in a Zeiss 210 CLSM using a Plan-NeoFluar (40 X Oil Dic, NA=1.3) objective. (A) Fluorescence signals detected in the control strain AFS10. (C) Fluorescence signals detected in the wild-type strain SU-1. The bright-field images related to A and C are shown in B and D, respectively. Representative non-specific signals are indicated with arrows. Bar, 50 μ m.

strain AFS10 (fractions R1, R2, and R3) and LW1432 (fractions L1, L2 and L3) did not show significant fluorescent signals compared to samples prepared from the same colony fractions from wild type SU-1 (fractions S1, S2, and S3) or CS10 (fractions C1, C2 and C3) (Fig. 4.6). These data are consistent with Western blot analysis of protein extracts isolated from the same colony fractions (Lee et al., 2002). OmtA was detected in the substrate level mycelium (Fig. 4.7, A; Fig 4.8, B) as well as conidiospore-bearing structures (Fig. 4.7, B; Fig. 4.8, A) located in fractions S1 and S2 at nearly equal intensity as in substrate level mycelium. The fluorescent signal was confined to discrete areas (patches) within cells (Fig. 4.7, A). However, due to limitations in resolution of CLSM, it was not clear if these areas are associated with particular organelles. Similar samples were also probed with anti-SKL antibodies that are expected to detect proteins targeted to peroxisomes and Woronin bodies (Fig. 4.7, C) (Keller et al., 1991; Valenciano et al., 1998). The observed fluorescent pattern was consistent with localization to these organelles. In addition, we used SYTOX Green to stain nuclei in fungal fractions (Fig. 4.7, D); again the fluorescent pattern was consistent with the expected results. Under the same magnification, immuno-fluorescence labeling pattern of OmtA (Fig. 4.7, A and B) was different from SKL or SYTOX staining (Fig. 4.7, C and D). Neither anti-SKL nor SYTOX generated the same “patchy” pattern as anti-OmtA.

In summary, the data suggest that, like Nor-1 and Ver-1, OmtA is evenly distributed in all cell types in a fungal colony and does not accumulate to highest levels in conidiophores. The fluorescent signal is not consistent with localization of OmtA to only peroxisomes, Woronin bodies, or nuclei. However, the data do not rule out the possibility that OmtA is localized to other cell locations as well as these specific organelles.

Quantitative fluorescence intensity analysis. The CLSM fluorescence intensities represent the abundance of Nor-1, Ver-1, and OmtA shown in three colony

Figure 4.6. OmtA protein localization in time-fractionated colonies of *A. parasiticus* SU-1, AFS10 (*afR* knockout), CS10 and LW1432 (*omtA* knockout) grown on YES agar for 72 h. Paraffin-embedded fungal sections were immuno-labeled with affinity purified OmtA PAb (20 µg/ml) followed by Alexa 488 conjugated goat anti-rabbit IgG. (A) Fluorescence images of SU-1 (S1, S2, and S3) and AFS10 (R1, R2, and R3). (B) Fluorescence images of CS10 (C1, C2 and C3) and LW1432 (L1, L2 and L3). All colony fractions were analyzed under the same instrument settings. Bars, 50 µm.

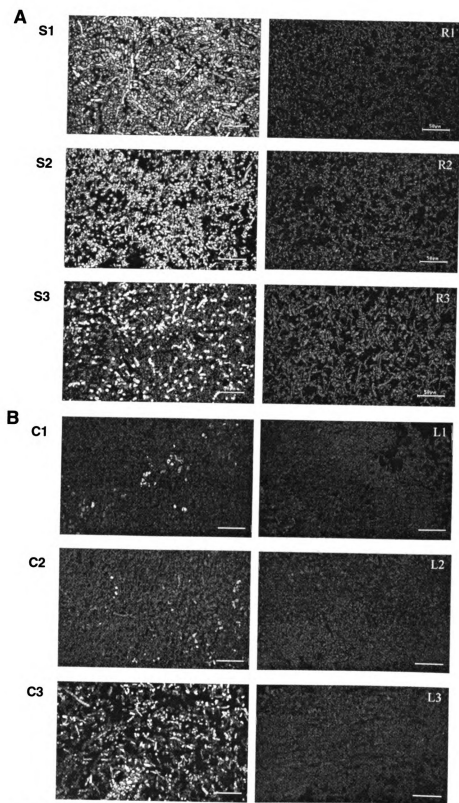


Figure 4.6

Figure 4.7. Protein localization using OmtA PAb and anti-SKL, and detection of nuclei using SYTOX Green. (A) Z-series overlay image of SU-1 (fraction S2) immuno-labeled with OmtA PAb. The image consists of an overlay of ten consecutive optical sections taken at Z-interval of 800 nm (step size). (B) Fluorescence images of vesicles of conidiophores of SU-1 (fraction S1) immuno-labeled with OmtA PAb. (C) Immuno-labeling of SU-1 (fraction S2) with anti-SKL. The magnification for the left panel is 400X and for right panel is 2,000 X. (D) Fluorescence image of nuclei in SU-1 (fraction S2) stained with SYTOX. The magnification for the left panel is 400X and for the right panel is 2,000 X. The bar in panels A, B, C, and D represents 10 μm .

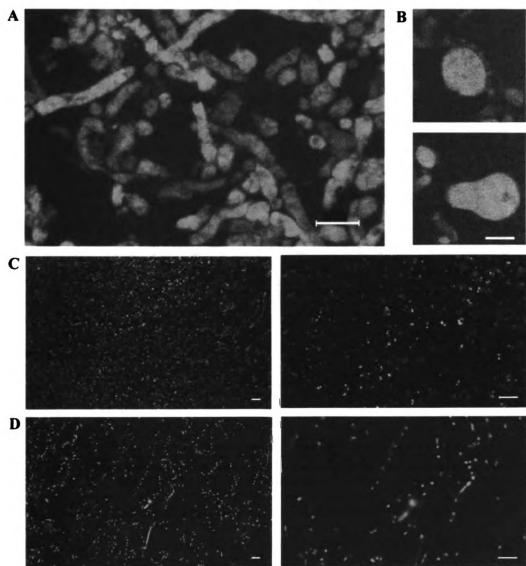


Figure 4.7

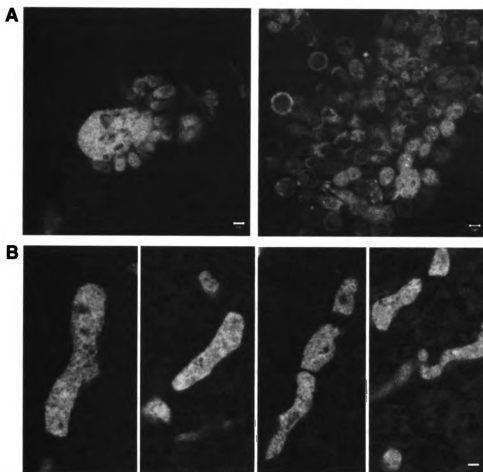


Figure 4.8. CLSM immuno-fluorescence detection of OmtA in *A. parasiticus* SU-1. Fungal cells derived from colony fraction S2 were immuno-labeled with the OmtA antibody followed by goat-anti-rabbit IgG conjugated with an Alexa 488 probe. Single optical sections were acquired using a Zeiss LSM5 Pascal CLSM with a Plan-APOCHROMAT objective (63 X Oil Dic, NA=1.4). (A) Immuno-fluorescence of OmtA was detected in conidiophores. (B) Immuno-fluorescence of OmtA was detected in hyphae. Bars = 2 μ m.

fractions of SU-1. Fluorescence intensities were quantified by measuring the pixel numbers on CLSM micrographs using the IQ Master Program (V2.31) image analysis software. The quantitative pixel analysis to analyze distribution of AF enzymes in colony fractions was consistent with qualitative detection by Western blot analysis and fluorescence microscopy (Lee et al., 2002; Lee et al. submitted). The control strain AFS10 did not produce significant levels of Nor-1, Ver-1 and, OmtA compared to SU-1. These data confirm that the highest quantity of these three aflatoxin enzymes occurs in fraction 2 (Table 4.1).

DISCUSSION

Because a close regulatory association between aflatoxin synthesis and conidiation has been demonstrated in several studies (Guzman-de-Pena and Ruiz-Herrera, 1997; Hicks et al., 1997, Adams et al., 1998), a close temporal and spatial association between AF protein expression and conidiospore development was hypothesized. To test this hypothesis, antibodies against several AF proteins were generated to immunolocalize these proteins. Previous studies (Liang, 1996; Zhou, 1998) utilized a fungal cell preparation technique for immuno-labeling that required digestion of the cell wall using Novozyme (Harris et al., 1994). However, in these early localization studies, variation in cell wall digestion resulted in significant artifacts. The paraffin-embedment and sectioning procedures developed and described in this study successfully preserved fungal mycelium, developmental structures, organelle structure, and protein antigenicity; they also eliminated the need for cell wall digestion, in turn generating consistent and reproducible immuno-labeling results. This technique provides a useful tool to localize proteins and possibly other compounds in fungal cells and colonies.

Despite the close regulatory relationship between sporulation and aflatoxin production, my data suggest that Nor-1, Ver-1, and OmtA are not produced exclusively in conidiophores as hypothesized. On the contrary, CLSM micrographs showed that these

Table 4.1. Quantative fluorescence intensity analysis of *A. parasiticus* SU-1 and AFS10 immuno-fluorescence labeled with Nor-1, Ver-1 and OmtA antibodies.

(Fungal colony)	(SU-1)			(AFS10)		
	<u>S1</u>	<u>S2</u>	<u>S3</u>	<u>R1</u>	<u>R2</u>	<u>R3</u>
Nor-1	229.5	858.4	260.9	15.2	18.7	62.3
Ver-1	144.4	297.9	166.5	68.7	89.2	42.3
OmtA	120.0	940.1	146.7	4.3	3.9	21.6

* The data represent the average pixel number in 20 images from each colony fraction.

proteins are distributed throughout the colony and in both conidiophores and vegetative hyphae. In fraction S2, the highest intensity of AF proteins was detected by CLSM and the signal was observed at similar levels in vegetative hyphae and conidiophores.

CLSM detected Nor-1 and Ver-1 mainly in the cytoplasm. These data are consistent with data from previous subcellular fractionation studies along with Western blot analysis. Nor-1 was mainly detected in the cytosolic fraction (Zhou, 1998), while Ver-1 was present in the cytosol (80%) and the microbody fraction (14%) (Liang, 1996). Based on CLSM data generated in the current study, detection of Ver-1 in particle-like structures by Liang (1996) (presumably microbodies), was an artifact. Cytosolic immuno-fluorescence labeling of Ver-1 was specific in SU-1 and not observed in the negative control strain AFS10. However, immuno-fluorescence of Ver-1 on the cell wall, spore coat, as well as particle-like structures was observed in both SU-1 and AFS10. Ver-1 displays 56% protein sequence similarity to scytalone reductase (Vidal-cros et al., 1994), and 66% identity and 82% similarity to polyhydroxynaphthalene reductase; both enzymes are involved in melanin biosynthesis. Melanins are dark pigments that accumulate in distinct layers of cell walls and spores of many fungi (Wheeler and Bell., 1988). Thus, the PAb against Ver-1 used in this study possibly exhibited cross-reactivity to the cell wall and the spores. In addition, immuno-gold labeling of Ver-1 observed by transmission electron microscopy (TEM) revealed that the labeling pattern of Ver-1 in particle-like structures in SU-1 and AFS10 was not specific to Ver-1. The organelle immuno-labeled by Ver-1 antibody in both SU-1 and AFS10 was identified to be the Woronin bodies. The appearance of this organelle was recently demonstrated in *A. parasiticus* using PAb against a C-terminal tri-peptide Peroxisomal Targeting Sequence I, SKL (Ser-Lys-Leu) (Lee, 2003). The fourteen percent of the Ver-1 associated with the microbody fraction detected by Liang (1996) was possibly due to this non-specific interaction.

Cells immuno-labeled with OmtA PAb and analyzed by CLSM showed patches of fluorescence within fungal cells suggesting that OmtA is confined to sub-cellular compartments. An alternative explanation is that OmtA is present in the cytoplasm and is thus excluded from cell organelles. To gain more information about sub-cellular localization, we labeled paraffin embedded sections to identify specific organelles; for example anti-SKL antibodies (Keller et al., 1991) were used to label peroxisomes and SYTOX Green was used to detect nuclei. Both probes generated small, regularly shaped signals consistent with the expected organelles, indicating that the double-membrane bound nuclei as well as single-membrane bound microbodies were well-preserved. These observations strongly suggest that we have minimized artifacts due to poor sample preparation. Images using both probes were different than with OmtA PAb.

Quantitative fluorescence intensity analysis performed in this study supported qualitative CLSM data for the distribution of AF enzymes in colony fractions. CLSM also generated important information for subsequent determination of sub-cellular localization of AF proteins using high resolution TEM. The specimen size required for TEM cell preparation is extremely small (approximately 1 μm^2 dimension to be sectioned into 100 nm thickness). Therefore, the finding that the S2 fraction exhibited the highest density of AF proteins allowed sample acquisition efficiently (from fraction S2) in order to detect these proteins at the sub-cellular level (Lee, 2003).

ACKNOWLEDGEMENTS

Special thanks to Dr. Shirley Owens (Center for Advanced Microscopy at Michigan State University) for help in quantification of fluorescence intensity and Dr. Jeff Cary (USDA, New Orleans, LA.) for providing the *aflR* knockout strain, AFS10.

Immuno-localization of OmtA is published in *Applied and Environmental Microbiology* (Lee, L.W., C.H. Chiou, and J.E. Linz. 2002. Function of native OmtA *in vivo* and expression and distribution of this protein in colonies of *Aspergillus parasiticus*. Appl. Environ. Microbiol. 68:5718-5727).

Immuno-fluorescence analysis of Nor-1 and Ver-1 is submitted for publication (Lee, L. W., C. H. Chiou, K. L. Klomparens, and J. E. Linz. 2003. Sub-cellular localization of aflatoxin biosynthetic enzymes in time-dependent fractionated colonies of *Aspergillus parasiticus*. Manuscript submitted to Arch. Microbiol.).

CHAPTER 5

Distribution and sub-cellular localization of the aflatoxin enzyme versicolorin B synthase (VBS) in time-fractionated colonies of *Aspergillus parasiticus*

ABSTRACT

Aflatoxins (AF) are highly toxic and carcinogenic fungal secondary metabolites. Aflatoxin biosynthesis in the filamentous fungi *Aspergillus parasiticus* and *A. flavus* requires a complex pathway consisting of at least eighteen enzymatic activities; one of these enzymes, versicolorin B synthase (VBS), catalyzes closure of the bisfuran ring in the racemic versiconal hemiacetal substrate to form versicolorin B. Bisfuran ring formation is important for AF toxicity as the structure is required for the subsequent creation of AFB₁-8,9 epoxide, a potent alkylating agent. I analyzed the localization of VBS in the AF producing strain *A. parasiticus* SU-1 grown on solid media using a colony fractionation technique developed previously. A highly specific polyclonal antibody, raised against a Maltose Binding Protein-VBS fusion protein synthesized in *Escherichia coli*, was utilized to detect VBS in SU-1 grown on a rich solid medium via immunofluorescence confocal laser scanning microscopy (CLSM) and immunogold transmission electron microscopy (TEM). VBS was found not only in vegetative hyphae but also in asexual developmental structures, called conidiophores. Western blot and CLSM analyses demonstrated the highest abundance of VBS in colony fraction S2 where cells had grown for 24 to 48h; this fraction also contained the highest levels of newly developed conidiophores. The highest abundance of AFB₁ also was detected in fraction S2, consistent with VBS abundance. At the sub-cellular level, CLSM and TEM detected VBS at similar levels in the cytoplasm and in ring-like structures surrounding nuclei; it is uncertain if enzymatically active VBS is present in either or both locations.

INTRODUCTION

Aflatoxins (AF), fungal secondary metabolites produced by filamentous fungi including *Aspergillus parasiticus*, *A. flavus*, *A. nomius*, and *A. tamarii*, are highly toxic and carcinogenic compounds (Cary et al., 2000; Eaton & Groopman, 1994; Cotty and Cardwell, 1999). AF contamination in commercial crops including corn, peanuts, tree nuts, and cottonseed has generated significant economic and human health concerns throughout the world (CAST, 2003). Among the members of the AF family, AFB₁ is considered the most dangerous as it is efficiently bioactivated by cytochrome P450 enzymes (particularly in the liver) to form the AFB₁-8,9 epoxide, a potent alkylating agent. The epoxide interacts with the N-7 position of guanine residues in double stranded DNA to generate AFB₁-N7-Gua DNA adducts (Bailey, et al., 1996; Mace, et al., 1997; Aguilar et al., 1993; Eaton and Gallagher, 1994). The tumor suppressor gene *p53* appears to be a frequent target of AFB₁ since mutation of *p53* is often seen in hepatic-cancer patients with high levels of AFB₁ exposure (Yang, et al., 1997). Our goal is to eliminate AF contamination in agricultural commodities and in turn to ensure product safety and consumer health.

AF biosynthesis utilizes a complex pathway requiring at least 18 enzymatic activities (Minto & Townsend, 1997; Payne, 1998; Bhatnagar et al., 2003). The structural genes that encode these aflatoxin enzymes, including *nor-1* (Trail et al., 1994), *ver-1* (Skory et al., 1992), *omtA* (Yu, et al., 1993), *vbs* (Silva et al., 1996), as well as one regulatory gene *aflR* (Chang et al., 1993; Woloshuk et al., 1994), are clustered in a 75 kb chromosomal region (Trail et al., 1995; Minto & Townsend, 1997; Payne and Brown, 1998; Cary et al., 2000; Bhatnagar et al., 2003). Although most AF biosynthetic genes have been cloned and characterized, the mechanisms that regulate AF biosynthesis are not completely understood. The positive-acting GAL4-type transcription factor AflR is required for AF biosynthesis (Chang et al., 1993; Ehrlich et al., 1999a; Ehrlich, et al., 2003). A recent report also described cluster-dependent positional effects on AF

biosynthesis. The *nor-1* promoter is positively regulated within the AF gene cluster whereas outside the cluster (*niaD* or *pyrG*), *nor-1* promoter activity decreases dramatically (Chiou et al., 2002).

To date, little is known about how or where aflatoxin enzymes interact at the cellular level to synthesize AFB₁. To address this issue, our laboratory developed a colony fractionation protocol and immuno-fluorescence and immuno-gold based microscopic methods to localize proteins involved in AF biosynthesis. Previously, we analyzed the distribution of OmtA, an enzyme involved in the later stages of AF biosynthesis (Lee et al. 2002). The highest abundance of OmtA was detected in fungal cells grown for 24 to 48 h (fraction S2) in *A. parasiticus* strain SU-1 grown on a solid medium (YES). Immuno-fluorescence confocal laser scanning microscopy (CLSM) detected OmtA in the cytoplasm and the protein frequently was confined to discrete areas in cells in this colony fraction. Transmission electron microscopy (TEM) together with immuno-gold labeling suggested that OmtA and the aflatoxin enzymes Nor-1 and Ver-1 are found in the cytoplasm; of particular interest, OmtA was also detected at high levels in vacuole-like organelles in cells residing near the substrate surface of the colony (Lee et al., manuscript submitted). These observations caused us to propose that early aflatoxin enzymes function in the cytoplasm while later pathway enzymes are localized to organelles either to protect cells from the toxic effects of late pathway intermediates or to reduce the level of aflatoxin synthesis via protein turnover. In this report, we investigate the localization of another key enzyme involved in AF biosynthesis, versicolorin B synthase (VBS), in *A. parasiticus* to determine if the data support or refute the proposed model.

VBS catalyzes the cyclization of the racemic versiconal hemiacetal substrate and closure of the bisfuran ring to form versicolorin B (Lin and Anderson, 1992; Anderson and Chung, 1994; Silva et al., 1996). The bisfuran ring structure is required for the subsequent creation of the AFB₁-8,9 epoxide and toxicity. *vbs* encodes a protein of 634

amino acids

116, 221.

flavin-dep

and does

The pred

VBS app

by SDS

and VB

mass is

VBS v

hetero

main

trans

reco

loca

was

hyp

new

gro

sec

betw

and

in r

tem

sug

amino acids (VBS) that contains 3 putative *N*-glycosylation sites at amino acid residues 116, 221, and 507 (Silva et al., 1996). VBS displays sequence similarity to several flavin-dependent oxidases and dehydrogenases but it does not catalyze a redox reaction and does not bind FAD or FMN to its truncated FAD binding domain (Silva et al., 1996). The predicted molecular mass of VBS based on the cDNA sequence is 70 kDa, yet native VBS appears as a homo-dimer with a monomeric molecular mass of 78 kDa (estimated by SDS-polyacrylamide gel electrophoresis). *N*-glycosidase F treatment of native VBS and VBS heterologously expressed in yeast revealed that the discrepancy in molecular mass is attributed to *N*-glycosylation (Silva et al., 1997). The N-terminus of the native VBS was also reported to be post-translationally modified (Silva et al., 1996). VBS heterologously expressed in *E. coli* was not active, whereas VBS expressed in yeast maintained its activity, suggesting that *N*-glycosylation and perhaps other post-translational modifications are essential for VBS activity (Silva et al., 1997).

In the current study, a highly specific PAb was produced in rabbits using a recombinant maltose binding protein (MBP)-VBS fusion expressed in *E. coli*. VBS localization was conducted by fluorescence-based CLSM and immuno-gold TEM. VBS was observed throughout a 72 h-old colony and was detected not only in vegetative hyphae but also at similar levels in conidiophores. The highest levels of VBS, AFB₁, and newly developed conidiophores were present in colony fraction S2 where the cells had grown for 24 to 48 h. These observations suggest a strong spatial association between secondary metabolism and asexual sporulation; a regulatory and temporal association between these processes was reported previously (Adams et al., 1998; Guzman-de Pann and Ruiz-Herrera, 1997; and Calvo et al, 2002).

At the sub-cellular level, VBS was detected in the cytoplasm and at similar levels in ring-like structures surrounding nuclei; based on morphology, these structures were tentatively identified as endoplasmic reticulum (ER). Computer-based sequence analysis suggested that VBS contains a putative signal peptide at the N-terminus. Because VBS is

N-link glycosylated, we propose that VBS is associated with the ER/golgi secretory pathway for transient co- and post-translational modification and localizes to the cytoplasm where it participates in aflatoxin synthesis. However, based on the data, it is currently uncertain if the ER, the cytoplasm, or both locations represent the final destination for VBS activity.

MATERIALS AND METHODS

Fungal strains and growth conditions. The wild type aflatoxin producing strain *A. parasiticus* SU-1 (NRRL5862, ATCC 56775) and a non-aflatoxin producing strain AFS10 (*aflR* knockout mutant, kindly provided by Dr. Jeffrey Cary, USDA, New Orleans, LA) (Cary et al., 2002) were used to study VBS and other AF enzymes. For liquid culture, a conidiospore suspension (2×10^7 conidiospores) was inoculated into a 250 ml Erlenmeyer flask containing 100 ml YES media (2% yeast extract, 6% sucrose, pH5.5) and incubated at 29°C with constant shaking (150 rpm) for 24 h to 72 h. For solid culture, conidiospores ($2 \times 10^5/\mu\text{l}$) were center inoculated onto YES agar (1.5%) overlaid with sterile cellophane membranes and cultured in the dark at 29°C for 24 h, 48 h, or 72 h.

Production of antibodies against native VBS. Native VBS purified from *A. parasiticus* SU-1 was kindly provided by Dr. Craig Townsend, Johns Hopkins University (McGuire et al., 1996). Approximately 30 μg of protein was mixed in a 1: 1 (V/V) ratio with TiterMax adjuvant (CytRx, Norcross, GA) and used to immunize two New Zealand White rabbits. After 30 d, a booster injection with the same dose of VBS/TiterMax emulsion was utilized. Twenty-one d later, the anti-serum was collected and the serum IgG was precipitated in 33% ammonium sulfate according to standard protocols (Ausubel et al., 2003).

Generation of MBP (Maltose Binding Protein)-VBS fusion protein. Three possible reading frames of the *vbs* exon II fragment were amplified by PCR based on the published sequence (Silva et al., 1996) using *A. parasiticus* SU-1 genomic DNA as a template. To generate VBS clones with each of the three possible reading frames, PCR amplification was conducted using three forward primers containing 23 nucleotides including an *EcoRI* restriction endonuclease site (underlined) [(1) 5' agaGAATTC-agAGGCTCGAAAGG-3', (2) 5' tagGAATTCcag AGGCTCGAAAG-3', and (3) 5'-ctaGAATTC-tcagAGGCTCGAAA-3'] and one reverse primer (5'-ATCAAAGCTT-GGTCTACTGCCAG-3') containing a *HindIII* restriction endonuclease site (underlined). Each 1.4 kb *vbs* fragment was individually cloned into the pMAL-c2 expression vector (New England Biolabs, Beverly, Mass.) to generate expression plasmids, pMAL-c2-vbs1, pMAL-c2-vbs2, and pMAL-c2-vbs3. These plasmids were transformed into *E. coli* to express the 94 kDa MBP-VBS fusion protein. The fusion protein was induced in large scale culture by addition of 0.5 mM IPTG at optimum cell density (O.D.₆₀₀ approximately 0.6). Cells were disrupted by a brief freeze and thaw cycle followed by sonication on ice (Sonifier cell disrupter W-350; Fisher Scientific, Pittsburgh, PA). The induced soluble MBP-VBS was purified with amylose resin according to the manufacturer's instructions (New England Biolabs, Beverly, Mass.).

Production and purification of PAb against MBP-VBS. Purified recombinant MBP-VBS was injected into two New Zealand White rabbits. Each rabbit was immunized subcutaneously with approximate 50 µg purified MBP-VBS mixed at a 1: 1 (V/V) ratio with TiterMax adjuvant (CytRx, Norcross, Ga). After 32 d, a booster injection with the same amount of protein/TiterMax emulsion was utilized. Anti-sera collection was performed after an additional 30-d and approximately 60 ml of anti-sera were obtained from each rabbit. Serum IgG was precipitated in 33% ammonium sulfate as described previously (Ausubel et al., 2003). Because immuno-gold TEM studies require low background signals, anti-VBS IgG was further purified by affinity

chromatography. The anti-VBS IgG was passed through a column containing proteins extracted from AFS10 (non-AF producing, does not synthesize VBS) grown in liquid YES medium for 48 h as described by Lee et al., (2002); the extracted proteins were conjugated to a resin mixture of Affi-Gel 10 and Affi-Gel 15 (BioRad, Hercules, Calif.). The flow-through fraction (containing the cleaned-up IgG) was dialyzed against phosphate buffered saline (PBS)(Ausubel et al., 2003) and used for immunogold-labeling on ultra-thin fungal sections (described below).

Time-dependent fractionation of fungal colonies. A 72 h-old colony grown on YES agar was fractionated according to Lee et al. (2002). Briefly, at 24 h intervals during growth, the culture plate was marked on the bottom to indicate the location of the outer margin of the colony. After 72 h of culture, the colony was dissected into 3 fractions (concentric rings) using these marks. Fractionation of 72 h-old SU-1 colonies (AF producing strain) generated fractions S1 (48 to 72 h), S2 (24 to 48 h), and S3 (0 to 24 h). Fractionation of AFS10 (*aflR* knockout mutant) resulted in analogous fractions R1, R2, and R3 (using the same scheme).

Fungal protein extraction. Mycelia from liquid culture were collected by filtration through miracloth (Calbiochem, La Jolla, Calif.) by aspiration. Mycelia from solid culture fractions were generated as described above and peeled directly from the cellophane membrane. The fungal mycelia were then pulverized under liquid nitrogen with a mortar and pestle and fungal proteins were extracted using TSA buffer (2 mM Tris-Cl, pH 8.0; 40 mM NaCl; and 0.025% sodium azide) containing complete protease inhibitors (2 tablets/10 ml buffer, Roche Molecular Biochemicals, Indianapolis, Ind.). The resulting extracts were centrifuged at 12,000 g for 20 min at 4°C to remove mycelia. The supernatant (fungal protein extract) was transferred to microcentrifuge tubes in small aliquots and stored at -80°C. Protein concentration was determined using Bio-Rad protein assay reagent (Bio-Rad, Hercules, Calif.) and bovine serum albumin (BSA, Sigma-Aldrich, St. Louis, Mo.) as a standard.

SDS-Polyacrylamide Gel Electrophoresis (SDS-PAGE) and Western blot analysis. SDS-PAGE was conducted using a standard procedure (Ausubel et al., 2003) to analyze expression of recombinant MBP-VBS and other fungal proteins. The molecular mass was determined by comparison to Low-Range Prestained SDS-PAGE standards or SDS-PAGE Molecular Mass Standards-low range (Bio-Rad, Hercules, Calif.). For immunoblotting, 30 to 60 µg of fungal proteins were separated by SDS-PAGE (electrophoresis on 10% or 12% polyacrylamide gels) and transferred onto PolyScreen PVDF membrane (Dupont Biotechnology Systems, NEN Research Products, Boston, Mass.). The membranes were blocked with 1% casein in TBST (10 mM Tris-Cl, pH 8.0; 150 mM NaCl; and 0.05% Tween 20) at RT for 1 h. The blots were probed with anti-VBS IgG (2 µg/ml) followed by goat anti-rabbit IgG alkaline phosphatase conjugate (Sigma-Aldrich, St. Louis, Mo.) as the secondary Ab probe (1: 5,000 dilution) at RT for 30 min. Reactive proteins were visualized using the BCIP/NBT colorimetric detection system (Roche Molecular Biochemicals, Indianapolis, Ind.).

Detection of AFB₁ in colony fractions. (i) Thin Layer Chromatography (TLC). Fungal colony fractions (from replica plates) were placed into glass scintillation vials for measurement of dry weight, followed by extraction of AFB₁ using 5 ml chloroform. The chloroform extract (5 µl) was dotted onto silica plates (LHPKD Silica Gel 60 A, 10 cm x 10 cm; Whatman International Ltd., Maidstone, England) for TLC with a solvent system consisting of 5% acetone/ 95% chloroform. AFB₁ was detected under long-wave UV light. **(ii) Enzyme-Linked-Immunosorbent-Assay (ELISA).** AFB₁ in each colony fraction was quantified by a competitive-sandwich ELISA method described previously (Pestka *et al.*, 1980). One ml of AF extract (in chloroform) was evaporated under N₂ and re-suspended in 0.5 ml methanol. The assay plates were coated with anti-AFB₁ antibodies (Sigma-Aldrich), incubated at 42°C over night and blocked with 1% BSA-PBS at 37°C for 30 to 60 min. Serially diluted samples as well as AFB₁ standard (Sigma-Aldrich) were mixed with the AFB₁-horse radish peroxidase (HRP)

conjugates (kindly provided by Dr. Pestka, Michigan State University) as a competitor, followed by incubation with the substrate ABTS (2,2'-Azino-bis(3)-ethylbenzothiazoline-6-sulfonic acid) to generate a detectable signal at an absorption wavelength at 405 nm. The concentration of AFB₁ was determined according to the standard curve. The levels of AFB₁ measured in a colony fraction were normalized to dry weight (AFB₁ [μ g]/fraction weight [g]).

Preparation of paraffin-embedded fungal sections and immuno-fluorescence labeling. Fungal samples were derived from a whole 48 h colony or colony fractions generated from a 72 h-old colony. The detailed procedure to prepare the paraffin-embedded fungal sections for immuno-fluorescence microscopy was described previously (Lee, et al., 2002). Specimens (5 mm) were cut from each colony fraction, fixed with Streck tissue fixative (Streck Laboratory Inc., Omaha, Nebr.) at 4° C overnight, followed by dehydration in a graded series of ethanol, and finally embedded in Paraplast (Sigma-Aldrich). Fungal sections (4-5 μ m thickness) were generated using a tissue section microtome (AO Spencer 820 microtome, Fisher Scientific) and attached to poly-L-Lysine (Sigma-Aldrich) coated coverslips (22 mm square) (Corning Glass Works, Corning, NY). Prior to immuno-labeling, sections required removal of paraffin by 100% xylenes, and re-hydration with decreasing concentrations of ethanol, followed by an antigen retrieval procedure (heating the sections in 10 mM citrate buffer, pH 6.0 at 95° C for 5 min and cooling at room temperature for 20 min). After blocking the samples with TBS containing 1% BSA and 0.1% saponin at 4° C overnight, the samples were immuno-labeled with one of the following primary antibodies: 20 μ g/ml of anti-VBS IgG (generated in this paper); 20 μ g/ml purified anti-OmtA IgG (Lee et al., 2002); 20 μ g/ml anti-Ver-1 IgG (Liang et al., 1997); or a 1:500 dilution of Nor-1 antiserum (Zhou, 1997; Lee et al., manuscript submitted) at room temperature for 1.5 h, followed by incubation with the secondary antibody conjugated with a fluorescent probe (Goat anti-rabbit IgG-

Alexa 488 conjugate [5 µg/ml]; Molecular Probes; Eugene, OR), at RT for 1 h. Selected coverslips were subsequently stained with SYTOX orange dye (Molecular Probes; Eugene, OR) to localize the nucleus.

Confocal Laser Scanning Microscopy (CLSM). To determine the distribution of VBS in colony fractions, fluorescence image acquisition and quantitative intensity analysis of one colony of SU-1 and AFS10 was conducted using a Zeiss Axioskop microscope equipped with a Meridian Insight confocal laser scanning system (Meridian Inc. Okemos, Mich.) as described by Lee, et al. (manuscript submitted). Due to damage to the detector in this microscope, the remaining samples were viewed using a Zeiss LSM5 Pascal Laser Scanning Microscope with the same 40X objective lens (Plan NEOFLUAR 40 X/ 1.3 Oil Dic, NA=1.3). High resolution single confocal images, extended focus image made from Z-stacks, or DIC (Differential Interference Contrast) images were taken using a Zeiss Plan-APOCHROMAT (63 X/ 1.4 Oil Dic, N.A.=1.4) objective. Detection of the Alexa 488 fluorescence probe (*Abs/Em* 495/519 nm) was conducted using a BP 505-530 emission filter set under excitation with the 488 nm argon-ion laser line and detection of SYTOX orange (*Abs/Em* 547/570 nm) was performed using the BP 560-615 nm emission filter set under the 543 nm helium-neon laser.

Quantitative fluorescence intensity analysis. Samples derived from three SU-1 replicate colonies were immuno-labeled with anti-VBS or OmtA and subjected to fluorescence intensity analysis by quantifying the pixel number in 20 randomly selected images. Pixels were analyzed using IQ Master Program (V2.31) image analysis software that accompanied the Meridian Insight laser-scanning microscope (Meridian Instrument, Inc., Okemos, Mich.) or on a Macintosh using a NIH image program (developed at the U.S. National Institutes of Health and available on the web: <http://rsb.info.nih.gov/nih-image/>). For the samples derived from the same immuno-labeling experiment (both SU-1 and the negative control AFS10), the CLSM images were acquired under identical

instrument settings. For each colony fraction, average pixel number in the 20 images was reported.

Statistical analysis. Fluorescence intensity data were statistically analyzed by a complete random design with a split-plot model using SAS software (SAS Institute Inc. Cary, NC) or two-way ANOVA using SigmaStat (SPSS Inc. Chicago, Ill.). The amount of AFB₁ in three colony fractions was analyzed by one-way ANOVA using SigmaStat. Statistical significance among samples was defined by a *P*-value not greater than 0.05.

Preparation of ultra-thin fungal sections, immuno-gold labeling, and TEM analysis. Ultra-thin sections were generated from colony fractions S2 and R2. Sample preparation and immuno-gold labeling followed the procedures described by Lee et al. (manuscript submitted). Briefly, samples were prepared by a freeze-substitution method (Flegler et al., 1995) and embedded in LR White resin (Ted Pella Inc., Redding, CA). Ultra-thin sections (90-100 nm) were generated using an MTX ultra-microtome (RMC, Tucson, AZ) and mounted onto formvar-coated nickel grids. Sections were immuno-labeled with column-purified anti-VBS IgG (50 µg/ml), followed by goat anti-rabbit IgG conjugated with 10 nm gold (Ted Pella. Inc., Redding, CA); sections were subsequently post-stained with 3% uranyl acetate for 20 min. Samples were observed using a JEOL 100CX II transmission electron microscope (Tokyo, Japan) at 100 kV acceleration voltage .

RESULTS

Generation of PAb against native fungal VBS. An anti-VBS PAb preparation was generated using native VBS purified from *A. parasiticus* SU-1 as an immunogen. Only 60 µg of VBS protein was available for immunization split between a primary and booster injection into two rabbits. The resulting PAb recognized VBS heterologously expressed in yeast but also appeared to cross-react with fungal proteins other than VBS. To remove cross-reactive antibodies, we pre-absorbed the IgG fraction with proteins in a

fungal extract isolated from SU-1 grown for 24 h in liquid YES culture (conditions which generate little detectable VBS expression). The resulting IgG recognized a single sharp band in heterologous VBS expressed in yeast (78 kDa) but several proteins in SU-1. Among these SU-1 proteins, two closely associated protein bands (one band equal to 78 kDa and a smaller band of approximately 72 kDa) appeared to be VBS based on pattern of accumulation; they were only detected at 48 h and 72 h but not at 24 h in the SU-1 extracts (Fig. 5.1). Although this clean-up procedure reduced the cross-reactivity, the remaining background signals could generate considerable artifacts during an immunocytochemistry study. Thus, anti-VBS antibodies with higher specificity were produced using an alternate procedure.

Expression of MBP-VBS fusion protein and production of PAb against VBS.

To assure production of full-length protein, we amplified (PCR) three reading frames of VBS exon II based on the published sequence (Silva et al., 1996) and cloned these PCR fragments into the pMAL-c2 expression vector to generate the MBP-VBS fusion proteins. *E. coli* harboring pMAL-c2-vbs1 expressed the expected 94 kDa MBP-VBS fusion protein (Fig. 5.2) whereas *E. coli* harboring pMAL-c2-vbs2 and pMAL-c2-vbs3 generated pre-maturely terminated protein products (molecular masses of 45 kDa and 55 kDa, respectively). Control *E. coli* carrying the backbone vector, pMAL-c2 (*malE::lacZ*) produced a 52 kDa MBP- β -galactosidase fusion protein (Fig. 5.2).

The MBP-VBS fusion protein was purified and injected into two rabbits to generate PAb. We initially intended to isolate VBS by removing MBP from the fusion protein using factor Xa (IEER, Ile-Glu-Glu-Arg recognition). However, treatment fragmented VBS as well (Fig. 5.3) even though there is no factor Xa cleavage site found in the VBS exon II sequence. Thus cleavage within VBS appeared to be non-specific. We consequently used the entire MBP-VBS fusion protein to generate PAb.

Based on Western blot analysis, PAb raised against MBP-VBS displayed a higher specificity (Fig. 5.4) than PAb raised against the native VBS (Fig. 5.1). The serum

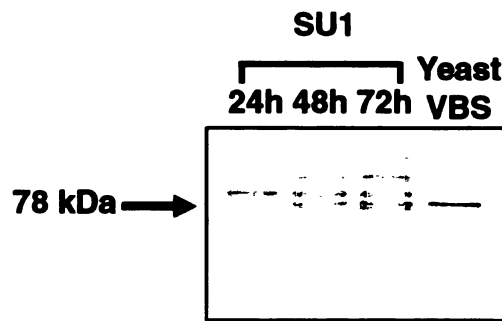


Figure 5.1. Western blot analysis of VBS detected by PAb raised against native fungal VBS. Fungal proteins were extracted from *A. parasiticus* SU-1 grown in liquid YES medium for 24 h, 48 h, and 72 h. Proteins were separated by SDS-PAGE (12% acrylamide gel), transferred onto PVDF membrane and probed with rabbit serum IgG raised against native VBS (2 $\mu\text{g}/\text{ml}$) that had been preabsorbed with protein isolated from SU-1 cultured in liquid YES medium for 24 h. Heterologous VBS expressed in yeast is shown as a control. The apparent molecular mass for the target protein is 78 kDa.

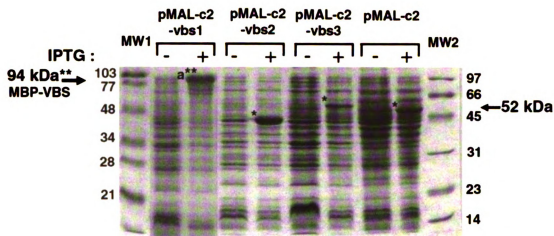


Figure 5.2. SDS-PAGE of recombinant MBP-VBS fusion proteins. Three reading frames of *vbs* exon II sequences were amplified from genomic DNA of SU-1 and PCR fragments cloned into pMAL-c2 expression vector generating three frame-shift plasmids, pMAL-c2-vbs1, pMAL-c2-vbs2, and pMAL-c2-vbs3 (see Materials and Methods) that were subsequently transformed into *E. coli* DH5 α . The in-frame MBP-VBS had the predicted molecular mass of approximately 94 kDa (a**). As a control, *E. coli* carrying the backbone vector, pMAL-c2 containing *malE::lacZ*, expressed only the MBP- β -galactosidase fusion protein (52 kDa). The induced fusion proteins (IPTG+) are indicated with symbols * or **.

Figure 5.3. MBP-VBS treated with Factor Xa to generate MBP (42 kDa) and VBS (52 kDa). The purified MBP-VBS (94 kDa) produced in *E. coli* was incubated with Factor Xa at RT for 0 h, 2 h, 4 h, 8 h, and 24 h. As a control, an equal amount of MBP-VBS without incubation with Factor Xa was set at RT for 8 h and 24 h. (A) SDS-PAGE analysis. Samples were separated by electrophoresis on a 10% polyacrylamide gel and stained with coomassie blue. Molecular mass markers are shown at both sides of the gel. (B) Western blot analysis. Samples separated by SDS-PAGE were transferred onto PVDF membrane. The blot was incubated with anti-VBS IgG (2 µg/ml, raised against native VBS) and Goat anti- rabbit IgG conjugated with alkaline phosphatase, followed by colorimetric detection by BCIP/NBT.

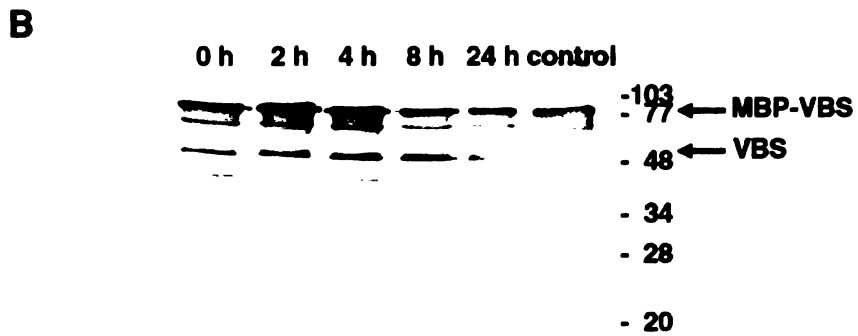
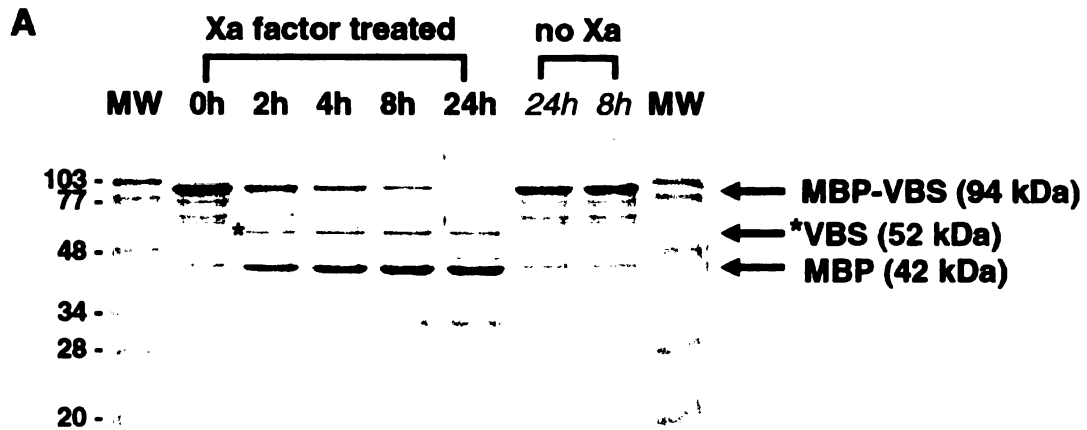


Figure 5.3

recognized VBS expressed in yeast and native VBS present in a 72 h culture of SU-1 grown in YES (Fig. 5.4, A). SU-1 cultured in YEP medium (contains peptone instead of sucrose and does not support AF biosynthesis) did not produce detectable VBS (Fig. 5.4, B). VBS was not observed in a 24 h SU-1 in YES liquid-shake culture (Fig. 5.4, A and C) while VBS was abundant at 48 h (Fig. 5.4, C).

Expression of VBS in *A. parasiticus* grown on solid medium. In liquid-shake culture, fungal cells are maintained as vegetative hyphae and also produce secondary metabolites at highest levels during a transition between active growth and stationary phase. However, normal developmental processes such as asexual sporulation are not observed under such growth conditions. Thus, I cultured *A. parasiticus* on a solid medium that supports native morphology and asexual development including the genesis of conidiophores and asexual conidiospores.

Western blot analysis using the highly specific VBS PAb (MBP-VBS) was conducted on fungal total proteins isolated from SU-1 and AFS10 colonies grown on solid YES medium for 24 h, 48 h, and 72 h (Fig. 5.5). No VBS was detected in the control strain AFS10 (Fig. 5.5, A and B). A 24 h-old SU-1 colony did not contain detectable VBS whereas colonies cultured for 48 h and 72 h did contain detectable levels of VBS (Fig. 5.5, A), a result similar to liquid-shake culture (Fig. 5.4, C). We then analyzed time-dependent expression of VBS; a 72 h-old SU-1 colony grown on solid YES was fractionated into S1 (48 to 72 h), S2 (24 to 48 h), and S3 (0 to 24 h); AFS10 was similarly fractionated to generate R1, R2, and R3. Western blot analysis detected VBS in all three SU-1 fractions but not in any AFS10 fraction (Fig. 5.5, B). Fraction S2 appeared to contain the highest abundance of VBS. Similar results for OmtA (Lee et al., 2002), Ver-1, and Nor-1 were reported previously (Lee et al., manuscript submitted). The intact form of VBS (78 kDa) appeared in all SU-1 samples and little degradation was apparent.

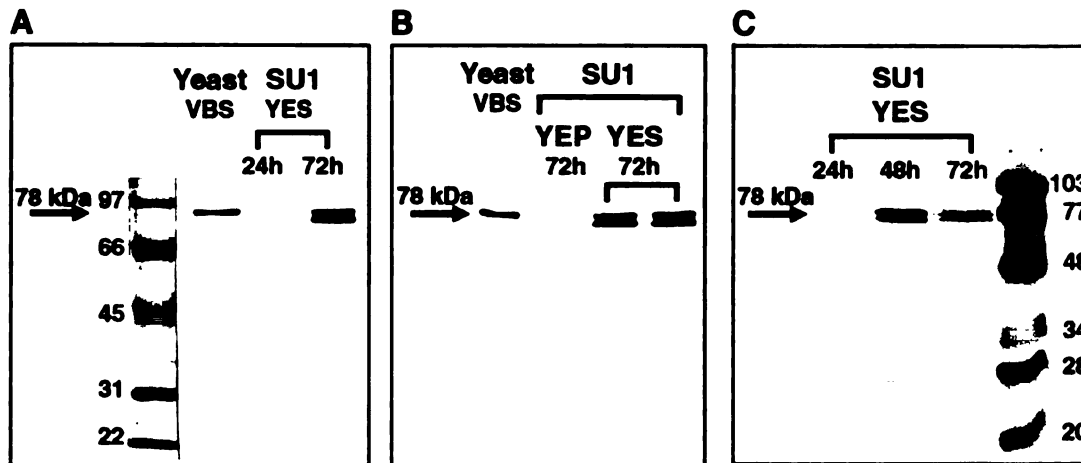


Figure 5.4. Western blot analysis of VBS produced in liquid shake culture using highly specific PAb raised against MBP-VBS. (A) Analysis of protein isolated from *A. parasiticus* SU-1 grown in liquid-shake YES (yeast extract sucrose) culture for 24 h or 72 h. (B) Analysis of proteins isolated from SU-1 grown in liquid-shake YES or YEP (yeast extract peptone) culture for 72 h. In panels A and B, samples were electrophoresed on 10% polyacrylamide gels and subsequently probed with a 1:5000 dilution of anti-serum. VBS expressed in yeast was used as a control. (C) Time-course expression of VBS in SU-1 grown in liquid-shake YES culture for 24 h, 48 h, and 72 h. Proteins were separated by electrophoresis on a 12% polyacrylamide gel and subsequently probed with 2 μ g/ml of serum IgG. The primary signal is shown with the molecular mass of 78 kDa.

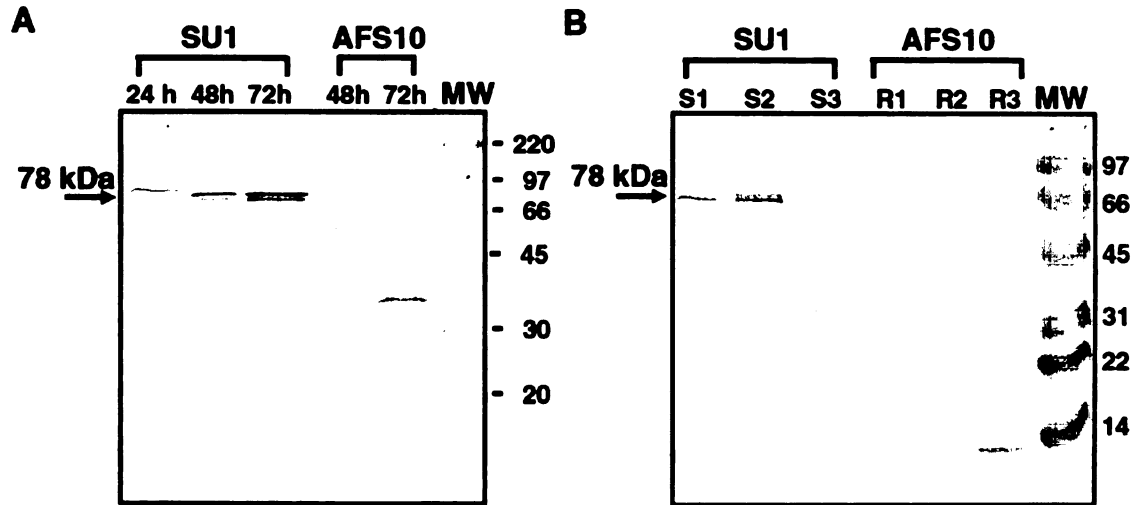


Figure 5.5. Western blot analysis of VBS expressed in *A. parasiticus* SU-1 colonies (solid culture) and colony fractions. (A) VBS expressed in *A. parasiticus* colonies of different ages. Proteins were isolated from colonies of SU-1 and AFS10 (*aflR* knockout strain) grown on solid YES medium for 24 h, 48 h and 72 h. (B) Distribution of VBS in time-dependent colony fractions. The 72 h-old colonies of SU1 and AFS10 grown on YES solid media overlaid with a cellophane membrane were divided into 3 fractions based on time of growth (S1: 48-72 h; S2: 24-48 h; S3: 0-24 h) according to Materials and Methods. Approximately 60 μ g of fungal proteins were loaded in each lane of a 12% polyacrylamide gel. Both blots were probed with specific anti-VBS IgG (2 μ g/ml). The molecular mass markers (MW) are shown on the right of each blot. Native VBS has a mass of 78 kDa.

Confocal Laser Scanning Microscopy (CLSM) of time-dependent expression of VBS in a 72 h-old fungal colony. Fungal tissues from three colony fractions (72 h-old SU-1 or AFS10 colonies grown on YES solid medium) were fixed and embedded in paraffin to generate sections for immuno-labeling. CLSM detected significant fluorescence in all SU-1 fractions (Fig. 5.6, A), while little fluorescence was observed in AFS10 (Fig. 5.6, B). Thus, the corresponding AFS10 bright field images are shown to indicate that similar numbers of the AFS10 cells were analyzed (Fig. 5.6, B, insets). Fluorescence intensity analysis via CLSM (Fig. 5.6, A) appeared to parallel Western blot analysis (Fig. 5.5, B) in that highest intensities were observed in fraction S2; here, VBS was present in both substrate level mycelia (Fig. 5.8, A, B, and C) and in conidiophores (Fig. 5.8, D). To confirm this observation, we immuno-localized VBS and OmtA in 2 additional colonies and analyzed the fluorescence intensity quantitatively.

Fluorescence intensity quantification and statistical analysis. Pixel analysis was performed on images generated from three independent colonies (designated A, B, and C)(Table 1). Pairwise comparison confirmed that the levels of OmtA in fraction S2 (cultured for 24 to 48 h) were significantly higher than the other two fractions of SU-1 (S2 vs. S1, $P=0.0003$; S2 vs. S3, $P < 0.0001$). The levels of VBS detected by fluorescent antibody were consistently higher in fraction S2 than in fractions S1 and S3 although the difference was not statistically significant (S2 vs. S1, $P=0.3529$; S2 vs. S3, $P=0.1230$).

Production of AFB₁ in colony fractions. TLC analysis did not detect AFB₁ in the control strain AFS10 while significant quantities of AFB₁ were detected in all 3 SU-1 fractions (Fig. 5.7). The quantity of AFB₁ extracted from fraction S2 was higher than from fractions S1 and S3 based on TLC (Fig. 5.7) and ELISA (Table 5.2), yet the difference was not statistically significant ($P=0.0589$).

Sub-cellular localization of VBS. Using CLSM and anti-VBS probes, fluorescent signals appeared in the cytoplasm of hyphae of SU-1 in fraction S2 and these

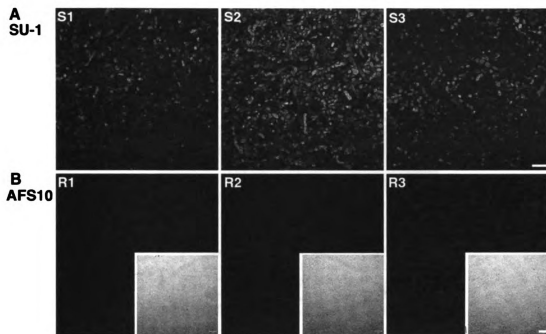


Figure 5.6. CLSM of VBS protein distribution in time-fractionated colonies of *A. parasiticus* SU-1 (S1, S2, S3) and AFS10 (R1, R2, and R3) grown on YES agar for 72 h. Paraffin-embedded fungal sections derived from various colony fractions (see Material and Methods) were immuno-labeled with anti-VBS IgG (20 $\mu\text{g}/\text{ml}$) followed by Alexa 488 conjugated goat-anti rabbit IgG. The associated bright field images (insets in B) demonstrate the numbers of AFS10 cells being analyzed. Bars, 10 μm .

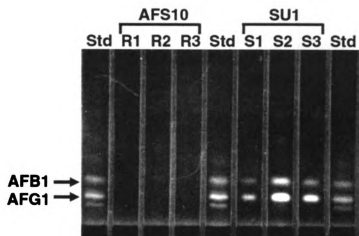


Figure 5.7. Thin Layer Chromatography analysis of AFB₁ accumulation in colony fractions. Colony fractions of *A. parasiticus* SU-1 (S1, S2, and S3) and AFS10 (R1, R2, and R3) were extracted in 5 ml chloroform and 5 μ l were resolved on silica plates. Aflatoxin standard (Std) is shown on both sides and in the middle lane. Fluorescence of AF was detected under long-wave UV light ($\lambda = 360$ nm).

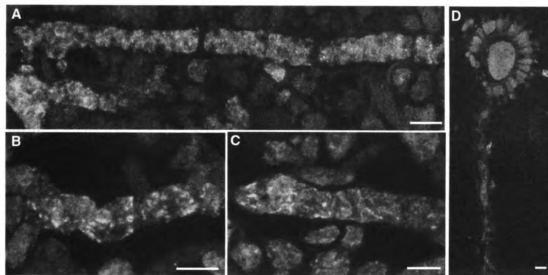


Figure 5.8. CLSM immuno-fluorescence of VBS of *A. parasiticus* SU-1 grown in solid culture. Immuno-fluorescence of VBS was detected in the hyphae of SU-1 shown as extended focus images of CLSM Z-stacks (A and B) and a single optical section (C). (D) Presence of VBS in a conidiophore shown in an extended focus image. Bars, 5 μ m.

Table 5.1. Quantitative fluorescence intensity analysis* of *A. parasiticus* SU-1 and AFS10 labeled with polyclonal antibodies to VBS and OmtA.

(Fungal colony)	(SU-1)			(AFS10)		
	<u>S1</u>	<u>S2</u>	<u>S3</u>	<u>R1</u>	<u>R2</u>	<u>R3</u>
VBS						
Colony A^a	18.46	42.37	15.02	9.48	9.77	8.06
B^b	11.60	29.00	6.22	5.75	5.73	7.25
C^b	6.48	11.92	5.05	3.00	3.26	3.89
OmtA						
Colony A^a	7.53	58.79	9.20	0.29	0.28	1.38
B^b	15.22	37.08	2.55	1.04	1.65	2.85
C^b	9.27	28.28	2.29	0.86	1.84	1.69

* The data represent the average pixel number of 20 images from each colony fraction.

a. Images of colony A were generated by the Meridian Insight confocal laser scanning system and pixel analysis by NIH image program.

b. Images of colony B and C were generated using the Zeiss LSM5 Pascal Laser Scanning Microscope and pixel analysis by NIH image program.

Table 5.2. Quantitative detection (ELISA) of AFB₁ in colony fractions of SU-1 cultured on YES solid media for 72 h.

(Fungal strain)	(SU-1)		
	S1	S2	S3
Colony A	295.59	490.41	245.83
Colony B	204.82	451.24	252.82

* The levels of AFB₁ measured in the colony fraction were normalized to AFB₁ (μg)/fraction weight (g).

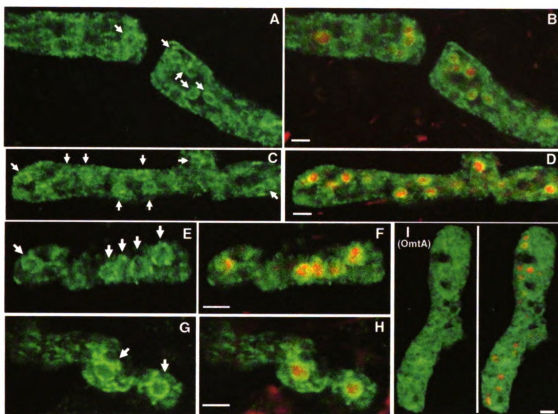


Figure 5.9. CLSM dual detection for localization of VBS and nuclei in *A. parasiticus* SU-1. Fungal sections generated from colony fraction S2 were immuno-labeled with anti-VBS IgG (20 $\mu\text{g}/\text{ml}$) followed by Alexa 488 conjugated goat-anti rabbit IgG (represented in green) and further stained with SYTOX orange dye to contrast the localization of nuclei (represented in red). Immuno-fluorescence of VBS (single green channel) is shown in panels A, C, E, and G. The ring-like fluorescence signals are indicated with arrows. The merged dual channel images indicating localization of VBS (represented in green) and nuclei (represented in red) are shown at the right of each of the image pairs (panels B, D, F, and H). Immuno-fluorescence pattern of OmtA (panel I, immuno-labeled with 20 $\mu\text{g}/\text{ml}$ anti-OmtA IgG) and nuclear staining are shown in the lower right corner. Bars, 2 μm . Images in this dissertation are presented in color.

were frequently associated with ring-like structures (Fig. 5.9, A, C, E, and G). We stained nuclei using SYTOX-orange fluorescent dye (*Abs/Em* 543/570) and found that the fluorescent ring-like structures were associated with the outside surface of the nuclei (Fig. 5.9, B, D, F, and H). The cytoplasmic labeling pattern of VBS was clearly different from OmtA (Fig. 5.9, I, lower right panel). Ultra-thin sections were immuno-labeled with column purified anti-VBS IgG followed by immuno-gold labeling; TEM analysis revealed that VBS was distributed within the cytoplasm and also concentrated in ring-like structures surrounding the nuclei in SU-1 (Fig. 5.10, C, D, E, and F), while no labeling was observed in those structures in AFS10 (Fig. 5.10, A and B). Within a single cell, several ring-like structures immuno-labeled with VBS antibodies were observed in both CLSM (Fig. 5.9, A, C, E, and G) and TEM (Fig. 5.10, panel E). It is not clear if the signals were associated with a membrane structure. The data suggested that VBS is localized in the cytoplasm and also likely in the ER (see below).

DISCUSSION

I initially used native VBS to generate PAb but encountered significant cross reactivity. This could possibly be due to the limited amount of purified VBS available (60 μ g for two rabbits) or that purified VBS still contained contaminating fungal proteins. Similar cross-reactivity was encountered using the glycosylated form of *A. niger* glucose oxidase to generate PAb to the native enzyme (Witteveen et al., 1992). Native VBS has been confirmed to be *N*-link glycosylated (Silva et al., 1997). If the glycosylated form of the antigen affects antibody specificity, the native VBS should have been treated with deglycosylating enzyme to remove the *N*-glycan moiety prior to immunization. Nevertheless, I chose an alternative way to generate highly specific antibodies using methods reported previously, e.g., anti-Ver-1 (Liang et al., 1997), anti-Nor-1 (Zhou and Linz, 1999), and anti-OmtA (Lee et al., 2002), and this approach proved fruitful.

Figure 5.10. Immuno-gold labeling of VBS in *A. parasiticus* AFS10 and SU-1 analyzed by TEM. Ultra-thin fungal sections derived from colony fractions R2 (AFS10 shown in Panels A and B) and S2 (SU-1 shown in Panels C, D, E and F) were immuno-labeled with column-purified anti-VBS IgG (50 µg/ml) followed by goat-anti rabbit IgG conjugated with gold particles (10 nm diameter). The large organelles shown in panels B, D, and F were generated at higher magnifications from the cognate hyphae shown in panels A, C, and E, respectively. Abbreviations: CW, cell wall; M, mitochondria; N, nuclei; V, vacuole. Bars represent 1 µm in panels A and E, 0.5 µm in panels B and D, and 250 nm in panels D and F. (This figure was generated by Lee, 2003).

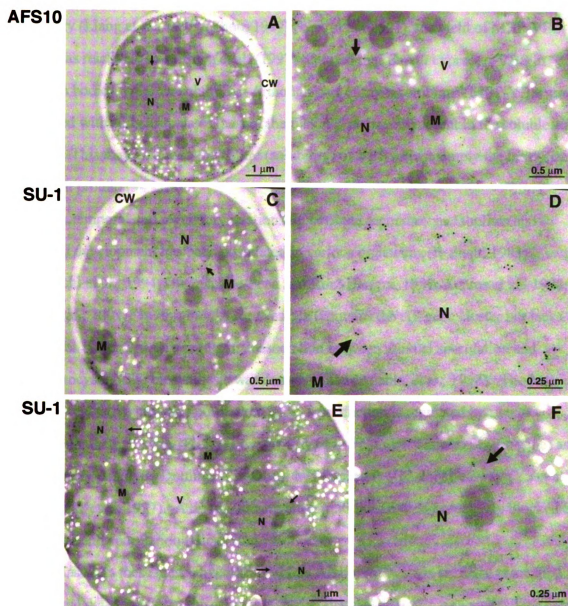


Figure 5.10

The *E. coli*- derived recombinant MBP-VBS fusion protein was generated and used as an immunogen. Compared to other MBP fusion proteins previously generated in our laboratory (Liang et al., 1996) (Zhou, 1997) (Lee, et al., 2001), the yield of MBP-VBS fusion was relatively low. Silva et al. (1997) reported that *E. coli* expresses VBS in inclusion bodies with low solubility. Although part of my recombinant MBP-VBS was associated with cell particulates, part of the fusion protein was present in the soluble fraction. This may be due to the nature (solubility) of VBS or just simply the large size of the fusion protein (94 kDa).

A temporal and regulatory relationship between secondary metabolism and microbial development has been postulated in various organisms (Bennett, 1983; Horinouchi et al., 1994, Guzman-De-Pena and Ruiz-Herrera, 1997; Adams et al., 1998; Calvo et al., 2002). In *A. nidulans* for example (contains the AF gene cluster but lacks the final enzyme, OrdA), a regulatory association between asexual sporulation and sterigmatocystin (ST) biosynthesis was demonstrated (Adams, et al., 1998). The balance between vegetative growth, sporulation, and ST production is regulated by two antagonistic factors, FlbA (Fluffy, Low brlA; *brlA* is a conidial vesicle specific gene) and FadA (Fluffy Autolytic Dominant) involved in a G-protein signaling pathway (Yu et al., 1996; Hicks et al, 1997). A dominant activation mutation in *fadA* completely blocked ST production and sporulation (Hicks et al., 1997).

Based on these data, I hypothesized that AF biosynthesis is spatially associated with fungal development at the cellular level and that AF enzymes are localized specifically in conidiophores (Lee et al., 2002?). However, recent data now clearly demonstrate that this hypothesis is not fully correct (Chapter 4); similar levels of VBS (this study), Nor-1, Ver-1, and OmtA (Chapter 4; Lee et al., submitted) were detected in vegetative hyphae and conidiophores. However, immuno-localization of VBS (this study) and OmtA, Nor-1, and Ver-1 (Chapter 4) detected the highest levels of these proteins and AFB₁ in fraction S2; interestingly, fraction S2 also contained the highest

numbers of newly developed conidiophores. According to Adams et al. (1998), conidiospores are generated approximately 24 h after germination of spores in the original inoculum. Consistent with these findings, conidiophores and conidiospores were observed in fractions S1 (48 to 72 h) and S2 (24 to 48 h) but not in fraction S3 (0 to 24 h). In addition, most conidiophores in fraction S2 were immuno-labeled with antibodies to VBS and OmtA but significantly fewer were labeled in fraction S1 suggesting that these proteins were present in newly developed conidiophores. Visual microscopic inspection of the conidiophores in fraction 2 confirms that many of these are immature and exist in various stages of development. In conclusion, our data support a spatial and temporal association between AF protein expression/AF production and sporulation at the colony level. I cannot rule out the possibility that protein stability or proteolytic degradation may contribute to our observations. The factors that directly participate in mediating this close association in *A. parasiticus* require further investigation.

In terms of sub-cellular localization of VBS, both CLSM and TEM indicated the presence of VBS in the cytoplasm as well as in ring-like structures adjacent to the nucleus. I attempted to identify a subcellular targeting signal in VBS using protein localization prediction programs found on the ExPASy Molecular Biology Server (<http://us.expasy.org>). Since no database is available for filamentous fungi, in most cases we used the sequence analysis database for yeast; occasionally data from animal or plant cells were used. These analyses predicted that VBS has a signal peptide (analyzed by iPOSRT, PSORT version 6.4, Signal IP V2.0, and Target P V1.0), suggesting VBS may be associated with the ER/Golgi secretory pathway. Using PSORTII, the possible subcellular localization for VBS was predicted as follows: Mitochondria: 43.5%; Cytoplasm: 21.7%; Golgi: 17.4%; Endoplasmic reticulum: 13.0%; and Vacuole: 4.3%.

The observed perinuclear localization of VBS is likely due to its association with the ER and possibly the Golgi. First, the sequence prediction analysis suggests that the close association of VBS with ring like structures is consistent with passage through an

ER/Golgi secretory pathway. VBS is a *N*-link glycosylated protein and the ER is the site for core-glycan (Glc3-Man9-GlcNAc₂) addition to the Asn residue.

Second, the perinuclear immuno-fluorescence labeling pattern of VBS is reminiscent of several proteins known to target the ER including calreticulin (Roderick et al., 1997; Dyer and Mullen, 2001; Wedlich-Söldner et al., 2002), ER mannosidase (Zuber et al., 2000), nephrin (Yan et al., 2002), and the vacuolar system-associated protein VASAP-60 (Brule et al., 2003).

Third, *N*-glycosylation of VBS is consistent with passage through an ER/Golgi pathway. Native VBS appeared as a doublet (78 kDa and 72 kDa) upon SDS-PAGE. Similar doublet bands have been detected by immuno-blotting of nephrin (Yan et al., 2002) and VASAP-60 (Brule et al., 2003). These proteins localize to ER and are thought to be post-translationally modified. In addition, it is well known that several co-translational and post-translational modifications take place specifically in the ER but not in the cytosol, including cleavage of the signal-peptide, *N*-link glycosylation, formation of disulfide bonds, and glyco-phosphatidylinositol (GPI)-anchoring (Ellgaard and Helenius, 2003 review). These observations allow us to predict that VBS is present in the ER for *N*-glycosylation and signal peptide cleavage; other VBS modifications might occur at that location as well.

It is not clear if VBS is associated with the Golgi for complex glycan modification. In filamentous fungi, the typical appearance of the Golgi apparatus with the classic dictyosome organization of stacked disc shape cisternae was not observed previously (Markham, 1995); however, a recent study detected the morphology of Golgi bodies in *A. niger* (Khalaj et al. 2001). Our CLSM and TEM micrographs did not show clear evidence that the Golgi bodies were being immuno-labeled. Also, the enzyme PNGase F, which was used to confirm that VBS is *N*-Glycosylated (Silva et al., 1997), cleaves intact oligosaccharide chains from the protein; therefore this method cannot determine if VBS is modified with complex glycans (Ausubel et al., 2003). In order to

determine the degree of complexity of the glycan attached onto VBS, other types of endoglycosidase and glycoamidase enzymes should be used (Ausubel et al., 2003).

N-glycosylation of VBS appeared to be significant for VBS activity and may play a role in stability. In general, protein *N*-glycosylation along the secretory pathway plays an important role in control of proper folding to the native tertiary and quaternary structure, and for subsequent translocation to the final cellular destination (Ellgaard and Helenius, 2003; Roth, 2002; Helenius and Aebi, 2001; Parodi, 2000). The *N*-glycosylation and ER protein control system provide proof reading mechanisms to ensure that the native conformation of newly synthesized proteins is maintained; in this regard, they are important for the fidelity of cellular functions (Ellgaard and Helenius, 2003 review). My data support the idea that *N*-glycosylation contributes to protein stability; VBS was significantly more stable than OmtA analyzed using similar methods (colony fractionation/Western blot data). A high proportion of intact VBS (78 kDa) remained in colony fraction S1 (48 to 72 h) compared to OmtA in this same fraction (Fig. 5.5 in this study compared to Fig. 5, Lee et al., 2002).

It is still uncertain if enzymatically active VBS is present in the ER, cytoplasm, or at both locations. VBS does not contain a typical C-terminal KDEL ER-retention signal (Teasdale and Jackson, 1996; Harter and Wieland, 1996), so presumably it is not an ER resident protein but is only transiently present for modification. However, in most cells studied to date, glycoproteins are transported along the secretory pathway and localized in the extracellular space, the plasma membrane, or in compartments that are involved in secretion and endocytosis (Ellgaard and Helenius, 2003). Therefore, an important issue to resolve is why VBS appears in the cytosol.

One possible explanation is that incorrectly folded, immature proteins can be retro-translocated from the ER into the cytosol for degradation through an ER-associated degradation (ERAD) process (Kostova and Wolf, 2003). However, the relative proportion of VBS found in the cytosol and the ER (approximately 50% in each location)

strongly suggests that the cytosolic localization of VBS is not likely due to this type of mechanism.

Another, more likely explanation is that, since VBS is involved in biosynthesis of a secondary metabolite (i.e. AF), targeting of this protein to its final cellular destination may be different from typical glycoprotein targeting in primary metabolism in higher eukaryotes. Perhaps the regular glycoprotein transport machinery is altered during secondary metabolism. In addition, we cannot rule out the possibility that although VBS appeared to be a cytosolic protein, it may be associated with a particular sub-cellular compartment yet the membrane structure was not preserved during cell preparation. Alternatively, VBS may be anchored in membrane structures while the bulk of the protein remains in the cytoplasm. In support of this, VBS is predicted to contain a putative transmembrane domain (PSORT version 6.4). Furthermore, mature VBS is a good candidate for a cytosolic protein because addition of a polar glycan generally increases solubility (Helenius and Aebi, 2001).

If VBS is functional in the cytosol, it will be interesting to determine if this enzyme interacts with other AF synthesizing enzymes that appeared in the cytoplasm (e.g. Nor-1, Ver-1, and OmtA; Lee et al., manuscript submitted). Based on our preliminary co-immuno-gold labeling of VBS and OmtA using TEM, these two proteins are in close proximity in the cytosol. Future experiments involved in co-localization of various AF synthesizing proteins either by GFP-linked or co-immuno-labeling techniques, subcellular fractionation to identify the organelles associated with AF synthesizing enzymes, and immuno-precipitation studies to determine interactions between AF proteins may provide insights about the coordination of these protein involved in AF biosynthesis.

ACKNOWLEDGEMENTS

Special thanks to Dr. Xudong Fan (Center for Advanced Microscopy at Michigan State University) for help in operating the jet-freezer.

Data in Chapter 5 were submitted for publication (Chiou, C. H., L. W. Lee, S. A. Owens, J. Whallon, K.L. Klomparens, C. A. Townsend, and J. E. Linz. Distribution and sub-cellular localization of the aflatoxin enzyme versicolorin B synthase (VBS) in time fractionated colonies of *Aspergillus parasiticus*. Fungal Genet. Biol.).

BIBLIOGRAPHY

- Adams, T. H., J. K. Wieser, and J.-H. Yu.** 1998. Asexual sporulation in *Aspergillus nidulans*. *Microbiol. Mol. Biol. Rev.* **62**:35-54.
- Adams T. H. and J-H. Yu.** 1998. Coordinate control of secondary metabolite production and asexual sporulation in *Aspergillus nidulans*. *Curr Opin Microbiol.* **1**:674-677.
- Aguilar, F., S. P. Hussain, and P. Cerutti.** 1993. Aflatoxin B₁ induces the transversion of G→T in codon 249 of the p53 tumor suppressor gene in human hepatocytes. *Proc. Natl. Acad. Sci. USA.* **90**:8586-8590.
- Akesson, H., E. Carlemalm, E. Everitt, T. Gunnarsson, G. Odham, and H-B Jansson.** 1996. Immunocytochemical localization of phytotoxins in *Bioplaris sorokiniana*. *Fungal Gene. Biol.* **20**:205-216.
- Amos, W. B., J. G. White, and M. Fordham.** 1987. Use of confocal imaging in the study of biological structure. *Appl. Optics* **26**:3239-3234.
- Anderson, H.W., E. W. Nehring, and W. R. Wichser.** 1975. Aflatoxin contamination of corn in the field. *J. Agric Food Chem.* **23**:775-782.
- Anderson, J.A., and C.H. Chung.** 1994. Conversion of versiconal acetate to versicolorin C in extracts from *Aspergillus parasiticus*. *Mycopathologia* **110**:31-35.
- Ashfold, A.E.** Dynamic pleiomorphic vacuole system: are they endosomes and transport compartments in fungal hyphae? In *Advances in Botanical Research incorporating Advances in Plant Pathology*. Callow, J. A. ed. Academic Press. San Diego, CA.
- Asao, T., G. Buchi, M. M. Abdel-Kader, S. B. Chang, E. L. Wick., and G. N. Wogan.** 1963. Aflatoxins B and G. *J. Am. Chem. Soc.* **85**:1706-1707.
- Aufauvre-Brown, A., C. M. Tang, and D. W. Holden.** 1993. Detection of gene-disruption events in *Aspergillus* transformants by polymerase chain reaction direct from conidiospores. *Curr Genet.* **24**:177-178.
- Ausubel F. M., R. Brent, E. Kingston, D. D. Moore, J. G. Seidman, J. A. Smith, and K. Struhl.** 2003. *Current Protocol in Molecular Biology*. John Wiley & Sons, New York, N. Y.
- Bailey, E. A., Iyer, R. S., Stine, M. P. Harris, T. M., and Essigmann, J. M.** 1996. Mutational properties of the primary aflatoxin B₁-DNA adduct. *Proc. Natl. Acad. Sci. USA.* **93**:1535-1539.

- Beckette, A., I. B. Health, and D. J. McLaughlin.** 1974. An Atlas of Fungal Ultrastructure, Longman, London.
- Bennett, W. J.** 1983. Secondary metabolism and differentiation in fungi, p. 1-32. *In* Bennett, J.W., and A. Ciegler. (ed.), Secondary metabolism and Differentiation in Fungi. Maecel Dekker, New York, N. Y.
- Betina, V.** 1995. Differentiation and secondary metabolism in some prokayotes and fungi. *Folia. Microbiol.* **40**:51-67.
- Bhatanagar, D., J. Yu, and K. C. Ehrlich.** 2002. Toxins of filamentous fungi. In Fungal Allergy and Pathogenecity. Breitenbach, M., R. Cramer, and S. B. Lehrer. eds. *Chem Immunol. Basel, Karger* **81**:167-206.
- Bhatnagar, D., K. C. Ehrlich, and T. E. Cleveland.** 2003. Molecular genetic analysis and regulation of aflatoxin biosynthesis. **61**:83-89.
- Blount, W. P.** 1961. Turkey "X" disease. *J. Brit. Turkey Fed.* **9**:52-54.
- Bodine, A. B., and D. R. Mertens.** 1983. Toxicology, metabolism, and physiological effects of aflatoxin in the bovine. pp. 46-50. In U. L. Diener, R. L. Asquith, and J. W. Dickens, Eds. Aflatoxin and *Aspergillus flavus* in corn. Souther Cooperative Series Bulletin 279. Auburn University, Auburn, Alabama.
- Borgia, P.T., L.E. Eagleton, and Y. Miao.** 1994. DNA preparations from *Aspergillus* and other filamentous fungi. *Biotechniques* **17**:431-432.
- Boutrif E.** 1995. FAO programmers for prevention, regulation, and control of mycotoxin in food. *Nat. Toxins.* **3**:322-326.
- Brown, D.W., J.H. Yu, H.S. Kellar, M. Fernandes, T.C., Nesbit, N.P. Keller, T.H. Adams, and T.J. Leonard.** 1996. Twenty-five coregulated transcripts defibe a sterigamatocystin gene cluster in *Aspergillus nidulans*. *Proc. Natl. Acad. Sci.* **93**:1418-1422.
- Brelje, T.C., M. W. Wessendorf, and R. L. Sorenson.** 1993. Multicolor laser scanning confocal immunofluorescence microscopy: Practical applications and limitations. In. *Cell Biological Applications of Confocal Microscopy* (B. Matsumoto, ed.) pp. 98-182. Academic Press, San Diego.
- Brule, S., R. Faure, M. Dore, D. W. Silversides, and J. G. Lussier.** 2003. Immunolocalization of vacuolar system-associated protein-60 (VASAP-60). *Histochem. Cell Biol.* **119**:371-381.

Buchanan, R. L., and D. F. Lewis. 1984. Regulation of aflatoxin biosynthesis: effects of glucose on activities of various glycolytic enzymes. *Appl. Environ. Microbiol.* **48**:306-310.

Butchko, R.A.E., T.H. Thomas, N.P. Keller. 1999. *Aspergillus nidulans* mutants defective in stc gene cluster regulation. *Genetics* **153**:715-720.

Calvo, A. M., R. A. Wilson, J. W. Bok., and N. P. Keller. 2002. Relationship between secondary metabolism and fungal development. *Micro. Mol. Biol. Rev.* **66**:447-459.

Carlsson, K., and N. Aslund. 1987. Confocal imaging for 3-D digital microscopy. *Appl. Optics* **26**:3232-3238.

Cary, J.W., N. Barnaby, N.K.C. Ehrlich, and D. Bhatnagar. 1999. Isolation and characterization of experimentally induced, aflatoxin biosynthetic pathway deletion mutants of *Aspergillus parasiticus*. *Appl. Microbiol. Biotechnol.* **51**:808-812.

Cary, J. J., J. E. Linz., and D. Bhatnagar. 2000. Aflatoxins: biological significance and regulation of biosynthesis. p. 317-362. *In* J. Cary, D. Bhatnagar, and J. Linz (ed.), *Microbial foodborne diseases: mechanisms of pathogenesis and toxin synthesis.* Technomic Publishing, Lancaster, Pa.

Cary, J. J., M. D. John, K. C. Ehrlich, M. S. Wright, S-H. Liang and J. E. Linz. 2002. Molecular and functional characterization of a second copy of the aflatoxin regulatory gene, AflR, from *Aspergillus parasiticus*. *Biochim Biophys Acta.* **1576**:316-323.

CAST. 2003. Council for Agricultural Science and Technology. Mycotoxins: Risks in plant, animal, and human system. Report 139.

Cenis, J.L. 1992. Rapid extraction of fungal DNA for PCR amplification. *Nucleic Acids Res.* **20**:2380.

Chang, P. K., C. D. Skory, and J. E. Linz. 1992. Cloning of a gene associated with aflatoxin B₁ biosynthesis in *Aspergillus parasiticus*. *Curr. Genet.* **21**:231-233.

Chang, P. K., J. W. Cary, D. Bhatnagar, T. E. Cleveland, J. W. Bennett, J. E. Linz, C. P. Woloshuk, and G. A. Payne. 1993. Cloning of the *Aspergillus parasiticus* apa-2 gene associated with the regulation of aflatoxin biosynthesis. *Appl. Environ. Microbiol.* **59**:3273-3279.

Chang, P. K., J. W. Cary, J. Yu, D. Bhatnagar, and T. E. Cleveland. 1995a. The *Aspelto* et al., 2001; ynthase gene, pksA, a homologs of *Aspergillus nidulans* wA, is required for a aflatoxin B₁ biosynthesis. *Mol. Gen. Genet.* **248**:270-277.

- Chang, P. K., D. Bhatnagar, D., K. C. Ehrlich, and T. E. Cleveland, and J. W. Bennett.** 1995b. Sequence variability in homologs of the aflatoxin pathway gene *aflR* distinguished species in the *Aspergillus* Section *Flavi*. *Appl. Environ. Microbiol.* **61**:40-43.
- Chang, P.-K. and J. Yu.** 2002. Characterization of a partial duplication of the aflatoxin gene *us* ATCC 56775. *Appl. Microbiol. Biotechnol.* **58**:632-636.
- Chiou, C. H., M. M. Miller, D. L. Wilson, F. Trail and J. E. Linz.** 2002. Chromosomal location plays a role in regulation of aflatoxin gene expression in *Aspergillus parasiticus*. *Appl. Environ. Microbiol.* **68**:306-315.
- Colling, A.J., and P. Markham.** 1985. Woronin bodies rapidly plug septal pores of severed *Penicillium chrysogenum* hyphae. *Experimental. Mycol.* **9**:80-85.
- Cotty, P. J., and D. Bhatnagar.** 1994. Variability among atoxigenic *Aspergillus flavus* strains in ability to prevent aflatoxin contamination and production of aflatoxin biosynthetic pathway enzymes. *Appl. Environ. Microbiol.* **60**:2248-2251.
- Cotty P.J. and K.F. Cardwell.** 1999. Divergence of West African and North American communities of *Aspergillus* section *Flavi*. *Appl. Environ. Microbiol.* **65**:2264-2266.
- Czymmek, K., J. H. Whallon, and Klomparens, K. L.** 1994. Confocal microscopy in mycological research. *Exp. Mycol.* **18**:275-293.
- Gould, J. R., G.-A. Keller, and S. Subramani.** 1987. Identification of a peroxisomal targeting signal at the carboxylterminus of firefly luciferase. *J. Cell. Biol.* **105**:2923-2931.
- Dyer, J. M. and R. T. Mullen.** 2001. Immunocytological localization of two plant fatty acids desaturases in the endoplasmic reticulum. *FEBS Lett.* **494**:44-47.
- D'Souza, C.A., B.N. Lee, and T. Adams.** 2001. Characterization of the role of the FluG protein in asexual development of *Aspergillus nidulans*. *Genetics* **158**:1027-1036.
- Eaton, D. L., and E. P. Gallagher.** 1994. Mechanisms of aflatoxin biosynthesis. *Annu. Rev. Pharmacol. Toxicol.* **34**:135-172.
- Eaton, D. L., and J. D. Groopman. (ed.)** 1994. The toxicology of aflatoxins: human health, veterinary, and agriculture Significance. Academic Press, San Diego, Calif.
- Ehrlich, K., J.W. Carry, and B.G. Montalbano.** 1999a. Characterization of the promoter for the gene encoding the aflatoxin biosynthetic pathway regulatory protein AFLR. *Biochim. Biophys. Acta* **1444**:412-417.

Ehrlich, K., B.G. Montalbano, and J.W. Carry. 1999b. Binding of the C6-zinc cluster protein, AFLR, to the promoters of aflatoxin pathway biosynthesis genes in *Aspergillus parasiticus*. *Gene* **230**:249-257.

Ehrlich, K., B.G. Montalbano, and P. J. Cotty. 2003. Sequence comparison of *aflR* from different *Aspergillus* species provide evidence for variability in regulation of aflatoxin production. *Fungal Genet. Biol.* **38**:63-74.

Ellis, W. O., J. P. Smith, B. K. Simpson, and J. H. Oldham. 1991. Aflatoxins in food: occurrence, biosynthesis, effects on organisms, detection, and methods of control. *Crit Rev. Food Sci. Nutr.* **30**:403-439.

Ellgaard, L. and A. Helenius. 2003. Quality control in the endoplasmic reticulum. *Nature Rev.* **4**:181- 191.

Farag, R. S., M. M. Rashed, and A. A. Abo-Hagger. 1996. Aflatoxin destruction by microwave heating. *Intl. J. Food Sci Nutri.* **47**:197-208.

Feng, G. H., and T. J. Leonard. 1995. Characterization of the polyketide synthase gene (*pksL1*) required for aflatoxin biosynthesis in *Aspergillus parasiticus*. *J. Bacteriol.* **177**:6246-6254.

Ferreira, A. V. B., and N. Glass. 1996. PCR from fungal spores after microwave treatment. *Fungal Genet Newsl.* **43**:25-26.

Flegler, S.L., J.W.Heckman, and K.L. Klopman. 1995. Scanning and transmission electron microscopy an introduction. Chapter 6. p.97- 150.

Ghebranious, N., and S. Sell. 1998. Hepatitis B injury, male gender, aflatoxin, and p53 expression each contribute to hepatocarcinogenesis in transgenic mice. *Hepatology.* **27**: 383-391.

Greenblatt, M. S., W. P. Bennett, M. Hollstein., and C. C. Harris. 1994. Mutations in the p53 tumor suppressor gene: clues to cancer etiology and molecular pathogenesis. *Cancer Res.* **54**:4855-4878.

Guzman-De-Pena, D., and J. Ruiz-Herrera. 1997. Relationship between aflatoxin biosynthesis and sporulation in . *Fungal Genet. Biol.* **21**:198-205.

Hamer, J. E. and W. E. Timberlake. 1987. Functional organization of the *Aspergillus nidulans trpC* promoter. *Mol. Cell Biol.* **7**:2352-2359.

Harris, C. C., M. and Hollstein. 1993. Clinical implications of the p53 tumor suppressor gene. *N. Engl. J. Med.* **329**:1318-1327.

- Harris, S. D., J. L. Morrell and J. E. Hamer.** 1994. Identification and characterization of *Aspergillus nidulans* mutants defective in cytokinesis. *Genetics*. **136**:517-532.
- Harter, C., and F. Wieland.** 1996. The secretary pathway: mechanisms of protein sorting and transport. *Biochim. Biophys. Acta*. **1286**:75-93.
- Helenius, A., and M. Aebi.** 2001. Intracellular functions of *N*-linked glycans. *Science* **291**:2364-2369.
- Henry, S. H., F. X. Bosch, T. C. Troxell, and P. M. Bolger.** 1999. Reducing liver cancer- Global control of aflatoxin. *Science* **286**:2453-2454.
- Herman, B.** 1998. Fluorescence microscopy. Bios Scientific Publisher, Springer-Verlag, New York, Inc. NY.
- Hicks, J. K., J.-H. Yu, N. P. Keller, and T. H. Adams.** 1997. *Aspergillus* sporulation and mycotoxin production both require inactivation of the FadA Ga protein-dependent signaling pathway. *EMBO. J.* **16**:4916-4923.
- Hoch, H. C., and R. C. Staples.** 1983. Ultrastructural organization of the non-differentiated uredosopre germling of *Uromyces phaseoli* variety *typica*. *Mycologia* **75**:795-824.
- Horinouchi, S., and T. Beppu.** 1994. A-factor as a microbial hormone that controls cellular differentiation and secondary metabolism in *Streptomyces griseus*. *Mol. Microbiol.* **12**:859-864.
- Horng, J. S., P. K. Chang, J. J. Pestka, and J. E. Linz.** 1990. Development of a homologous transformation system for *Aspergillus parasiticus* with the gene encoding nitrate reductase. *Mol. Gen. Genet.* **224**:294-296.
- Hsia, C. C., D. E., Klenier, C. A. Axiotis, A. DiBidceglie, A. M. Nomura, D. E. Stemmermann, and E. Tabor.** 1992. Mutations of *p53* gene in hepatocellular carcinoma: roles of hepatitis B virus and aflatoxin contamination in the diet. *J. Natl. Cancer. Inst.* **84**:1638-1641.
- Hussein, H. S., and J. M. Brasel.** 2001. Toxicity, metabolism, and impact of mycotoxins on humans and animals. *Toxicology* **167**:101-134.
- IARC.** 1993. IARC monographs on the evaluation of carcinogenic risks to humans. Some naturally occurring substances: food items and constituents, heterocyclic aromatic amines and mycotoxins. Lyon, France:IARC. **56**, 245-345.
- Ito, Y., S. W. Peterson, D. T., Wicklow, and T. Goto.** 2001. *Aspergillus pseudotamarii*, a new aflatoxin producing species in *Aspergillus* section *Flavi*. *Mycol. Res.* **105**:233-239.

- Jackson, P. E. and J. D. Groopman.** 1999. Aflatoxin and liver cancer. *Bailliere's Clin. Gastro.* **13**:545-555.
- Jedd, G. and N.-H. Chua.** 2000. A new self-assembled peroxisomal vesicle required for efficient resealing of the plasma membrane. *Nat. Cell Biol.* **2**:226-231.
- Johnson, L. M., V. A. Bankaitis, and S. D. Emr.** 1987. Distinct sequence determinants direct intracellular sorting and modification of a yeast vacuolar protease. *Cell* **48**:875-885.
- Kale, S. P., D. Bhatnagar, and J.W. Bennett.** 1994. Isolation and characterization of morphological variants of deficient in secondary metabolite production. *Mycol. Res.* **98**: 645-652.
- Kato, J. A. Suzuki., H. Yamazaki, Y. Ohinishi, and S. Horinouchi.** 2002. Control by A-factor of a metalloendopeptidase gene involved in areal mycelium formation in *Streptomyces griseus*. *J. Bact.* **184**:6016-6025.
- Keller, G.A.** 1991. Evolutionary conservation of a microbody targeting signal that targets protein to peroxisomes, glyoxisomes and glycosome. *J. Cell. Biol.* **114**:893-904.
- Keller, N. P. and T. M. Hohn.** 1997. Metabolic pathway gene clusters in filamentous fungi. *Fungal. Genet. Biol.* **21**:17-29.
- Khalaj, V., J. L. Brookman, and G. D. Robson.** 2001. A study of the protein secretory pathway of *Aspergillus niger* using a glucoamylase-GFP fusion protein. *Fung. Genet. Biol.* **32**:55-65.
- Kinsey, J. A. and J. A. Rambosek.** 1984. Transformation of *Neurospora crassa* with the cloned *amdH* (glutamate dehydrogenase) gene. *Mol. Cell Biol.* **4**:117-122.
- Klinlosky, D. J.** 1997. Protein transport from the cytoplasm into the vacuole. *J. Membrane Biol.* **157**:105-115.
- Klich, M.A., E. J. Mullaney, C. B. Daly, and J. W. Cary.** 2000. Molecular and physiological aspects of aflatoxin and sterigmactocystin biosynthesis by *Aspergillus tamarii* and *A. ochraceoroseus*. *Appl. Microbiol. Biotechnol.* **53**:605-609.
- Kostova, Z., and D. H. Wolf.** 2003. For whom the bell tolls: protein quality control of the endoplasmic reticulum and the ubiquitin-proteasome connection. *EMBO J.* **22**:2309-2317.
- Krishnamachari, K. A. V. R., R. V. Bhat., V. Nagarajan, and T. B.. G. Tilac.** 1975, Hepatitis due to aflatoxicosis. *Lancet* **1**:1061-1063.

- Kurylowicz, W., W. Kurzatkowski, and J. Kurzatkowski.** 1987. Biosynthesis of benzylpenicillin by in *Penicillium chrysogenum* and its golgi apparatus. Arch. Immunol. Ther. Exp. **35**:699-724.
- Kusumoto, K. I., K. Yabe, Y. Nogata, and H. Ohta.** 1998. Transcript of a homolog of aflR, a regulator gene for aflatoxin synthesis in *Aspergillus parasiticus*, was not detected in *Aspergillus oryzae* strains. FEMS Microbiol. Letts. **169**:303-307.
- Kwon, Y.H., K.S. Wells., and H. C. Koch.** 1993. Fluorescence confocal microscopy: Applications in fungal cytology. Mycologia **85**:721-733.
- Lasky, T., and L. Magder.** 1997. Hepatocellular carcinoma p53 G>T trasnversion at codon 249: the fingerprint of aflatoxin exposure? *Environ. Health. Perspect.* **105**:392-397.
- Lecellier, G., and P. Silar.** 1994. Rapid methods for nucleic acids extraction from Petri dish-grown mycelia. Curr Genet. **25**:122-123.
- Lee, A. B., and T. A. Cooper.** 1995. Improved direct PCR screen for bacteria colonies: Wooden toothpicks inhibit PCR amplification. BioTechniques **18**:225-226.
- Lee, B. N., and T. Adams.** 1994. The *Aspergillus nidulans fluG* gene is required for production of an extracellular developmental signal. Genes Dev. **8**:641-651.
- Lee, L.W., C.H. Chiou, and J.E. Linz.** 2002. Function of native OmtA *in vivo* and expression and distribution of this protein in colonies of *Aspergillus parasiticus*. Appl. Environ. Microbiol. **68**:5718-5727.
- Lee, L.W.** Functional analysis of *omtA* and subcellular localization of aflatoxin enzymes in *Aspergillus parasiticus*. PhD Dissertation, Michigan State University, East Lansing.
- Lee, L. W., C. H. Chiou, K. L. Klomparens, and J. E. Linz.** 2003. Sub-cellular localization of aflatoxin biosynthetic enzymes in time-dependent fractionated colonies of *Aspergillus parasiticus*. Manuscript submitted to Arch. Microbiol.
- Lenderfeld, T., D. Ghali, M. Wolschek, E. M. Kubicek-Pranz, and C. P. Kubicek.** 1993. Subcellular compartmentation of penicillin biosynthesis in *Penicillium chrysogenum*. J. Biol. Chem. **268**:665-671.
- Liang, S.-H.** 1996. The function and expression of the *ver-1* gene and localization of the Ver-1 protein involved in aflatoxin B₁ biosynthesis in *Aspergillus parasiticus*. PhD Dissertation, Michigan State University, East Lansing.
- Liang S.-H., C. D. Skory and J. E. Linz.** 1996. Characterization of the function of the *ver-1* and *ver-1B* genes, involved in aflatoxin biosynthesis in *Aspergillus parasiticus*. Appl Environ Microbiol. **62**:4568-4575.

- Liang, S.H., T-S Wu, R. Lee, F.S. Chu, and J.E. Linz.** 1997. Analysis of mechanisms regulating expression of the ver-1 gene, involved in aflatoxin biosynthesis. *Appl. Environ. Microbiol.* **63**:1058-1065.
- Lin B. K., and J. A. Anderson.** 1992. Purification and properties of versiconal cyclase from *Aspergillus parasiticus*. *Arch. Biochem. Biophys.* **293**:67-70.
- Ling, M., F. Merante, and B. H. Robinson.** 1995. A rapid and reliable DNA preparation method for screening a large number of yeast clones by polymerase chain reaction. *Nucleic Acids Res.* **23**:4924-4925.
- Lunn, R. M., Y. J. Zhang, L. W. Wang, C. J. Chan, P. H. Lee, C. H. Lee, W. Y. Tsai, and R. M. Santella.** 1997. *p53* mutations, chronic hepatitis B virus infection, and aflatoxin exposure in hepatocellular carcinoma in Taiwan. *Cancer Res.* **57**:3471-3477.
- Mace, K., F. Aguilar, J. S. Wang, P. Vautravers, M. Gomez-Lechon, F. J. Gonzalez, J. Groopman, C. Harris, and M. A. Pfeifer.** 1997. Aflatoxin B1-induced DNA adduct formation and *p53* mutations in CYP450-expressing human liver cell lines. *Carcinogenesis* **18**:1291-1297.
- Mahanti, N., D. Bhatnagar, J. W. Cary, J. Joubert, and J. E. Linz.** 1996. Structure and function of fas-1A, a gene encoding a putative fatty acid synthase directly involved in aflatoxin biosynthesis in *Aspergillus parasiticus*. *Appl. Environ. Microbiol.* **62**:191-195.
- Mannon, J., and E. Johnson.** 1985. Fungi down on the farm. *New Scientist* **105**:12-16.
- Markham, P.** 1995. Organelles of filamentous fungi. Pp. 75-98. *In* N. A. R. Gow, and G. W. Gooday (ed), *The growing fungus*, 1st ed. Chapman & Hall, London, UK.
- Marin, S., V. Sanchis, R. Saenz, A. J. Ramos, I. Vinas, and N. Magan.** 1998. Ecological determinants for germination and growth of some *Aspergillus* and *Penicillium* spp. from grain. *J. Appl. Microbiol.* **84**:25-36.
- Markham, P., and A. J. Collinge.** 1987. Woronin bodies of filamentous fungi. *FEMS Microbiol. Rev.* **46**:1-11.
- Marth, E. H., and M. P. Doyle.** 1979. Update on molds: Degradation aflatoxin. *Food Technol* **33**:81-87.
- Massey, T. E., R. K. Stewart, J. M. Daniels, and L. Liu.** 1995. Biochemical and molecular aspects of mammalian susceptibility to aflatoxin B₁ carcinogenicity. *Proc. Soc. Exp. Biol. Med.* **208**:213-227.

- Matushima K., K. Yashiro, Y. Hanya, K. Abe, K. Yabe, and T. Hamasaki.** 2001. Absence of aflatoxin biosynthesis in koji mold (*Aspergillus sojae*). *Appl. Microbiol. Biotechnol.* **55**:771-776.
- Maxewell, D.P., V.N. Armentrout, and L.B. Graves.** 1977. Microbodies in plant pathogenic fungi. *Annal. Rew. Phyto.* **15**:119-134.
- McGuire, S. M., J. C. Silva, E. G. Casillas, and C. A. Townsend.** 1996. Purification and characterization of Versicolorin B Synthase from *Aspergillus parasiticus*. Catalysis of the stereodifferentiating cyclization in aflatoxin biosynthesis essential to DNA interaction. *Biochemistry* **35**:11740-11486.
- McLean, M. and M. F. Dutton.** 1995. Cellular interactions and metabolism of aflatoxin: an update. *Pharmac. Ther.* **65**:163-192.
- Meyers D. M., G. Obrian, W. L. Du, D. Bhatnagar, and G. A. Payne.** 1998. Characterization of *aflJ*, a gene required for conversion of pathway intermediates to aflatoxin. *Appl. Environ. Microbiol.* **64**:3713-7.
- Min, J., M. T. Arganoza, J. Ohrnberger, C. Xu, and R.A. Akins.** 1995. Alternative methods of preparing whole-cell DNA from fungi for dot-blot, restriction analysis, and colony filter hybridization. *Anal Biochem.* **225**:94-100.
- Miller, B. L., K. Y. Miller, K. A. Roberti, and W. E. Timberlake.** 1987. Position-dependent and -independent mechanisms regulate cell-specific expression of the *SpoC1* gene cluster of *Aspergillus nidulans*. *Mol. Cell Biol.* **7**:427-434.
- Miller, M. J.** 2003. Transcriptional regulation of the *Aspergillus parasiticus* aflatoxin biosynthesis pathway gene *nor-1*. Ph.D. Dissertation, Michigan State University, East Lansing.
- Minto, R. E. and C. A. Townsend.** 1997. Enzymology and molecular biology of aflatoxin biosynthesis. *Chem. Rev.* **97**:2537-2555.
- Minsky, M.** 1961. Microscopy apparatus. U.S. Patent 3013467.
- Minsky, M.** 1988. Memoir on inventing the confocal scanning microscope. *Scanning* **10**:128-138.
- Montalto, G. M. Cervello, L. Giannitrapani, F. Dantona, A. Terranova, and L. A. M. Castagnetta.** 2002. Epidemiology, risk factors, and natural history of hepatocellular carcinoma. *Ann. N.Y. Acad. Sci.* **963**:13-20.
- Motomura, M., N. Chihaya, T. Shinozawa, T. Hamasaki, and K. Yabe.** 1999. Cloning and characterization of the O-Methyltransferase I gene (*dmtA*) from associated with the conversion of demethylstrigmatocystin to sterigmatocystin of dihydro-

- demethylsterigmatocystin to dihydrosterigmatocystin in aflatoxin biosynthesis. *Appl. Environ. Microbiol.* **65**:4987-4994.
- Muchen, K. F. , R. P. Misra, and M. Z. Humayun.** 1983. Sequence specificity in aflatoxin B1-DNA interactions. *Proc. Natl. Acad. Sci. USA* **80**:6-10.
- Müller W.H., T.P. van der Krift, A.J.J. Krouwer, H.A.B. Wosten, L.H.M. van der Voort, E.B. Smaal, and A.J. Verkleij.** 1991. Localization of the pathway of the penicillin biosynthesis in *Penicillium chrysogenum*. *EMBO Journal.* **10**:489-495.
- Ngindu, A., P. R. Kenya, D. M. Ocheng, T. N. Omonde, W. Ngare, D. Gatei, B. K. Johnson, J. A. Ngira, H. Nandwa, J. Jansen, J. N. Kaviti, and T. A. Siongok.** 1982. Outbreak of acute hepatitis caused by aflatoxin poisoning in Kenya. *Lancet* **1**:1346-1348.
- Ohneda, M., M. Arioka., H. Nakajima, and K. Kitamoto.** 2002. Visualization of vacuoles in *Aspergillus oryzae* by expression of CYP-EGFP. *Fungal Genet. Biol.* **37**:29-38.
- Ohsumi, K., M. Arioka, H. Nakajima, and K. Kitamoto.** 2002. Cloning and characterization of a gene (*avaA*) from *Aspergillus nidulans* encoding a small GTPase involved in vacuole biogenesis. *Gene.* **291**:77-84.
- Paddock, S. W.** An introduction to confocal imaging. *Confocal Microscopy Methods and Protocols.* Ed. S. Paddock Human Press Inc. Totowa, NJ. *Meth. Mol. Biol.* **122**:1-34.
- Parodi, A. J.** 2000. Rold of N-oligosaccharide endoplasmic reticulum processing reactions in glycoprotein folding and degradation. *Biochem. J.* **348**:1-13.
- Paul, G. C., C. A. Kent, and C. R. Thomas.** 1994. Hyphal vacuolation and fragmentation in *Penicillium chrysogenum*. *Biotechnol. Bioeng.* **44**:655-660.
- Payne, G.** 1998. Process of contamination by aflatoxin-producing fungi and their impact on crops. pp 279-306. In K. K. S. Sinha and D. Bhatnagar (Eds.) *Mycotoxins in Agriculture and Food Safety.* Marcel Dekker, Inc. New York.
- Payne, G. A., and M. P. Brown.** 1998. Genetics and physiology of aflatoxin biosynthesis. *Annu. Rev. Phytopathol.* **36**:329-362.

Pestka, J.J., P. K. Gaur, and F. S. Chu. 1980. Quantification of aflatoxin B1 and aflatoxin B1 antibody by an enzyme-linked immunosorbent microassay. *Appl. Environ. Microbiol.* **40**:1027-1031.

Prieto R., G. L. Yousibova, and C. P. Woloshuk. 1996. Identification of aflatoxin biosynthetic genes by genetic complementation in a mutant of *Aspergillus parasiticus* lacking the aflatoxin gene cluster. *Appl. Environ. Microbiol.* **62**:3567-3571.

Raymond, C. K., C. J. Roberts, K. E. Moore, I. Howald, and T. H. Stevens. 1992. Biogenesis of the vacuole in *Saccharomyces cerevisiae*. *Int. Rev. Cytol.* **139**:59-120.

Reiß, J. 1982. Development of *Aspergillus parasiticus* and formation of aflatoxin B1 under the influence of conidiogenesis affecting compounds. *Arch. Microbiol.* **133**:236-8.

Roderick, H. L., A. K. Campbell, and D. H. Llewellyn. 1997. Nuclear localisation of calreticulin in vivo is essential by its interaction with glucocorticoid receptors. *FEBS Lett.* **405**:181-185.

Roth, J. 2002. Protein N-Glycosylation along the secretory pathway: relationship to organelle topography and function protein quality control and cell interactions. *Chem. Rev.* **102**:285-303.

Sharma, P. R., and D. K. Salunkhe. 1991. Mycotoxin and phytotoxins in human and animal health. Boca Raton, CRC Press.

Shen, H. M., and C. H. Ong. 1996. Mutations of the *p53* tumor suppressor gene and *ras* oncogenes in aflatoxin hepatocarcinogenesis. *Mut. Res.* **366**:23-44.

Siller, W. G., and D.C. Ostler. 1961. The histopathology of an enterohepatic syndrome of turkey poults. *Vet. Rec.* **73**:134-148.

Silva, J. C., R. E. Minto, C. E. Barry, K. A. Holland, and C. A. Townsend. 1996. Isolation and characterization of the versicolorin B synthase gene from *Aspergillus parasiticus*. *J. Biol. Chem.* **271**:13600-13608.

Silva, J. C. and C. A. Townsend. 1997. Heterologous expression, isolation, and characterization of Versicolonin B Synthase from *Aspergillus parasiticus*. *J. Biol. Chem.* **272**:804-813.

Sinnhuber, R. O., J. D. Hendriks, J. H. Wales, and G. B. Putnam. 1977. Neoplasms in rainbow trout, a sensitive animal model for environmental carcinogenesis. *Ann. N. Y. Acad. Sci.* **298**:389-408.

Skory, C. D., J. S. Horng, J. J. Pestka, and J. E. Linz. 1990. Transformation of *Aspergillus parasiticus* with a homologous gene (*pyrG*) involved in pyrimidine biosynthesis. *Appl. Environ. Microbiol.* **56**:3315-3320.

- Skory, C. D., J. S. Horng, J. J. Pestka, and J. E. Linz.** 1992. Isolation and characterization of a gene from *Aspergillus parasiticus* associated with the conversion of versicolorin A to sterigmatocystin in aflatoxin biosynthesis. *Appl. Environ. Microbiol.* **58**:3527-3537.
- Skory, C. D., P.-K. Chang, and J. E. Linz.** 1993. Regulated expression of the *nor-1* and *ver-1* genes associated with aflatoxin biosynthesis. *Appl. Environ. Microbiol.* **59**:1642-1646.
- Spear, R. N., D. Cullen., and J. H. Andrews.** 1999. Fluorescent labels, confocal microscopy, and quantitative image analysis in study fungal biology. *Methods In Enzymol.* **307**:607-623.
- Steiner, J.J., C.J. Poklemba, R.G. Fjellstrom, and L.F. Elliott.** 1995. A rapid one-tube genomic DNA extraction process for PCR and RAPD analysis. *Nucleic Acids Res.* **13**:2569-2570.
- Subramani, S.** 1996. Protein translocation into peroxisomes. *J. Biol. Chem.* **271**:32483-32486.
- Tarutani, Y., K. Ohsumi, M. Arioka, H. Nakajima, and K. Kitamoto.** 2001. Cloning and characterization of *Aspergillus nidulans vpsA* gene which is involved in vacuolar biogenesis. *Gene* **268**:23-30.
- Teasdale, R. D., and M. R. Jackson.** 1996. Signal mediated sorting of membrane proteins between the endoplasmic reticulum and the Golgi apparatus. *Annu. Rev. Cell Dev. Biol.* **12**:27-54.
- Tenney, K. I. Hunt, J. Sweigard, J. I. Pounder, C. McClain, E. J. Bowman, and B. J. Bowman.** 2000. *hex1*, a gene unique to filamentous fungi, encodes the major protein of the Woronin body and functions as a plug for septal pores. *Fungal Genet. Biol.* **31**:205-217.
- Thurmm, M.** 2000. Structure and function of the yeast vacuole and its role in autophagy. *Microsc. Res. Tech.* **51**:563-572.
- Timberlake, W. E. and E. C. Barnard.** 1981. Organization of a gene cluster expressed specifically in the asexual spores of *A. nidulans*. *Cell* **26**:29-37.
- Timberlake, W. E. and M. A. Marshall.** 1989. Genetic engineering of filamentous fungi. *Science* **244**:1313-1317.
- Trail, F., P-K Chang, and J. E. Linz.** 1994. Structural and functional analysis of the *nor-1* gene involved in the biosynthesis of aflatoxin by *Aspergillus parasiticus*. *Appl. Environ. Microbiol.* **60**:3315-3320.

- Trail, F., N. Mahanti, and J. E. Linz.** 1995a. Molecular biology of aflatoxin biosynthesis. *Microbiology* **141**:755-765.
- Trail, F., N. Mahanti, M. Rarick, R. Mehigh, S.-H. Liang, R. Zhou, and J.E. Linz.** 1995b. Physical and transcriptional map of an aflatoxin gene cluster in *Aspergillus parasiticus* and functional disruption of gene involved early in the aflatoxin pathway. *Appl. Environ. Microbiol.* **61**:1665-1673.
- Van der Kamp, M., A. J. M. Driessen, and W. N. Konings.** 1999. Compartmentalization and transport in B-Lactam antibiotic biosynthesis by filamentous fungi. *Antonie van Leeuwenhoek.* **75**:41-78.
- Van der Lende, T. R., M. van de Kamp, M. van den Berg, K. Sjollema, R. A. L. Bovenberg, M. Veenhuis, W. N. Konings and A. J. M. Driessen.** 2002. δ -(L- α -aminoadipyl)-L-cysteinyl-D-valine synthetase, that mediates the first committed step in penicillin biosynthesis, is a cytosolic enzyme. *Fungal Gene. Biol.* **37**:49-55.
- Valenciano, S., J.R. De Lucas, I. Van der Klei, M. Veenhuis, and F. Laborda.** 1998. Characterization of *Aspergillus nidulans* peroxisomes by immunoelectron microscopy. *Arch. Microbiol.* **170**:370-376.
- Van Egmond, H. P.** 1993. Rationale for regulatory programmes for mycotoxins in human foods and animal feeds. *Food Addit. Contam.* **10**:29-36.
- van Gorcom, R. F., P. J. Punt, P. H. Pouwels, and C. A. van den Hondel.** 1986. A system for the analysis of expression signals in *Aspergillus*. *Gene* **48**:211-217.
- van Zeijl, C. M. J., E. H. M. van de Kamp, P.J. Punt, G. C. M. Selten, B. Hauer, R.F.M. van Gorcom, and C. A. M. J. J. van der Hondel.** 1998. An improved colony-PCR method for filamentous fungi for amplification of PCR-fragments of several kilobases. *J. Biotech.* **59**:221-224.
- Verdoes, J. C., P. J. Punt, A. H. Stouthamer, and C. A. M. J. J. van den Hondel.** 1994. The effect of multiple copies of the upstream region on expression of the *Aspergillus niger* glucoamylase encoding gene. *Gene* **145**:179-187.
- Vidal-cros, A., F. Viviani, G. Labesse, M. Boccara, and M. Gaudry.** 1994. Polyhydroxy-naphthalene reductase involved in melanin biosynthesis in *Magnaporthe grisea*-purification, cDNA cloning and sequencing. *Eur. J. Biolchem.* **219**:985-992.
- Voeltz, G. K., M. M. Rolls, and T. A. Rapoport.** 2003. Structural organization of the endoplasmic reticulum. *EMBO reports* **3**:944-950.
- Wada, Y. and Y. Anraku.** 1994. Chemiosomic coupling of ion transport in the yeast vacuole: its role in acidification inside organelles. *J. Bioenerg. Biomembr.* **26**:631-637.

- Wang, H., S. E. Kohalmi, and A.J. Culter.** 1996. An improved method for polymerase chain reaction using whole yeast cells. *Anal Biochem.* **237**:145-146.
- Waterham, H. R., and J. M. Cregg.** 1999. Peroxisome biogenesis. *BioAssays* **19**:57-66.
- Watson, A. J., L. J. Fuller, D. J. Jeemes, and D. B. Archer.** 1999. Homologs of aflatoxin biosynthesis genes and sequence of aflR in *Aspergillus oryzae* and *Aspergillus sojae*. *Appl. Environ. Microbiol.* **65**:307-310.
- Wedlich-Söhlender, R. I. Schulz, A. Straube, and G. Steinberg.** 2002. Dynein supports motility of endoplasmic reticulum in the fungus *Ustilago maydis*. *Mol. Cell. Biol.* **13**:965-977.
- Wendland, B., S. D. Emr, and H. Riezmanet.** 1998. Protein traffic in the yeast endocytic and vacuolar protein sorting pathways *Curr. Opin. Cell. Biol.* **10**:512-522.
- Whallon, J. H.** 1998. Introduction to laser scanning confocal microscopy. Laser Scanning Microscope Laboratory, Michigan State University. East Lansing, Mich.
- Wheeler, M. H. and A. A. Bell.** 1988. Melanins and their importance in pathogenic fungi. *Current Topics in medical Mycology.* **2**:338-387.
- Wicklow, D. T., and O. L. Schotwell.** 1983. Intrafungal distribution of aflatoxins among conidia and sclerotia of *Aspergillus flavus* and *Aspergillus parasiticus*. *Can. J. Microbiol.* **29**:1-5.
- Wild, C. P., G. J. Hudson, and G. Sbbioni.** 1992. Dietary intake of aflatoxins and the level of albumin-bound aflatoxin in peripheral blood in The Gambia, West Africa. *Cancer Epidemiol. Biomarkers Prev.* **1**:229-234.
- Wilson, D. L.** 1998. Expression analysis of an aflatoxin *nor-1/uidA* reporter fusion in *Aspergillus parasiticus*. Master Thesis, Michigan State University, East Lansing.
- Wilson, D. M., and G. A. Payne.** 1994. Factors Affecting *Aspergillus flavus* Group Infection and Aflatoxin Contamination of Crops. In Eaton, D.L. and Groopman, J.D. (Eds), *The Toxicology of Aflatoxins.* Academic Press, SanDiego. pp309-346.
- Witteveen, C. F.B., M. Veenhuis, and J. Visser.** 1992. Localization of glucose oxidase and catalase activities in *Aspergillus niger*. *Appl. Environ. Microbiol.* **58**:1190-1194.
- Woloshuk, C. P., K. R. Foutz, J. F. Brewer, D. Bhatnagar, T. E. Cleveland, and G. A. Payne.** 1994. Molecular characterization of *aflR*, a regulatory locus for aflatoxin biosynthesis. *Appl. Environ. Microbiol.* **60**:2408-2414.

- Woloshuck, C. P. and R. Prieto.** 1998. Genetic organization and function of the aflatoxin B1 biosynthetic genes. *FEMS Micro. Lett.* **160**:169-176.
- Xu, J.R., and J. E. Hamer.** 1995. Spore PCR. *Fungal Genet Newsl.* **42**:80.
- Yan, K., J. Khoshnoodi, V. Ruotsalainen., and K. Tryggvason.** 2002. *N*-link glycosylation is critical for the plasma membrane localization of Nephrine. *J. Am. Soc. Nephrol.* **13**:1385-1389.
- Yang, M., H. Zhou, R.Y. C. Kong, W. F. Fong, L. Ren, , X. Liao, Y. Wang, W. Zhuang, and S. Yang.** 1997. Mutations at codon 249 of *p53* gene in human hepatocellular carcinomas from Tongan, China. *Mutat. Res.* **381**:25-29.
- Yu, J., J. W. Cary, D. Bhatnagar, T. E. Cleveland, N. P. Keller, and F. S. Chu.** 1993. Cloning and characterization of a cDNA from *Aspergillus parasiticus* encoding an O-methyltransferase involved in aflatoxin biosynthesis. *Appl. Environ. Microbiol.* **59**:3546-3571.
- Yu, J., Chang, P. K., J. W. Cary, D. Bhatnagar, and T. E. Cleveland.** 1997. *avnA*, a gene encoding a cytochrome P-450 monooxygenase, is involved in the conversion of averantin to averufin in aflatoxin biosynthesis in *Aspergillus parasiticus*. *Appl. Environ. Microbiol.* **63**:1349-1356.
- Yu, J., P. K. Chang, E. C. Ehrlich., J. W. Cary, B. Montalbano., J. M. Dyer, D. Bhatnagar, and T. E. Cleveland.** 1998. Characterization of the critical amino acids of an *Aspergillus parasiticus* cytochrome P-450 mono-oxygenase encoded by *ordA* involved in biosynthesis of aflatoxin B₁, G₁, B₂ and G₂. *Appl. Environ. Microbiol.* **64**:4834-4841.
- Yu, J., P. K. Chang, D. Bhatnagar, and T. E. Cleveland.** 2000. Cloning of a sugar utilization gene cluster in *Aspergillus parasiticu*. *Biochem. Biophys. Acta* **1493**:211-214.
- Yu, J., P. K. Chang, D. Bhatnagar, and T. E. Cleveland.** 2002. Cloning and functional expression of an esterase gene in *Aspergillus parasiticus*. *Mycopathologia.* **156**:227-234.
- Yu, J. H., J. Weisser, and J. H. Adams.** 1996. The *Aspergillus* FlbA RGS domain protein antagonizes G-protein signaling to block proliferation and allow development. *EMBO J.* **15**:5184-5190.
- Zhou, R.** 1997. The function, accumulation, and localization of the Nor-1 protein involved in aflatoxin biosynthesis; the function of the *fluP* gene associated with sporulation in *Aspergillus parasiticus*. Ph.D. Dissertation, Michigan State University, East Lansing.
- Zhou, R., and J. E. Linz.** 1999. Enzymatic function of the Nor-1 protein involved in aflatoxin biosynthesis in *Aspergillus parasiticus*. *Appl. Environ. Microbiol.* **65**:5639-5641.

Zhou,
associ
Genet

Zube
immu
trimm

Zhou, R., R. Rasooly, and J. E. Linz. 2000. Isolation and analysis of fluP, a gene associated with hyphal growth and sporulation in *Aspergillus parasiticus*. *Mol. Gen. Genet.* **264**:514-520.

Zuber, C., M. J. Spiro., B. Guhl, R. G. Spiro., and J. Roth. 2000. Golgi apparatus immunolocalization of endomannosidase suggests post-endoplasmic reticulum glucose trimming: implications for quality control. *Mol. Biol. Cell.* **11**:4227-4240.

MICHIGAN STATE UNIVERSITY LIBRARIES



3 1293 02504 7865